

# Materials Horizons

Accepted Manuscript

This article can be cited before page numbers have been issued, to do this please use: U. S. Schubert, F. Behrendt and M. Gottschaldt, *Mater. Horiz.*, 2024, DOI: 10.1039/D4MH00315B.



This is an Accepted Manuscript, which has been through the Royal Society of Chemistry peer review process and has been accepted for publication.

Accepted Manuscripts are published online shortly after acceptance, before technical editing, formatting and proof reading. Using this free service, authors can make their results available to the community, in citable form, before we publish the edited article. We will replace this Accepted Manuscript with the edited and formatted Advance Article as soon as it is available.

You can find more information about Accepted Manuscripts in the [Information for Authors](#).

Please note that technical editing may introduce minor changes to the text and/or graphics, which may alter content. The journal's standard [Terms & Conditions](#) and the [Ethical guidelines](#) still apply. In no event shall the Royal Society of Chemistry be held responsible for any errors or omissions in this Accepted Manuscript or any consequences arising from the use of any information it contains.

Surface functionalized cryogels – Characterization methods, recent progress in preparation and application View Article Online  
DOI: 10.1039/D4MH00315B

**MH-REV-03-2024-000315.R1**

**Wider impact statement (max. 200 words)**

In this review, an overview about recent developments in the preparation of functionalized cryogels based on synthetic polymers, biopolymers and combination thereof as well as analytical methods used for their quantitative or qualitative characterization is given. Cryogels are sponge-like materials prepared by cryogelation possessing interesting features. Most importantly their interconnected pore structure distinguishes them from other porous materials. In addition, the functionalization of cryogels enables their use in a wide variety of different fields of application, *e.g.* the adsorption of certain molecules, catalysis, 3D cultivations or tissue engineering. Quantification of the successful cryogel functionalization is essential to ensure quality levels in cryogel research and enables comparability and reproducibility. It is necessary to optimize the functionalization based on different strategies in order to improve *e.g.* drug-delivery capabilities, stimuli-responsivity or for providing new tissue-like environments. This review will help researchers select suitable modification strategies for desired functionalities and provides an overview about recently applied analytical methods suitable for the evaluation of the successful cryogel functionalization. As future cryogel research will presumably be more directed towards multifunctional cryogels and the exploration of new fields of applications, the appropriate proof and quantification of the functionalization is inevitable for further improvements in this regard.



## ARTICLE

# Surface functionalized cryogels – Characterization methods, recent progress in preparation and application

Florian Behrendt,<sup>\*a,b,c</sup> Michael Gottschaldt<sup>a,b</sup> and Ulrich S. Schubert<sup>a,b,c,d</sup>Received 00th January 20xx,  
Accepted 00th January 20xx

DOI: 10.1039/x0xx00000x

Cryogels are polymeric materials possessing a sponge-like microstructure and have attracted significant attention within recent decades. Research has focused on their composition, fabrication techniques, characterization methods as well as potential or existing fields of applications. The use of functional precursors or functionalizing ligands enables the preparation of cryogels with desired properties such as biocompatibility or responsivity. They can also possess adsorptive properties or can be used for catalytical purposes. Although a very brief overview about several functional (macro-)monomers and functionalizing ligands has been provided by previous reviews for certain cryogel applications, so far there was no particular focus on the evaluation of the functionalization success and the used characterization methods. This review will provide a comprehensive overview about different characterization methods most recently used for the evaluation of cryogel functionalization. Furthermore, new functional (macro-)monomers and subsequent cryogel functionalization strategies are discussed, based on synthetic polymers, biopolymers and a combination of both. This review highlights the importance of the functionalization aspect in cryogel research in order to produce materials with tailored properties for certain applications.

## 1. Introduction

Cryogel research has gained significant interest due to the remarkable properties of these materials, which are easy to fabricate. In contrast to other porous polymer materials, cryogels contain an interconnected network of macropores enabling for example the supply of nutrients or the transport of substances through these materials.<sup>1, 2</sup> Various studies have been conducted to investigate the influence of several synthesis parameters such as the temperature, freezing rate, monomer and cross-linker concentration as well as additives and solvents.<sup>3</sup> Among a variety of different preparation techniques, cryopolymerization of precursors derived from synthetic polymers such as poly(acrylamide)<sup>4</sup> or polyvinylalcohol,<sup>5</sup> or natural biopolymers like gelatin or collagen<sup>6</sup> at sub-zero temperatures has proven to be a suitable method.<sup>7</sup> Freezing of the precursor solution leads to the formation of solvent crystals acting as pore templates within an unfrozen surrounding microphase in which the polymerization of the precursor molecules takes place. Subsequent thawing and washing results in highly porous materials which can be freeze-dried afterwards. Based on the interconnected network of macropores, mechanically stable and highly permeable

materials are obtained which are applied in tissue engineering,<sup>8-12</sup> heavy metal adsorption,<sup>13</sup> treatment of wastewater,<sup>14, 15</sup> drug delivery,<sup>9, 16</sup> chromatographic separation,<sup>17-23</sup> biomedical applications,<sup>24-28</sup> bioreactor scaffolds<sup>29, 30</sup> or for the 3D cultivation or immobilization of cells or bacteria.<sup>31-34</sup> In particular, in recent years, molecular imprinted cryogels for adsorption purposes<sup>35-37</sup> and injectable cryogels for biomedical applications<sup>38, 39</sup> have emerged. So far, reviews mainly focused on the different cryogel fabrication methods, the effect of certain parameters on the gel properties and applications.

Cryogel characterization typically comprises the examination of the pore structure by mercury intrusion porosimetry, micro-computed tomography or microscopy techniques such as scanning electron microscopy, environmental scanning electron microscopy or confocal laser scanning microscopy.<sup>13, 17, 25, 26, 40, 41</sup> A very detailed review from Martinez-Garcia *et al.* provides an overview about the aforementioned characterization techniques to evaluate the microarchitecture of cryogels for cellular applications.<sup>42</sup> Mechanical properties are determined by the use of dynamic shear and compressive measurements, atomic force microscopy, nano-indentation, rheological measurements or micromagnetic resonance elastography.<sup>13, 17, 25, 26</sup>

The preparation of functionalized cryogels can be achieved by the use of specific comonomers, *via* subsequent cryogel surface modification, by the use of functionalized particles or filler materials for the preparation of composite cryogels,<sup>40, 41, 43-45</sup> or by repeated cryogelation leading to the formation of interpenetrating networks with multiple cross-linking.<sup>40, 41</sup>

<sup>a</sup> Laboratory of Organic Chemistry and Macromolecular Chemistry (IOMC), Friedrich Schiller University Jena, Humboldtstraße 10, 07743 Jena, Germany.

<sup>b</sup> Jena Center for Soft Matter (JCSM), Friedrich Schiller University Jena, Philosophenweg 7, 07743 Jena, Germany.

<sup>c</sup> Cluster of Excellence Balance of the Microverse, Friedrich Schiller University Jena, Jena, Germany.

<sup>d</sup> Abbe Center of Photonics (ACP), Albert-Einstein-Straße 6, 07743 Jena.



Surface modification include grafting of polymer chains,<sup>41</sup> functionalization with growth factors,<sup>9, 26</sup> or cell-adhesive peptides such as RGD for improved cellular response.<sup>9</sup>

One of the few examples in which the functionalization of cryogels is highlighted explicitly with respect to the capture of target molecules, is represented by the review from Bakhshpour *et al.*. Therein, functional cryogels created from functional monomers or by cryogel surface modification with specific binding ligands are reviewed for the use in protein separation and the removal of metal ions, highlighting the adsorptive target, the kind of functional monomer or functional ligand and the adsorption capacity.<sup>24</sup> Nevertheless, there is a lack of the evaluation of the successful functionalization or the quantification of the cryogel functionalization.

In previous reviews, only Fourier-transform infrared spectroscopy (FTIR) has been mentioned for the evaluation of cryogel functionalization which is not a quantitative method.<sup>7, 17</sup> In the review of Damania *et al.* the use of x-ray photoelectron spectroscopy and elemental analysis for the quantitative evaluation of the elemental composition was described very briefly but there was no discussion of further characterization methods for the analysis of the functionalization of cryogels.<sup>7</sup>

Very recently, Danielsen *et al.* published a comprehensive review about the molecular characterization of polymer

networks.<sup>46</sup> Different analytical techniques are described in detail for the characterization of the cryogel precursors, the gelation process, the network structure, and its mechanics and dynamics. Techniques for the analysis of the network structure target the swelling, morphology, structure and topology, as well as the permeability. For the evaluation of the chemical structure, a very brief overview is given about the use of solid-state NMR (ssNMR) spectroscopy which enables both qualitative and quantitative analysis. However, an extensive description about how exactly the functionalization of cryogels was characterized and successfully proven is still missing and has never been reported so far to the best of our knowledge.

In this review, we will discuss the preparation of functional cryogels from functional monomers or by the subsequent modification of cryogels with functional ligands (**Figure 1**). Herein, we will distinguish between recently emerging functional monomers and different functionalization approaches of cryogels, based on synthetic polymers and biopolymers as well as their combination. A special focus is on the evaluation of the successful cryogel functionalization. Thus, a short overview is first given about different analytical methods recently used for the direct and indirect analysis of cryogel functionalization, the quantification of adsorbed species, and methods for the evaluation of bacterial and cell cultures.

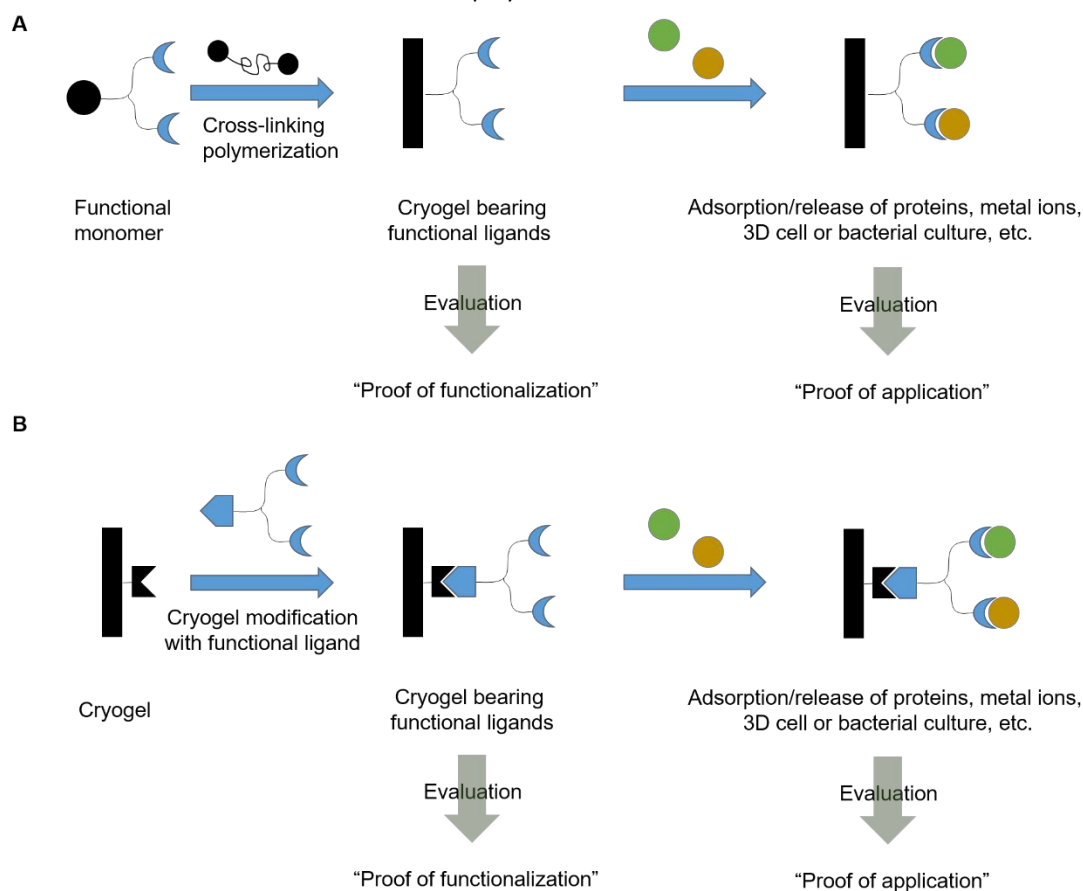


Figure 1 Schematic representation of the functionalization of cryogels by the use of functional monomers (A) or by the subsequent modification of cryogels with functional ligands (B) for the adsorption of target molecules such as proteins or heavy metal ions.



## 2. Characterization and quantification of cryogel functionalization - Analytics

A variety of different analytical methods exist for the evaluation and quantification of the degree of functionalization of cryogels depending on the functional ligand. In the following section, the main analytical methods will be discussed which are either used for the direct analysis of the cryogel functionalization (**Section 2.1**), the indirect determination of the cryogel functionalization (**Section 2.2**) or the quantification of adsorbed species (**Section 2.3**). Additionally, methods for the evaluation of bacterial and cell culture are summarized (**Section 2.4**).

### 2.1 Direct analysis of cryogel functionalization

As cryogels represent a class of insoluble polymeric networks, the direct evaluation of their functionalization requires specific analytical methods. Therefore, ssNMR typically applied in order to gain information about the cryogel composition on a qualitative basis.<sup>47, 48</sup> In comparison with the respective liquid NMR spectra of the monomers, band assignment is simplified. The presence of characteristic bands of the monomers in the cryogel spectra together with an absence of double bond carbon atoms indicates the successful incorporation of the functional monomer into the cryogel network.

The elemental and molecular composition of cryogels can be analyzed by energy-dispersive X-ray spectroscopy (EDX). This technique is commonly applied in material science for surface characterizations and enables both a qualitative and quantitative analysis of the cryogel functionalization among other methods, such as wavelength-dispersive X-ray spectroscopy (WDX) and X-ray photoelectron spectroscopy (XPS). The presence of sulfur atoms or metal atoms serves as a proof for the functionalization with biomolecules like enzymes or proteins containing metals in their sub-units.<sup>49-51</sup> Furthermore, a quantification of the functionalization is also possible. For instance, the amount of immobilized *N*-acetyl cysteine onto poly(AAm-MMA) cryogels was calculated based on the sulfur stoichiometry.<sup>52</sup> The amount of covalently attached ferrocene was quantified based on the iron content.<sup>53</sup>

Alternatively, inductively coupled plasma (ICP) enables the direct determination of the amount of metal ions within cryogels upon an acidic digestion of the gel.<sup>53</sup> Dried, iron containing cryogel pieces are treated with a mixture of 96% H<sub>2</sub>SO<sub>4</sub>/65% HNO<sub>3</sub> followed by microwave irradiation. Afterwards the solutions are subjected to inductively coupled plasma-optical emission spectroscopy (ICP-OES) analysis.

Another method for the determination of the composition is represented by elemental analysis. This method allows a qualitative evaluation of the cryogel functionalization but also the quantitative determination of heteroatomic functional ligands such as vinylimidazole,<sup>54</sup> *N*-methacryloyl aspartic acid,<sup>55</sup> para-aminobenzoic acid,<sup>56</sup> para-aminopyridine,<sup>56</sup> nicotinamide,<sup>57</sup> 3-(prop-3-ynylloxycarbonylamino)-phenyl

boronic acid,<sup>58</sup> or ortho-phospho-L-tyrosine<sup>48</sup> based on the nitrogen,<sup>54-57</sup> boron,<sup>58</sup> or phosphorous content.

For the qualitative evaluation of cryogel functionalization, common spectroscopic characterization methods can also be applied such as FTIR, Raman spectroscopy or fluorescence spectroscopy. FTIR and Raman allow to detect functional groups and, thus provide information about the presence of functional monomers or ligands within the cryogels. Usually, cryogel FTIR or Raman spectra are compared with the spectra of the corresponding monomers or functionalizing ligands for peak assignment. An absence of the vinyl signals in FTIR (C=C-stretching vibration at 1630 to 1660 cm<sup>-1</sup>, =CH<sub>2</sub> at 2952 cm<sup>-1</sup> and =CH<sub>2</sub> distortion at 927 cm<sup>-1</sup>) together with the presence of characteristic bands of the monomers or functionalizing ligands serves as indication of a successful cryogel functionalization. For instance, the immobilization of L-asparaginase onto p(HEMA-GMA) cryogels was confirmed by the presence of two new peaks in the IR spectrum at 1650 cm<sup>-1</sup> and 1537cm<sup>-1</sup>, assigned as the vibration of the C=O groups (amide I) and a combination of the C-N stretching and N-H vibration in the protein backbone (amide II) respectively which are characteristic for enzymes or proteins.<sup>49</sup> For the functionalization of epoxide containing cryogels, an absence of the epoxide band (900 to 910 cm<sup>-1</sup>) often serves as an additional proof of the successful ligand attachment on the cryogels.

Fluorescence spectroscopy can be used for the qualitative evaluation of cryogel functionalization with adamantly modified peptides which were attached to acryloyl-cyclodextrin based cryogels.<sup>59</sup> Adamantane and cyclodextrin form a fluorescent complex *via* host-guest interactions. Thus, an increasing fluorescence signal in the course of the reaction serves as qualitative measure for the successful peptide functionalization.

Microscopy techniques such as confocal laser scanning microscopy (CLSM) or immunofluorescence microscopy allow for the observation of the incorporation and spatial distribution of peptides bearing a fluorescence label such as dansyl chloride<sup>60</sup> or proteins previously labeled with fluorescent dyes such as DyLight488 and DyLight594.<sup>61</sup>

Contact angle measurements enables the investigation of the physical properties of cryogels but also can be a proof of ligand functionalization, for instance the incorporation of lauryl acrylate as hydrophobic monomer resulting in the creation of water-repelling materials.<sup>62</sup>

In summary, a variety of analytical methods enable a qualitative and non-destructive evaluation of cryogel functionalization such as ssNMR, FTIR, Raman, fluorescence spectroscopy, CLSM, immunofluorescence microscopy or contact angle measurements. By the use of EDX, WDX, XPS, ICP-OES and elemental analysis, a quantification of the functionalization is even possible. Amongst all of the aforementioned analytical



techniques, ICP-OES remains the only destructive method for the direct evaluation of cryogel functionalization.

## 2.2 Indirect determination of cryogel functionalization

The amount of immobilized ligand can also be determined indirectly by measuring the ligand concentration in solution before and after the functionalization with common analytical methods such as spectrophotometry, or fluorescence spectroscopy.<sup>63</sup> The difference between the two concentrations corresponds to the amount of ligand immobilized on the cryogels. Depending on the kind of ligand to be immobilized, different methods exist for their determination. Fluorescence spectroscopy also allows a qualitative assessment of the success of the functionalization with peptide sequences bearing fluorescent labels such as pyrene.<sup>59</sup>

The most commonly used method for the indirect determination of ligand functionalization is represented by spectrophotometry which allows to determine the concentration of a variety of different immobilized ligands such as sugars,<sup>64, 65</sup> enzymes,<sup>49, 51, 66-68</sup> proteins,<sup>50</sup> antibodies,<sup>69</sup> metal ions,<sup>70, 71</sup> peptides,<sup>72</sup> and amino acids in solution.<sup>73</sup> This technique is often coupled with colorimetric assays such as the Bradford method,<sup>49, 66, 68, 69</sup> the Habeeb assay,<sup>61, 74, 75</sup> or the dinitrosalicylic acid method (DNS method).<sup>64</sup>

The Bradford method utilizes Coomassie Brilliant Blue G-250 as a protein-binding substrate. The protein-dye complex exhibits an increased molar absorbance and is quantified at 595 nm. The Habeeb assay (TNBS assay) takes advantage of the formation of an orange-colored compound by the reaction of 2,4,6-trinitrobenzenesulfonic acid (TNBS) with primary amines, which can be detected at 335 nm (Figure 2).

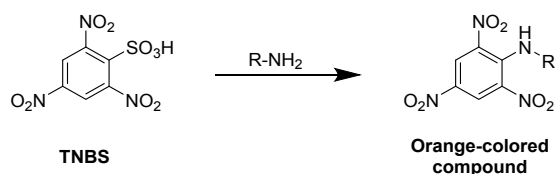


Figure 2 Schematic representation of the underlying reaction of the Habeeb assay (TNBS assay) for the determination of amines by the reaction with 2,4,6-trinitrobenzenesulfonic acid.

Since the reaction of free amines with the TNBS substrate takes place in a stoichiometric fashion, the amount of free amine groups in proteins can be quantified. Thus, this method allows to quantify the methacrylation of proteins such as gelatin or bovine serum albumine based on the amount of free amine groups after the modification relatively to the amount of free amines of the unmodified protein.<sup>61, 74</sup>

Reducing sugars such as *N*-acetyl glucosamine can also be determined spectrophotometrically upon treatment with 3,5-dinitrosalicylic acid (DNS) (Figure 3).<sup>64</sup> This technique was first reported by Sumner *et al.* in which the sugar containing solution is treated with the DNS reagent and heated in a boiled

water bath for 5 min.<sup>76</sup> The reaction yields the corresponding aldonic acid and 3-amino-5-nitrosalicylic acid which can be quantified at 575 nm.

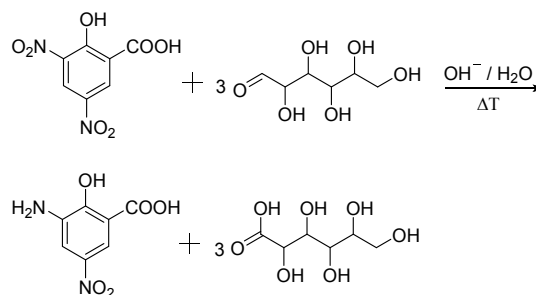


Figure 3 Schematic representation of the determination of reducing sugars using the dinitrosalicylic acid method, yielding 3-amino-5-nitro-salicylic acid and the corresponding aldonic acid.

The Kjeldahl method represents a commonly applied technique for the indirect determination of nitrogen containing molecules such as proteins or amino acids like tryptophan or phenylalanine.<sup>77-79</sup> At first, boiling in concentrated sulfuric acid in the presence of a catalyst, for example  $K_2SO_4$  or  $TiO_2$ , to drive decomposition of the nitrogen containing sample and to the formation of  $(NH_4)_2SO_4$ .<sup>80</sup> The subsequent addition of sodium hydroxide releases ammonia which is distilled and trapped in a known volume of boric acid.<sup>80</sup> After completion of the distillation process, the ammonia trapped-acid solution is titrated (Figure 4).<sup>80</sup> The amount of nitrogen is equal to the concentration of ammonium ions determined by titration.<sup>80</sup>

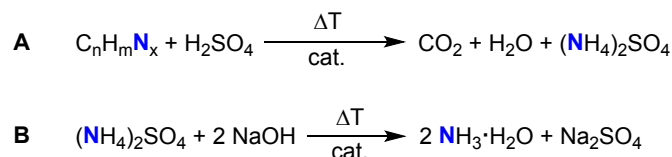


Figure 4 Schematic representation of the quantification of nitrogen containing molecules using the Kjeldahl method. (A) Decomposition of the nitrogen containing sample into ammonium sulfate by boiling in concentrated sulfuric acid. (B) Addition of sodium hydroxide leads to the formation of ammonia followed by distillation. The ammonia is trapped in a bath of acid (e.g. boric acid) which can then further be titrated.

Alternatively, a gravimetric method can also be considered to determine the amount of attached ligand. For instance, for the determination of immobilized tris(hydroxymethyl)amino-methane (Tris), the cryogels were dry weighed before and after the functionalization with Tris.<sup>81</sup> The mass difference of the cryogel before and after the functionalization corresponds to the amount of Tris attached to the cryogels for which a mass increase of  $5.32 \pm 0.23\%$  after the functionalization was measured.

The subsequent cryogel modification with functional ligands is most commonly realized by the covalent attachment onto cryogel surfaces bearing epoxide moieties. The determination of the epoxide ligand density on cryogels can be determined using a titrimetric method (Figure 5).<sup>82</sup> Treatment of epoxide



containing cryogels with an aqueous thiosulfate solution leads to a nucleophilic ring-opening and the production of hydroxide ions in a stoichiometric fashion. The concentration of OH<sup>-</sup> ions can be quantified by acid-base titration and directly correlates with the amount of epoxide groups on the cryogels.

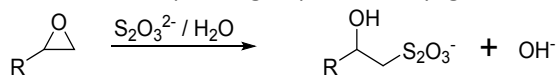


Figure 5 Schematic representation of the determination of the cryogel epoxide density using a titrimetric method. The epoxide ring-opening reaction by a nucleophilic attack of thiosulfate ions in aqueous solution leads to an equimolar formation of hydroxide ions which can be quantified by acid-base titration.<sup>83</sup>

The pyridine-HCl method represents an alternative method for the determination of the epoxide group density on cryogels which is based on the same titrimetric principle (Figure 6).<sup>66</sup>

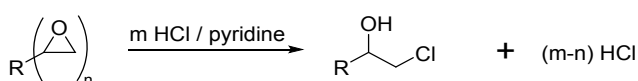


Figure 6 Schematic representation of the determination of the cryogel epoxide density using the pyridine-HCl method. HCl reacts with the epoxide groups in a stoichiometric fashion and the remaining HCl is titrated with NaOH.

The authors claim that treatment with an excess of HCl/pyridine leads to the stoichiometric reaction of the epoxide groups with hydrochloric acid.<sup>84</sup> The remaining HCl is then titrated with NaOH solution. The difference between the initial and final amount of HCl is equal to the amount of epoxide groups present on the cryogel.

Most of the aforementioned reported methods rely on the indirect quantification of the cryogel functionalization by the determination of the ligand concentration before and after the functionalization and are, therefore, considered non-destructive with respect to the final cryogels. These include spectrophotometry or fluorescence spectroscopy. Gravimetry enables the determination of the amount of ligand functionalization based on the weight difference of the dried cryogels before and after the functionalization. The Kjeldahl method represents a titrimetric method by which nitrogen containing ligands in solution are quantified upon acidic decomposition, alkalization and titration of the formed ammonia. As lots of functionalization approaches are directed towards the modification of cryogel epoxy groups with functional ligands, it can be beneficial to determine the amount of epoxide groups on the cryogels. By the covalent attachment of either thiosulfate or chloride ions due to a nucleophilic ring-opening of the epoxide, stoichiometrically formed hydroxide ions can be titrated and are considered equal to the amount of epoxide groups. Due to the resulting change in the chemical structure, further use of these particular samples can be limited.

### 2.3 Methods for the quantification of adsorbed species

As already mentioned before, spectrophotometry also plays an important role in cryogel research for the indirect quantification

of the adsorption or release of antibodies,<sup>54</sup> (co)enzymes,<sup>50, 55, 77, 82, 85, 86</sup> heavy metal ions,<sup>87-89</sup> dyes,<sup>90-93</sup> hormones,<sup>56, 94</sup> drugs,<sup>95, 96</sup> bacteria,<sup>58, 97</sup> proteins,<sup>98</sup> or phenolic compounds.<sup>51</sup> The adsorption capacity (A) is calculated based on the difference between the initial and final concentration of the adsorbent as follows:

$$A = \frac{(c_{\text{initial}} - c_{\text{final}})}{m_{\text{Cryogel}}} * V$$

In case of the metal ion detection in solution, xylenol orange or iminodiacetic acid are commonly used as color developing agents or coordination agents.<sup>87, 88</sup> The corresponding metal complex with either xylenol orange or iminodiacetic acid is quantified at 572 to 575 nm or 730 nm, respectively. In a few cases, the Bradford method can be applied for the quantification of adsorbed proteins,<sup>64, 78, 99-101</sup> enzymes,<sup>79, 99, 102</sup> and antibodies.<sup>48, 69-71, 73</sup>

To quantify the adsorption of heavy metal ions onto cryogels in an indirect manner, ICP-OES,<sup>55, 56, 103</sup> inductive coupled plasma-mass spectrometry (ICP-MS),<sup>57, 104</sup> inductively coupled plasma-atomic emission spectroscopy (ICP-AES),<sup>105</sup> atomic absorption spectroscopy (AAS)<sup>106</sup> or stripping voltammetry<sup>52</sup> are commonly applied which represent already well-known techniques for the quantification of metal ions in solution. The amount of adsorbed metal ions such as Pb<sup>2+</sup>,<sup>52, 103, 105</sup> Cu<sup>2+</sup>,<sup>55, 56</sup> Ag<sup>+</sup>,<sup>56</sup> Zn<sup>2+</sup>,<sup>52, 56</sup> As<sup>5+</sup>,<sup>104, 106</sup> Cr<sup>6+</sup>,<sup>104</sup> or Cd<sup>2+</sup>,<sup>52</sup> is determined from the difference between the initial and final concentration of metal ions in the adsorbing solution.

Alternatively, EDX and XPS allow the direct analysis of adsorbed metal ions<sup>60, 87-89, 99, 105</sup> or sulfur containing drugs<sup>96</sup> on cryogel surfaces on an either qualitative or quantitative basis.

In combination with homogenous colorimetric enzymatic assays, spectrophotometry also allows for the quantification of adsorbed LDL-cholesterol.<sup>65</sup> At first, cholesterol esters are hydrolyzed to free cholesterol and the corresponding fatty acids by cholesterol esterase enzyme (Figure 7A). In the presence of oxygen, cholesterol oxidase enzyme first mediates the reaction of LDL-cholesterol to 4-cholestenone and hydrogen peroxide (Figure 7B). The peroxidase enzyme can use the formed hydrogen peroxide for the reaction with *N*-ethyl-*N*-(2-hydroxy-3-sulfopropyl)-3,5-dimethoxyaniline sodium salt (DAOS) and 4-aminoantipyrine to form a colored quinonimine (Figure 7C). The amount of quinonimine is direct proportional to the amount of LDL-cholesterol and is quantified spectrophotometrically.

Additionally, HPLC allows to monitor the adsorption and release of lysozyme or to determine the amount of adsorbed cholesterol on cryogels indirectly by calculating the initial and final concentration in solution.<sup>81, 107</sup>

Gravimetric analysis allows the evaluation of the sorption of oils and organic solvents into hydrophobic cryogels.<sup>62</sup> Herein, the adsorption capacity is calculated from the cryogel mass after



adsorption divided by the initial mass in the dried state before and after the adsorption.

View Article Online  
DOI: 10.1039/D4MH00315B

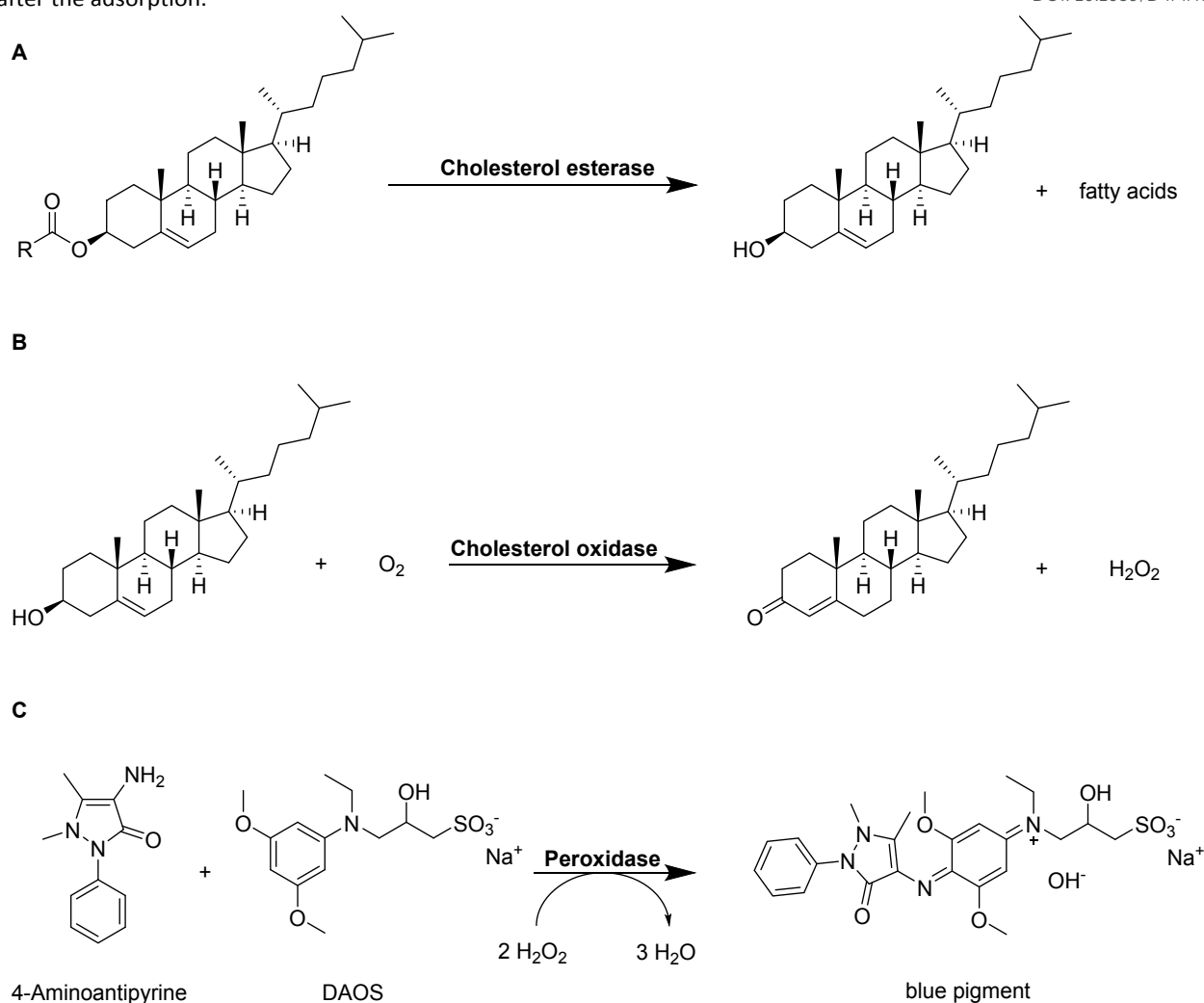


Figure 7 Schematic representation of the determination of LDL-cholesterol by a homogenous colorimetric enzymatic assay.<sup>112</sup> Cholesterol esters are hydrolyzed into free cholesterol and fatty acids by cholesterol esterase enzyme (A). Free cholesterol reacts with oxygen to 4-cholesten-3-one and hydrogen peroxide catalyzed by cholesterol oxidase (B). The formed hydrogen peroxide creates a colored pigment upon reaction with 4-aminoantipyrine and *N*-ethyl-*N*-(2-hydroxy-3-sulfopropyl)-3,5-dimethoxyaniline sodium salt (DAOS) which is quantified by spectrophotometry (C).

Spectroscopic methods such as FTIR and fluorescence spectroscopy allow both qualitative and quantitative investigations of the adsorption or release of substances from cryogels. FTIR spectroscopy can indicate the coordination of metal ions with binding ligands on cryogel surfaces by the shift of signals to lower frequencies and the decrease of the signal intensities.<sup>55, 56, 70, 71, 99, 100, 105</sup> On the other hand, fluorescence spectroscopy enables the quantification of loading and release of fluorescent dyes from cryogels in an indirect manner.<sup>108</sup> The loading and distribution of dyes within cryogels can be observed by confocal laser scanning microscopy on a qualitative basis.<sup>108</sup>

The ELISA assay allows for the indirect quantification of the loading of signaling proteins, which is equal to the difference between the initial and final protein concentration in solution.<sup>109</sup> Antibodies are used to label the proteins. Attached

proteins are labeled by, for example, the subsequent attachment of streptavidin-conjugated horseradish peroxidase. The amounts of antibodies and thus, proteins in solution are determined using spectrophotometry by a colorimetric reaction catalyzed by horseradish-peroxidase. Herein, tetramethylbenzidine is transformed into 3,3',5,5'-tetraene-4,4'-diimine (Figure 8).





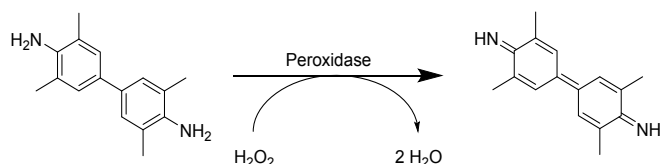


Figure 8 Schematic representation of the peroxidase catalyzed reaction of tetramethylbenzidine to 3,3',5,5'-tetramethyl-[1,1'-bi(cyclohexylidene)]-2,2',5,5'-tetraene-4,4'-diimine.

Flow cytometry enables the quantification of virus elution from cryogels. Monolayers of HEK cells are treated with virus elution supernatants followed by measuring the percentage of green fluorescent protein (GFP) expression after 72 hours.<sup>110</sup>

By the use of confocal laser scanning microscopy, the adsorption of proteins bearing fluorescence labels such as a fluorescein isothiocyanate or tetramethylrhodamine isothiocyanate can be qualitatively assessed.<sup>111</sup> Lastly, the amount of adsorbed Cu(II) ions can be qualitatively evaluated by PEI probing which is described as the formation of a blue Cu-PEI complex.<sup>60</sup>

In summary, the quantification of adsorbed species is most commonly realized by the use of indirect, non-destructive analytical methods such as spectrophotometry, ICP, AAS, stripping voltammetry, HPLC, gravimetry, fluorescence spectroscopy or ELISA assays. The quantification is based on the difference of either the ligand concentration or the masses of dried cryogels before and after the functionalization. Alternatively, EDX, XPS, FTIR, CLSM or PEI probing represent methods for the direct, non-destructive evaluation of cryogel functionalization in a quantitative or qualitative manner, respectively.

#### 2.4 Methods for the evaluation of bacterial and cell culture

Aforementioned we described different analytical characterization techniques necessary to confirm the successful cryogel characterization (Sections 2.1 and 2.2). Additionally, analytical methods were highlighted in order to proof the further applicability based on the functionalization (Section 2.3). Furthermore, it is also important to demonstrate the successful functionalization based on the biological properties which is described in this section.

For the quantification of the cellular proliferation and the viability, a variety of colorimetric assays exist such as the AlamarBlue assay,<sup>63, 113-120</sup> the PrestoBlue assay,<sup>121, 122</sup> the MTT assay,<sup>72, 95, 123-126</sup> the MTS assay,<sup>59, 60, 127-129</sup> or the WST-8 assay,<sup>61, 74</sup>. All of these assays enable the evaluation of the cell proliferation and viability by measuring the metabolic activity using different chemical transformations. Herein, a substrate is subjected to the cells leading to the formation of a colored product which is detected and quantified by fluorescence spectroscopy. In case of the AlamarBlue assay<sup>63, 113-117</sup> and the PrestoBlue assay<sup>121, 122</sup>, the substrate resazurin is reduced to resorufin (Figure 9).

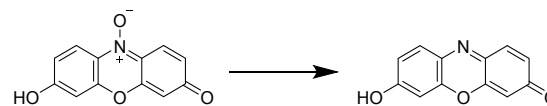


Figure 9 Schematic representation of the underlying reaction of the Alamar/PrestoBlue assay. Resazurin is reduced by viable cells to resorufin.

The MTT assay, MTS assay and WST-8 assay rely on the reduction of various tetrazolium dyes such as 3-(4,5-dimethylthiazol-2-yl)-2,5-diphenyltetrazolium bromide (MTT), (3-(4,5-dimethylthiazol-2-yl)-5-(3-carboxymethoxyphenyl)-2-(4-sulfophenyl)-2H-tetrazolium) (MTS) or (2-(2-methoxy-4-nitrophenyl)-3-(4-nitrophenyl)-5-(2,4-disulfophenyl)-2H-tetrazolium) (WST-8) to the corresponding formazan (Figure 10).



## ARTICLE



Assay	R <sub>1</sub>	R <sub>2</sub>	R <sub>3</sub>	X <sup>+/-</sup>
MTT				Br <sup>-</sup>
MTS				
WST-8				Na <sup>+</sup>

Figure 10 Schematic representation of the underlying chemical reactions of the colorimetric assays which utilize the reduction of tetrazolium dyes such as 3-(4,5-dimethylthiazol-2-yl)-2,5-diphenyltetrazolium bromide (MTT), (3-(4,5-dimethylthiazol-2-yl)-5-(3-carboxymethoxyphenyl)-2-(4-sulfophenyl)-2H-tetrazolium) (MTS) or (2-(2-methoxy-4-nitrophenyl)-3-(4-nitrophenyl)-5-(2,4-disulfophenyl)-2H-tetrazolium) (WST-8) to the corresponding formazan.

For the qualitative assessment of bacterial and cellular immobilization on cryogels, a variety of different microscopy methods can be applied. This enables the observation of bacterial or cellular morphologies and their distribution among the sample. Most commonly, confocal laser scanning microscopy<sup>47, 59-61, 63, 95, 110, 113-115, 117, 121, 123, 127, 130, 136, 137</sup> or fluorescence microscopy<sup>63, 74</sup> are applied which require the staining of bacteria or cells and the gel matrix with fluorescent dyes prior to the actual investigation. In the following **Table 1** the most commonly used dyes for staining cellular cytoplasm or nuclei are summarized. Labeling of the gel matrix can be achieved by the use of polymerizable fluorescent monomers

such as rhodamine acrylate,<sup>47, 63</sup> or rhodamine-NHS modified methacrylated hyaluronic acid,<sup>115</sup> the functionalization of cryogels prior to the culture with peptides bearing fluorescence labels such as dansyl or pyrene<sup>59, 60</sup> or rhodamine NHS,<sup>114</sup> or the labeling of the gel surface after the culture with red fluorescent polystyrene microspheres (Fluospheres™).<sup>130, 137</sup> Bright-field microscopy or optical microscopy can be applied by the use of cresyl violet staining<sup>59, 60, 127</sup> or methylene blue staining,<sup>67</sup> respectively. In contrast, scanning electron microscopy allows for the visualization of bacterial and cellular morphologies within the cryogel matrix without the need of a fluorescence label.<sup>47, 61, 110, 136</sup>

Cell type	Cytoplasm staining	Nuclei staining	Gel fluorescence	Ref.
Mameliella CS4, Marinobacter CS1	Individual staining with NIR680 and DAPI		Rhodamine acrylate as comonomer	47
PC-12 rat pheochromacytoma cells, NIH 3T3 mouse embryonic fibroblasts	Celltracker Green CMFDA	DAPI	Peptide containing gel with dansyl labeling	59
Human skin fibroblasts, human umbilical vein endothelial cells	Phalloidin CruzFluor™ 647	DAPI	Peptide containing gel with dansyl or pyrene labeling	60
L929 fibroblasts	Celltracker Deepred	DAPI	Rhodamine acrylate as comonomer	63



Journal Name	ARTICLE			
Human tonsil-derived mesenchymal stem cells, human umbilical vein endothelial cells	AlexaFluor488 phalloidin	DAPI	/	View Article Online DOI: 10.1039/D4MH00315B
Murine breast cancer cells (NIH/4T1, CRL-2539)	AlexaFluor488 phalloidin	DAPI	Rhodamine –NHS prior to cell culture	114
Primary chondrocytes	AlexaFluor488 phalloidin	DAPI	Rhodamine-NHS coupling to amine-HA-MA monomer	115
Porcine chondrocytes	AlexaFluor488 rhodamine phalloidin	DAPI	/	121
Human dermal fibroblasts	AlexaFluor660 phalloidin	DAPI	/	110
Breast cancer cells (MCF-7)	Phalloidin	DAPI	/	136
Murine B16F10-OVA cells	Phalloidin	DAPI	/	123
Peripheral blood mononuclear cells	Calcein-AM		Fluospheres™ gel surface labeling after culture	137
PC-12 rat pheochromacytoma cells, SH-SY5Y human neuroblastoma cells	DAPI		Autofluorescence	127
3T3 mouse embryonic fibroblasts cells	AlexaFluor488-phalloidin	DAPI	/	135
Human aortic endothelial cells	AlexaFluor647-phalloidin	DAPI	/	120

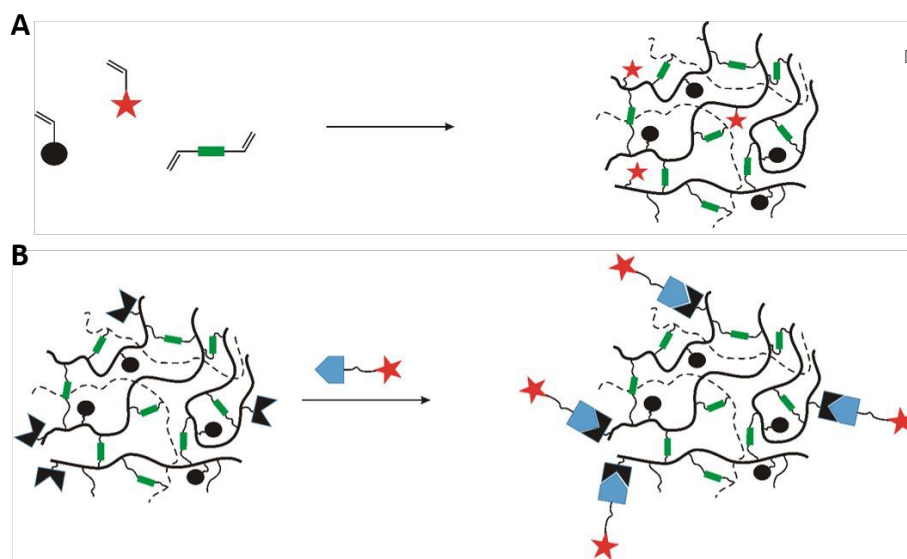
Table 1 Overview about different dyes applied for the morphological observation of bacteria and cells *via* confocal laser scanning microscopy.

### 3. Functional cryogels based on synthetic polymers

In recent years, there has been an increase in the use of synthetic polymers for the preparation of functional cryogels. In comparison with biopolymers, synthetic polymers exhibit favorable features such as their low cost and availability, as well as the possibility to tailor precisely their chemical structure. This

allows to obtain materials with well-defined properties. In the following section, the preparation of functionalized cryogels based on synthetic polymers and the proof of their functionalization will be discussed. Herein, recently emerging functional monomers for the preparation of cryogels by free radical cross-linking polymerization will be examined (**Figure 11A**). Additionally, the subsequent modification of synthetic polymer based cryogels with functional small molecules, biomolecules and biopolymers (**Figure 11B**) is also described.





View Article Online  
DOI: 10.1039/D4MH00315B

Figure 11 Schematic representation of the preparation of functionalized cryogels based on synthetic polymers using either free radical cross-linking polymerization of functional monomers (A) or *via* modification with small molecules, biomolecules and biopolymers (B).

### 3.1 Functional monomers

Within the last decade, a variety of functional monomers emerged as summarized in Table 2. This includes vinyl aromatic monomers such as vinylimidazole (VIm),<sup>54, 85, 87, 88</sup> 4-vinylpyridine (VP),<sup>90, 128</sup> 4-vinylphenylboronic acid (VPBA),<sup>94</sup> and *m*-acrylamidophenylboronic acid (AAPBA)<sup>138</sup> as well as (4-vinyl-benzyl)-*N*-methyl-D-glucamine (VBMG),<sup>104</sup> zwitter-ionic monomers such as sulfobetaine methacrylate (SBMA)<sup>91, 95</sup> or acrylamidopropyltrimethyl ammonium chloride (APTMACl),<sup>106</sup> or sulfonated monomers as sulfopropyl acrylate (SPA)<sup>108</sup> and sulfopropyl methacrylate (SPMA).<sup>128</sup> Furthermore, dimethylsulfoniopropionate-hydroxyethyl methacrylate ester (DMSP-HEMA),<sup>47</sup> 2-aminoethyl methacrylate hydrochloride (AEMA-HCl),<sup>97</sup> *N*-methacrylamido aspartic acid (Asp-MA),<sup>55</sup> lauryl acrylate,<sup>62</sup> oligo(poly(ethylene glycol)fumarate) (OPF)<sup>127</sup> or 2-(methacryloyloxy)ethyl trimethylammonium chloride (MAETAC)<sup>127</sup> were also used (Figure 12). The use of these new functional monomers allowed for the preparation of cryogel materials for the adsorption of heavy metal ions,<sup>87, 88, 104, 106</sup> proteins,<sup>54</sup> enzymes,<sup>85</sup> dyes,<sup>90, 91</sup> small molecules,<sup>55, 94</sup> bacterial capture<sup>47, 97</sup> or biomedical applications.<sup>95, 127, 128</sup>

Although it appears reasonable to determine the exact amount of incorporated functional monomer, the success of the functionalization is most commonly evaluated in a solely qualitative manner by the use of FTIR, NMR or Raman (Table 2). A few examples report the use of elemental analysis for the exact determination of the amount of functional monomer.<sup>54, 55, 139, 140</sup> For instance, the incorporation of 24.5 mg g<sup>-1</sup> VIm in p(VIm-HEMA) cryogels allowed for the adsorption of 21 mg g<sup>-1</sup> IgG whereas plain p(HEMA) cryogels adsorbed less than 1 mg g<sup>-1</sup>.<sup>54</sup> Besides the direct determination of functional monomer content by elemental analysis, the presence of characteristic signals at 1530 cm<sup>-1</sup> (ring C-H and C=N vibration) confirmed the presence of VIm in the cryogel.<sup>87</sup> p(VIm) cryogels demonstrated selective Cu<sup>2+</sup> adsorption in comparison with other metal ions such as Ni<sup>2+</sup>, Zn<sup>2+</sup>, Co<sup>2+</sup>, Pb<sup>2+</sup> and Cd<sup>2+</sup>.<sup>87</sup> 131.8 mg g<sup>-1</sup> Cu<sup>2+</sup> ions were adsorbed as determined by spectrophotometry, which was 2-4 times more compared to the other metal ions. Only in case of Cu<sup>2+</sup>, the entire metal ion content was completely adsorbed whereas the removal efficiencies for the other metal ions revealed lower values ranging from approx. 40 to 95%.



## ARTICLE

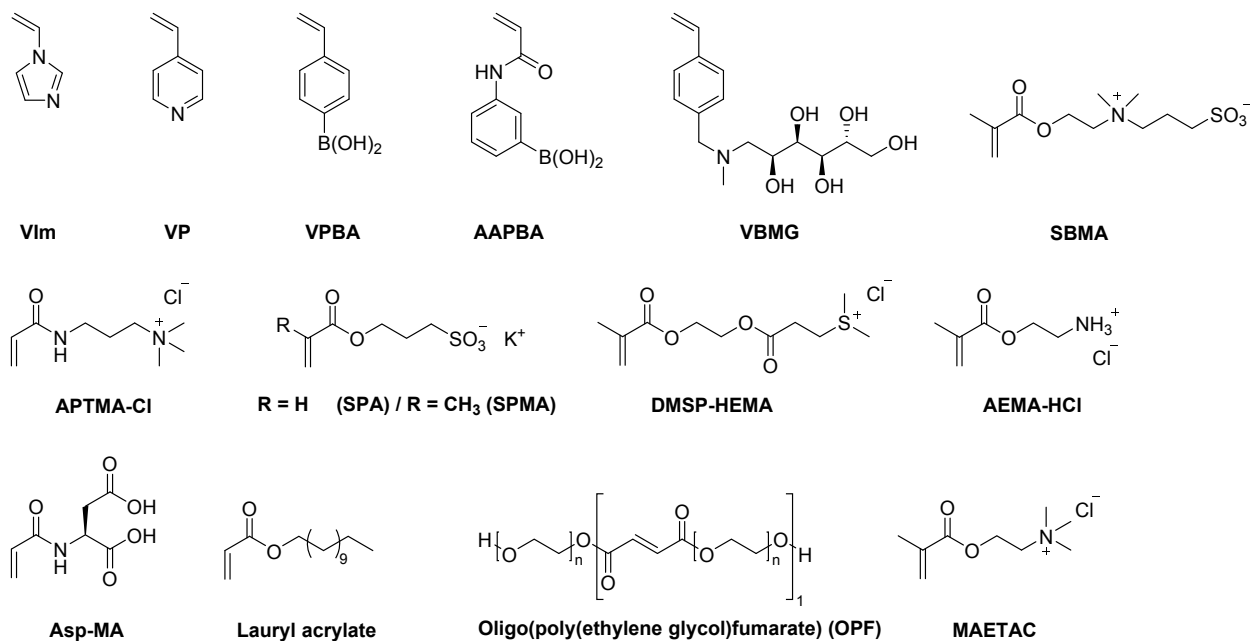


Figure 12 Schematic representation of recently emerging functional monomers used for the preparation of functional synthetic polymer based cryogels.



Table 2 Overview about synthetic polymer based cryogels using recently emerging functional monomers.

View Article Online

DOI: 10.1039/D4MH00315B

Composition	Proof of functionalization	Application	Proof of application	Ref.
VIm, HEMA, MBAAm	EA, FTIR	IgG adsorption	Spectrophotometry	54
		Laccase purification		85
VIm, MBAAm, (PEGDA)	FTIR	Adsorption of Cu <sup>2+</sup> , Ni <sup>2+</sup> , Zn <sup>2+</sup> , Co <sup>2+</sup> , Pb <sup>2+</sup> , Cd <sup>2+</sup>	Spectrophotometry	87
			XPS, EDX	88
VP, MAA, DMAAm, MBAAm		Removal of methylene blue		90
p(DMAAm-MABP-VPBA)	n/a	Dopamine capture and release	Spectrophotometry	94
p(AAm-AAPBA), p(AAm-AATris), MBAAm	<sup>1</sup> H NMR	Shape-memory cryogel	/	138
VBMG, HEMA, MBAAm	FTIR	Removal of As <sup>5+</sup> and Cr <sup>6+</sup>	ICP-MS	104
SBMA, TMBEMPA-Br		Dye adsorption	Spectrophotometry	91
SBMA, HEMA, EGDMA	n/a	Cancer immunotherapy	Spectrophotometry Live/dead staining (CLSM)	95
APTMA-Cl, MBAAm	FTIR	Removal of As <sup>5+</sup>	AAS	106
SPA, PEGDA	FTIR, Raman	Controlled dye release (BODIPY, Dil)	Fluorescence spectroscopy, CLSM	108
SPMA, VP, MBAAm	FTIR	Tissue engineering	MTS assay	128
DMSP-HEMA, MBAAm, DMAAm, ARhoB	ssNMR	Scaffold for marine bacterial culture	SEM, CLSM	47
AEMA-HCl, HEMA, MBAAm	n/a	<i>E. coli</i> capture	CFU analysis Spectrophotometry	97
Asp-MA, HEMA, EGDMA Cu <sup>2+</sup>	FTIR, EA OES	Adsorption of vit. B12	Spectrophotometry	55
Lauryl acrylate, EGDMA	FTIR	Sorption of oils and organic solvents	Gravimetric analysis	62
OPF, MAETAC, PEGDA		Neural tissue engineering	MTS assay, microscopy (bright-field, CLSM)	127

With PEGDA as additional cross-linker besides *N,N'*-methylenebisacrylamide, Hou *et al.* reported the simultaneous separation of oil-water mixtures and the adsorption of Cu<sup>2+</sup> at the same time by p(VIm) cryogels which might be advantageous for the treatment of toxic waste water.<sup>88</sup> The cryogel enabled the separation by preventing the oil layer from penetrating through the cryogel. The excellent removal of more than 95% of initial Cu<sup>2+</sup> ions from different oil-water mixtures containing benzene, toluene, diesel oil, cyclohexane or ethyl acetate were demonstrated.

Elemental analysis was applied to determine the amount of Asp-MA as functional ligand in p(Asp-MA-HEMA) cryogels for the adsorption of vitamin B12.<sup>55</sup> The content of Asp-MA in the cryogel discs was found to be 123.4 μmol g<sup>-1</sup>. Additionally, the presence of bands at 1073 cm<sup>-1</sup> (symmetrical C-N stretching) and 1449 cm<sup>-1</sup> (asymmetrical C-N stretching) confirmed the successful incorporation of Asp-MA in the cryogel networks. The subsequent immobilization of Cu<sup>2+</sup> was found to be 135.2 μmol g<sup>-1</sup> as determined by ICP-OES. The Cu<sup>2+</sup> functionalized p(Asp-MA-HEMA) discs were able to rapidly adsorb approx. 417 mg g<sup>-1</sup> of vitamin B12 within 10 min whereas plain

p(Asp-MA-HEMA) only revealed a B12 adsorption of less than 20 mg g<sup>-1</sup>. No loss in the adsorption capacity after four adsorption-desorption cycles was observed demonstrating the excellent reusability of these new types of cryogels. Desorption of vitamin B12 was achieved by the use of 1 M NaCl. Compared to other literature examples, this reported system exhibited a cost-effective and facile way for the adsorption of vitamin B12.

### 3.2 Functional cryogels via modification of synthetic polymer based cryogels

Besides the use of functional monomers bearing polymerizable groups, the subsequent modification of cryogels with plain, unmodified molecules of interest enables to introduce desired functionalities and/or properties. In contrary to functional monomers, they can be directly used without requiring chemical modifications, exhibiting a wider applicability to small functional molecules, biomolecules and biopolymers.

#### 3.2.1 Modification with small functional molecules

The functionalization of synthetic polymer based cryogels with small functional molecules such as tris(hydroxymethyl)aminomethane (Tris),<sup>81, 82</sup> iminodiacetic



acid (IDA),<sup>89, 99, 100</sup> *para*-amino benzoic acid (pABA),<sup>56</sup> *para*-amino pyridine (pAPyr),<sup>56</sup> nicotinamide,<sup>57</sup> *para*-amino benzenesulfonamide (pABSA)<sup>102</sup> or cibacron blue F3GA<sup>98</sup> is most commonly realized by the direct attachment towards reactive epoxide groups on cryogel surfaces (Table 3, Figure 13).

The subsequent incorporation of such functional molecules, as aforementioned allows for the adsorption of proteins,<sup>81, 82, 102</sup> enzymes<sup>81, 82, 102</sup> or metal ions.<sup>57, 89</sup> The immobilization of metal ions also enables the use for protein capture by immobilized metal-affinity chromatography (IMAC).<sup>56, 99, 100</sup>

**Table 3.** Modification of synthetic polymer based cryogels with small functional molecules *via* the direct coupling towards reactive epoxide groups on cryogel surfaces.

Composition	Modification	Coupling strategy	Proof of functionalization	Application	Proof of application	Ref.
AGE, AAm HEMA, MBAAm	Tris		Titrimetric method	Lysozyme binding	Spectrophotometry	82
AGE, AAm MBAAm			Gravimetric analysis		HPLC	81
GMA, HEMA MBAAm	IDA, Cu <sup>2+</sup> , Ca <sup>2+</sup> , Fe <sup>3+</sup>	Epoxide	FTIR, EDX	BSA and PPL adsorption	Spectrophotometry (Bradford method)	99
AGE, AAm MBAAm	IDA, Fe <sup>2+</sup> , Zn <sup>2+</sup> , Ni <sup>2+</sup> , Co <sup>2+</sup> , Cu <sup>2+</sup>		FTIR	BSA adsorption	Spectrophotometry (Bradford method)	100
AGE, PEGDA MBAAm	IDA		FTIR	Cu(II) removal	XPS, EDX Spectrophotometry	89
GMA, HEMA EGDMA	pABA/ pAPyr, Cu <sup>2+</sup> , Ag <sup>+</sup> , Zn <sup>2+</sup>		FTIR, EA ICP-OES	Insulin adsorption	Spectrophotometry	56
	NAA		FTIR, EA	Heavy metal adsorption	ICP-MS	57
AGE, AAm MBAAm	pABSA		FTIR	Lactoperoxidase adsorption	Spectrophotometry (Bradford method)	102
	Cibacron Blue F3GA			Adsorption of BSA	Spectrophotometry	98

Typically, allyl glycidyl ether (AGE) or glycidyl methacrylate (GMA) are used as functional monomers for the preparation of epoxide containing cryogels. For example, Tris was used as affinity ligand for the adsorption of lysozyme onto p(AGE-AAm) cryogels.<sup>81, 82</sup> The amount of immobilized Tris was either determined based on the epoxide group density or the mass differences of freeze-dried cryogels before and after the Tris functionalization. For the determination of the epoxide group density, the cryogels were treated with aqueous thiosulfate solution for 30 min at 30 °C. The nucleophilic epoxide ring-opening by the attacking thiosulfate anion resulted in the formation of a stoichiometric amount of hydroxide ions which were titrated with 0.1 M HCl for the indirect quantification of the epoxide groups. The amount of epoxide groups and thus, the amount of immobilized Tris was found to be 25 μmol g<sup>-1</sup> allowing for the adsorption of 360 mg g<sup>-1</sup> lysozyme. Aside from affinity ligands such as tryptophan, phenylalanine or histidine, this has been the highest reported amount of adsorbed lysozyme.

In recent years, the incorporation of IDA as affinity ligand for the adsorption of proteins by immobilized metal-affinity chromatography (IMAC)<sup>99, 100</sup> or the removal of Cu<sup>2+</sup> from wastewater treatment<sup>89</sup> has never been quantified. The

reaction of IDA with the cryogel epoxide groups within the last decade was typically confirmed by FTIR by the intensity decrease of the epoxide bands at 910 and 750 cm<sup>-1</sup> (C-O-C), the presence of a broad band at 3700 to 3200 cm<sup>-1</sup> (ring-opening of epoxide group) or the N-H bending vibration at 1500 cm<sup>-1</sup>. Among different metal ions tested by Wan *et al.* for IMAC, Cu<sup>2+</sup> exhibited the highest affinity to both porcine pancreatic lipase (PPL) and bovine serum albumine (BSA), with adsorption capacities of 150.14 mg g<sup>-1</sup> and 154.11 mg g<sup>-1</sup>, respectively.<sup>99</sup> Additionally, Nascimento *et al.* demonstrated the excellent reusability of p(AGE-AAm)-IDA-Cu<sup>2+</sup> cryogels for BSA adsorption as the adsorption capacity was still above 50 mg g<sup>-1</sup> after the fifth adsorption-desorption cycle.<sup>100</sup> Desorption of BSA was realized by the use of 0.2 M imidazole buffer.

For a potential application to remove Cu<sup>2+</sup> from wastewater, p(AGE) cryogels were functionalized with IDA.<sup>89</sup> With increasing amount of AGE monomer present in the cryogel, the amount of adsorbed Cu<sup>2+</sup> increased as well due to the increasing amount of IDA ligand. The Cu<sup>2+</sup> adsorption reached its maximum at pH 6 with an amount of 76.49 mg g<sup>-1</sup>. After five adsorption-desorption cycles, the adsorption capacity decreased to 57.85 mg g<sup>-1</sup> assigned to an incomplete desorption of Cu<sup>2+</sup> by the use of 1 M HCl.



## ARTICLE

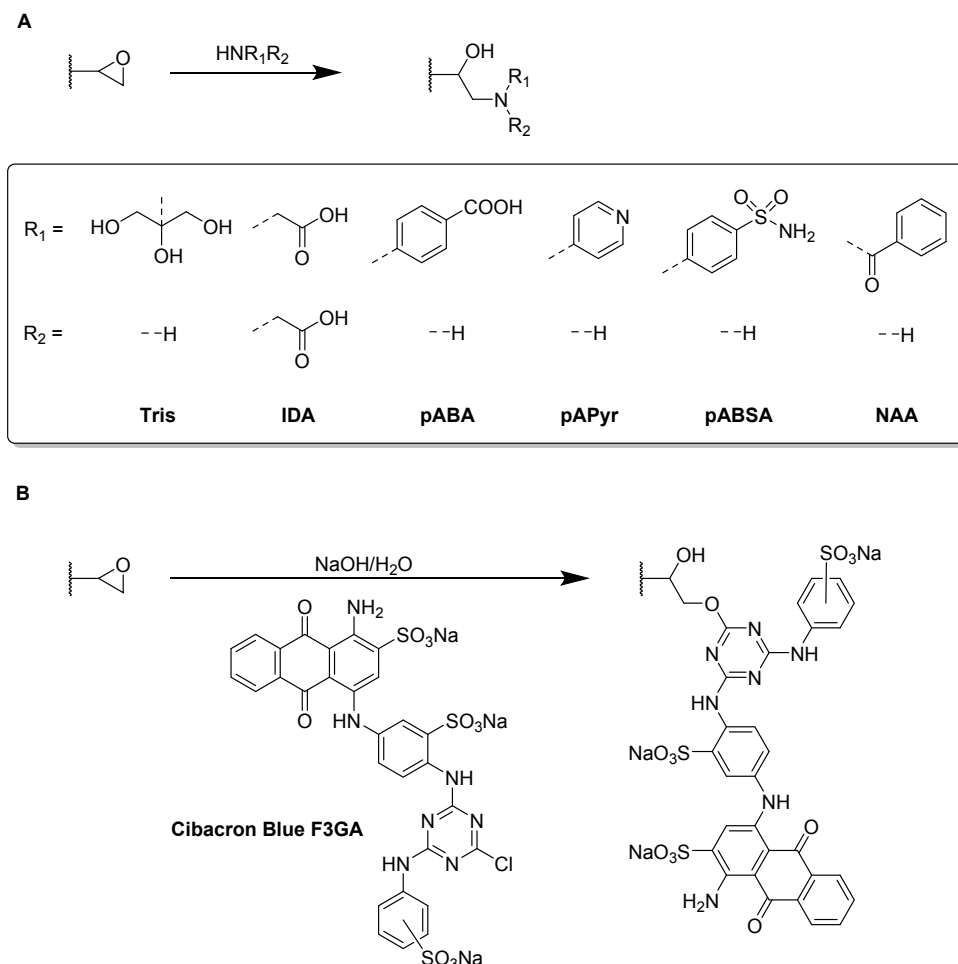


Figure 13 Schematic representation of the direct functionalization of synthetic polymer based cryogels with amine containing small functional molecules (A) such as tris(hydroxymethyl)aminomethane (Tris), iminodiacetic acid (IDA), para-amino benzoic acid (pABA), para-amino pyridine (pAPyr), para-amino benzenesulfonamide (pABSA) and nicotinamide (NAA), or cibacron blue F3GA (B) via the direct coupling towards epoxides on cryogel surfaces.

Nicotinamide was utilized as functionalization for the simultaneous adsorption of 15 different heavy metal ions.<sup>57</sup> Elemental analysis confirmed the successful ligand attachment of approx.  $1710.71 \mu\text{mol g}^{-1}$  nicotinamide onto p(GMA-HEMA) cryogels. The presence of bands in the FTIR spectrum at  $3367 \text{ cm}^{-1}$  (amide stretching) or  $1617 \text{ cm}^{-1}$  and  $1398 \text{ cm}^{-1}$  (aromatic -C=C- stretching) served as additional proof. By the incorporation of nicotinamide as coordinating ligand, a total amount of 687 mg heavy metal ions was adsorbed whereas unmodified p(GMA-HEMA) cryogels were only able to adsorb

387 mg. After five adsorption-desorption cycles in which 1 M NaCl was utilized for metal desorption no significant reduction of the adsorption capacities was observed.

Besides the direct coupling of small functional molecules by the reaction of amines with epoxide groups, a spacer or small molecule can react with the epoxides first introducing a different surface functionality (Table 4, Figure 14 and 15). This enables the use of a wider range of different molecules and modification strategies as this technique is not only limited to amine containing functional molecules.





Table 4 Modification of synthetic polymer based, epoxide-containing cryogels with small functional molecules by the use of different coupling strategies.

Composition	Modification	Coupling strategy	Proof of functionalization	Application	Proof of application	Ref.
AGE, AAm, MBAAm	Aniline	Amination of epoxides, GA	FTIR	Adsorption of BSA	Spectrophotometry (Bradford method)	101
	Enrofloxacin	Amination of epoxides, EDC/NHS	Habeeb assay ELISA	Biopanning of phages	Monoclonal phage ELISA	75
	Ethynyl ferrocene	Click chemistry	FTIR, EDX ICP	Redox-active cryogels	Cyclic voltammetry, differential pulse voltammetry	53
	Ethynyl pyrene		FTIR	Hg <sup>2+</sup> sensor	Fluorescence measurements	141
	PCAPBA		FTIR, EA	Capture of <i>E. coli</i> and <i>S. epidermidis</i>	Spectrophotometry	58

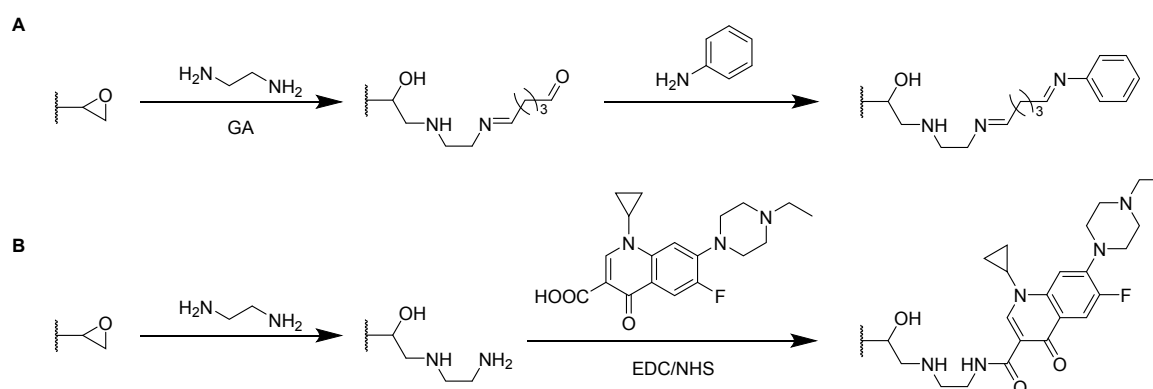


Figure 14 Schematic representation of the functionalization of synthetic polymer based cryogels with small functional molecules via coupling towards epoxides using an amine spacer either in combination with glutaraldehyde (GA) for the attachment of aniline (glutaraldehyde method (A)) or with EDC/NHS for the direct coupling of enrofloxacin (B).

By the use of a diamine spacer, such as ethylenediamine, the resulting amino-group bearing cryogel can be further modified with protein-affinity ligands such as aniline using glutaraldehyde (Figure 14A) or directly coupled to carboxylic acid containing drugs such as enrofloxacin by EDC/NHS chemistry (Figure 14B). An obvious advantage of the inclusion of spacer molecules might be the reduction of steric effects for the latter attachment of the molecule of interest which should theoretically result in a higher coupling efficiency, in particular when using large molecules such as biopolymers for the modification.<sup>142</sup> In case of the aniline functionalization, no quantification of ligand functionalization was carried out which could easily have been performed for instance by the use of the Kjeldahl method.

Zhang *et al.* described the preparation of enrofloxacin functionalized p(AGE-AAm) cryogels for phage biopanning.<sup>75</sup> After attachment of ethylenediamine, the amount of amino groups on the cryogel was qualitatively evaluated by the use of the Habeeb assay (TNBS assay). Unfortunately, the subsequent functionalization of the amine-modified cryogel with the drug using EDC/NHS chemistry was only qualitatively assessed indirectly by the use of an ELISA assay. The drug-coupled cryogel was herein treated with rabbit anti-enrofloxacin polyclonal antibody, followed by anti-rabbit/horseradish peroxidase IgG for antibody labeling. The assay is further based on the

peroxidase catalyzed transformation of a substrate such as tetramethylbenzidine in the presence of hydrogen peroxide into a colored compound, 3,3',5,5'-tetramethyl-[1,1'-bi(cyclohexylidene)]-2,2',5,5'-tetraene-4,4'-diimine, which can be detected by spectroscopy (Figure 8, Section 2.3).

Click chemistry represents an alternative strategy for the attachment of alkyne-carrying small functional ligands onto epoxide cryogels upon nucleophilic ring-opening with sodium azide. For instance, ethynyl ferrocene was covalently attached onto azide-modified p(AAm-AGE) cryogels in order to prepare redox-active materials (Figure 15A).<sup>53</sup> So far, ferrocene functionalization has only been realized by physical entrapment within cryogels rather than covalent attachment. FTIR confirmed the successful modifications by the presence of the azide band (2100 cm<sup>-1</sup>) and its disappearance after the click reaction with ethynyl ferrocene. The presence of 0.5 g Fe/100 g dry cryogel was determined by ICP after acidic cryogel digestion which was in accordance with EDX. EDX confirmed the homogenous distribution of Fe as well as the absence of entrapped copper from the click reaction. Cyclic voltammetry and differential pulse voltammetry indicated a well-defined quasi-reversible redox couple for the ferrocene functionalized gels, comparable to plain ferrocene. The electroactivity was retained even after 500 cycles demonstrating its long-term stability. In contrast, no electroactivity was observed in case of



epoxide-containing or azide-modified cryogel precursors. The attachment of ethynylpyrene onto azide modified p(AGE-AAm) cryogels allowed for the preparation of  $\text{Hg}^{2+}$  sensing materials,

although the functionalization was only qualitatively evaluated by FTIR.<sup>141</sup>

DOI: 10.1039/D4MH00315B

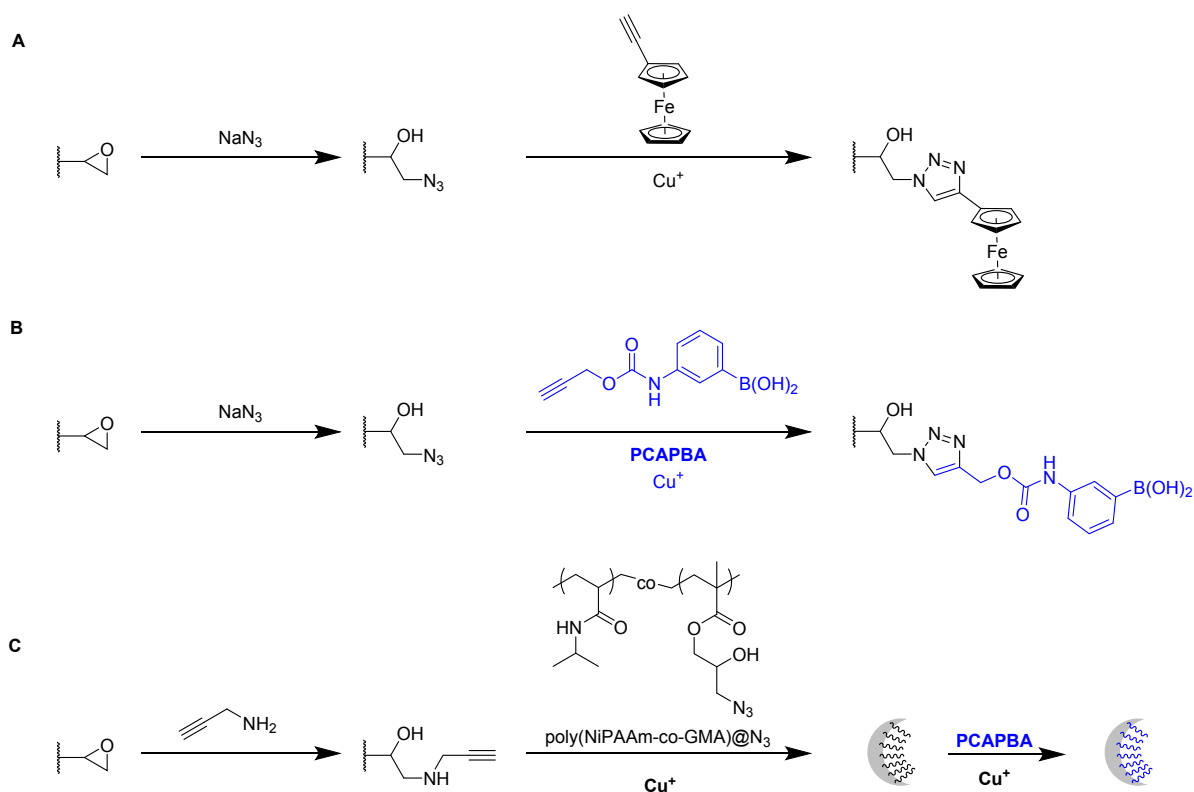
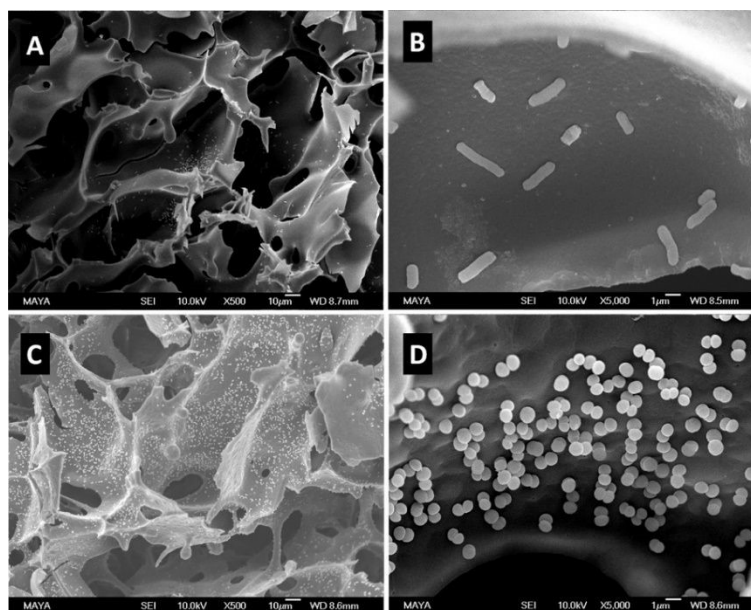


Figure 15 Schematic representation of the functionalization of synthetic polymer based cryogels with small functional molecules *via* click-chemistry upon the attachment of clickable azide (A, B) or alkyne moieties (C).

The attachment of 3-(prop-3-ynoxy carbonylamino)-phenylboronic acid (PCAPBA) for bacteria capture was quantified by elemental analysis according to the boron content.<sup>58</sup> 0.0031 mol  $\text{g}^{-1}$  PCABA were attached *via* Cu(I) catalyzed azide-alkyne cycloaddition onto azide modified p(AGE-AAm) cryogels (Figure 15B). In order to achieve a higher amount of functionalization, propargylamine treated p(AGE-AAm) cryogels were modified with an azide-tagged polymer, p(NiPAAm-co-GMA) $\text{@N}_3$  by click chemistry, prior to the functionalization with PCAPBA which was found to be 0.057 mmol  $\text{g}^{-1}$  (Figure 15C). The disappearance of the epoxide bands (875  $\text{cm}^{-1}$  and 910  $\text{cm}^{-1}$ ) together with the presence of azide (2037  $\text{cm}^{-1}$ ), alkyne (2100 to 2140  $\text{cm}^{-1}$ ) or phenyl hydrogen

signals (785  $\text{cm}^{-1}$  and 1065  $\text{cm}^{-1}$ ) in the FTIR spectra served as additional proof for the chemical transformations. The incorporation of PCAPBA enabled the adsorption of *S. epidermidis* and *E. coli* as gram-positive and gram-negative model bacteria (Figure 16). The number of adsorbed bacteria significantly increased compared to the corresponding azide precursors and also correlated with the functionalization amount of PCABA. In comparison with other separation materials utilizing nanoparticles, cryogels enable bacterial adsorption in a more convenient chromatographic mode. Similar binding capacities were obtained after three adsorption-desorption cycles in which bacterial desorption was realized with 0.5 M fructose in PBS buffer.





View Article Online  
DOI: 10.1039/D4MH00315B

Figure 16 SEM images of multiple boronic acid ligands containing cryogels with bound *E. coli* (A,B) and *S. epidermidis* (C,D) on. The scale bars are 10  $\mu\text{m}$  in (A,C) and 1  $\mu\text{m}$  in (B,D). Reproduced under terms of the CC-BY license with permission.<sup>58</sup> Copyright 2022, The Authors, published by the American Chemical Society.

Besides the direct functionalization of epoxides, a variety of further chemical reactions can be used to introduce desired functionalities which are summarized in Table 5.

Small functional molecules can be attached by direct reactions of amine-containing cryogels (Figure 17A),<sup>103</sup> amidoximation

(Figure 17B),<sup>105</sup> azo coupling (Figure 17C),<sup>86</sup> Hofmann rearrangement followed by GA treatment (Figure 17D)<sup>92</sup> and *via* thiol-maleimide click reaction (Figure 17E),<sup>111</sup> which allowed for the adsorption of metal ions,<sup>103, 105, 143</sup> enzymes,<sup>86</sup> proteins,<sup>111</sup> or dyes.<sup>92</sup> Unfortunately, the functionalization was only qualitatively evaluated, mostly by FTIR.

Table 5 Overview about of alternative coupling strategies for the subsequent modification of synthetic polymer based cryogels with small functional molecules.

Composition	Modification	Coupling strategy	Proof of functionalization	Application	Proof of application	Ref.
AllAm, MAAm, AA, MBAAm	Me-NCS	Reaction with amine groups		Removal of $\text{Pb}^{2+}$	ICP-OES	103
Acrylonitrile, AA, MBAAm	Hydroxylamine	Amidoximation	FTIR	Adsorption of $\text{Pb}^{2+}$	FTIR, XPS, EDX ICP-AES	105
MA-Tyr-OMe, HEMA, MBAAm	1-Naphthyl-amin	Azo coupling		Lysozyme capture	Spectrophotometry	86
AAM, MBAAm	bPEI	Hofmann rearrangement, GA	FTIR, ssNMR	Removal of remazol black B		92
FuMaMA or PEG-FuMaMA; PEGMeMA, PEGDMA	Biotin-SH	Thiol-maleimide click reaction	FTIR	Adsorption of TRITC-streptavidin	Fluorescence microscopy	111

The modification of p(AllAm-MAAm-AA) cryogels with methyl isothiocyanate enabled the adsorption of 164.41  $\text{mg g}^{-1}$   $\text{Pb}^{2+}$  ions superior to literature known systems such as biomaterial based adsorbents, composite materials or activated carbon (Figure 17A).<sup>103</sup> Simultaneous adsorption experiments of a mixture of metal ions ( $\text{As}^{3+}$ ,  $\text{Cd}^{2+}$ ,  $\text{Cr}^{6+}$ ,  $\text{Hg}^{2+}$ ,  $\text{Pb}^{2+}$ ) revealed a high selectivity for the adsorption of lead ions with removal efficiencies for the different metal ions (6.1%, 9.5%, 13.4%, 56.7% and 83.5% respectively).

The use of hydroxylamine as functionalizing ligand could even further increase the adsorption of  $\text{Pb}^{2+}$  as reported by Chen *et*

*al.* which resulted in a removal efficiency of 99.8% and an adsorption capacity of 650  $\text{mg g}^{-1}$  after 7 adsorption-desorption cycles (Figure 17B).<sup>105</sup> Desorption of  $\text{Pb}^{2+}$  ions from the cryogels was realized by the use of 1 M HCl. FTIR demonstrated the successful modification by a reduction of the  $\text{C}\equiv\text{N}$  stretching vibration ( $2240\text{ cm}^{-1}$ ) together with an increase of the signal at  $1654\text{ cm}^{-1}$ , dedicated to the  $\text{C}=\text{N}$  stretching vibration. A new band appeared at  $933\text{ cm}^{-1}$  assigned as the N-O stretching vibration.

1-Naphthylamin as hydrophobic ligand was attached to p(HEMA-MATyr-OMe) cryogels *via* diazotation (Figure 17C).<sup>86</sup> Specific bands in the IR spectra at  $1750\text{ cm}^{-1}$  (aromatic



substitution pattern) or at  $1400\text{ cm}^{-1}$  (skeletal C=C stretching vibration) confirmed the successful ligand functionalization. This enabled a 19.6 increase of the adsorption of lysozyme ( $105.8\text{ mg g}^{-1}$ , spectrophotometrically determined) in comparison with unfunctionalized p(HEMA-MATyr-OMe) cryogels. Among other examples in literature, this system exhibited the second highest amount of adsorbed lysozyme, besides an earlier work from the same group utilizing naphthylamine functionalized p(HEMA-MAHis) cryogels.<sup>144</sup> After 30 successive adsorption-desorption cycles, the adsorption capacity decreased only by 3% demonstrating the excellent reusability of the functionalized cryogels. Desorption of lysozyme was carried out by the use of 0.05 M of phosphate buffer (pH 7.0).

The successful modification of p(AAm) cryogels with PEI by Hofmann rearrangement and GA treatment was confirmed by FTIR and  $^{13}\text{C}$  solid-state NMR (ssNMR) (Figure 17D).<sup>92</sup> The appearance of new signals at  $2953\text{ cm}^{-1}$  and  $2863\text{ cm}^{-1}$  (C-H stretching) as well as at  $1560\text{ cm}^{-1}$  (N-H bending) confirmed the successful ligand coupling. This was in accordance with ssNMR which revealed the presence of new signals at 142.646 ppm and 156.601 ppm belonging to the imine groups. The cryogel exhibited a high adsorption capacity for Remazol black of  $201\text{ mg g}^{-1}$  as determined by spectrophotometry after 6 h with high removal rates of 98.42% whereas unmodified p(AAm) cryogels only exhibited dye removal capacities of 68%. In this regard, these materials were superior to most of the commonly used Remazol black adsorbents based on activated carbon or nanoparticles.

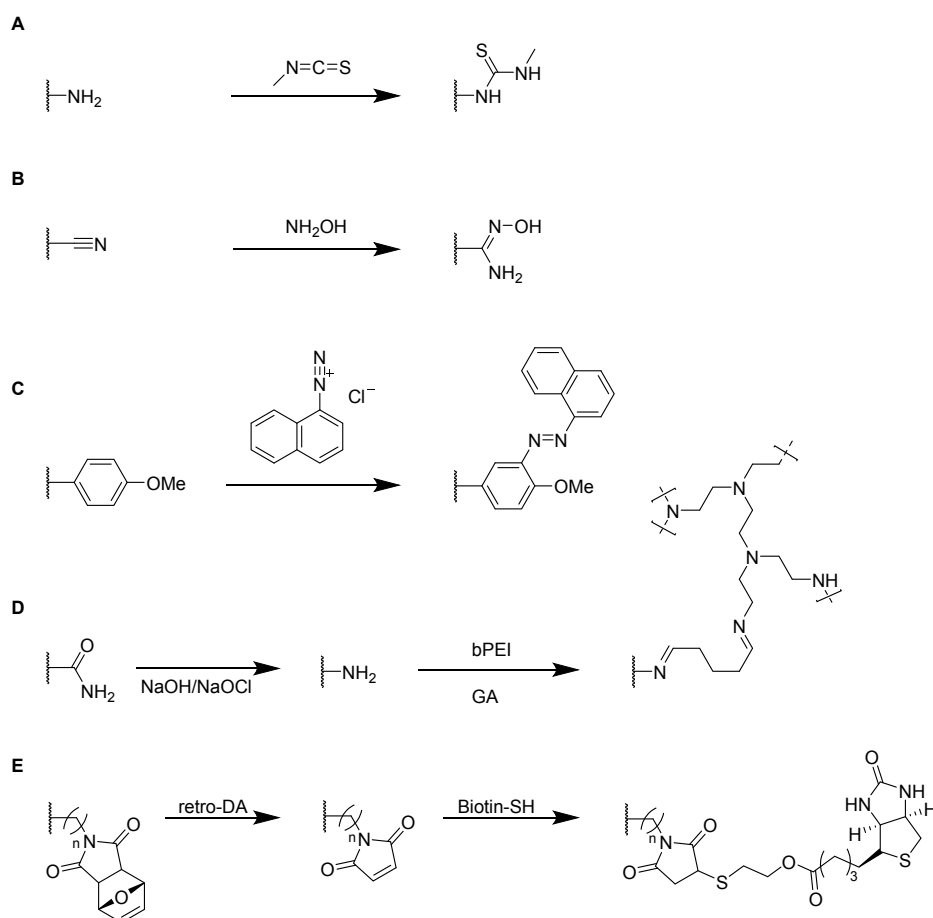


Figure 17 Schematic representation of alternative coupling strategies for the preparation of synthetic polymer based cryogels containing small functional molecules. Reaction of amine crygel surfaces with methyl isothiocyanate (A). Amidoximation of cryogels containing nitrile groups with hydroxylamine (B). Azo coupling of naphthalene diazonium chloride towards methyl tyrosine containing cryogels (C). Hofmann reaction of pAAm cryogels followed by the attachment of bPEI by glutaraldehyde (GA) (D). Thiol-maleimide click reaction for the introduction of biotin-thiol after retro-Diels Alder reaction (E).

In summary, small functional molecules are most commonly attached onto synthetic polymer based cryogels bearing epoxide groups in a direct manner or subsequently to the attachment of a diamine spacer or clickable group. The density of epoxide groups can be determined by a titrimetric method. The successful ligand

attachment can be quantified by gravimetry, elemental analysis or ICP upon acidic digestion. Alternative functionalization strategies are represented by the reaction with methyl isothiocyanate, hydroximation, azo coupling or thiol-maleimide click reactions. In



these cases, the successful modification was only qualitatively assessed by the use of FTIR and ssNMR.

### 3.2.2 Modification with biomolecules (sugars, amino acids, peptides)

Small biomolecules like sugar units or amino acids are most commonly attached to epoxide containing cryogel surfaces for the adsorption of proteins,<sup>64, 78</sup> enzymes<sup>77, 79</sup> or steroids.<sup>107</sup> Besides this, alternative methods rely on the use of click reactions<sup>111</sup>, EDC/NHS coupling<sup>52, 110</sup> or the attachment of functional ligands *via* host-guest interactions (Table 6, Figure 11 and 12).<sup>59, 60</sup>

Table 6 Overview about subsequent modification strategies of synthetic polymer based cryogels with biomolecules.

	Composition	Modification	Coupling strategy	Proof of functionalization	Application	Proof of application	Ref.
Sugars	FuMaMA or PEGFuMaMA, PEGMeMA, PEGDMA	Mannose-SH	Thiol-maleimide click reaction	FTIR	Adsorption of FITC-Con A	Fluorescence microscopy	111
	GMA, HEMA, MBAAm	$\beta$ -CD	Epoxide		Cholesterol removal	HPLC	107
		GlcNAc		Spectrophotometry (DNS method), FTIR	Lectin capture	Spectrophotometry (Bradford method)	64
Amino acids	AGE, AAm, MBAAm	Trp	Amination of epoxides, GA	Kjeldahl method, FTIR	Lysozyme adsorption	Spectrophotometry	77
		Trp, Phe			Protein binding	Spectrophotometry (Bradford method)	78
		Phe			Lysozyme adsorption		79
	AAm, MMA, MBAAm	Ac-Cys-OH			EDC/NHS	EDX, FTIR	Removal of Zn <sup>2+</sup> , Cd <sup>2+</sup> , Pb <sup>2+</sup>
Peptides	Acryloyl-CD, HEMA, PEGDA	Ada-Ahx-GGRGD, Ada-Ahx-GGGHK, (CuSO <sub>4</sub> , PEI)	Host-guest interaction	Fluorescence spectroscopy, CLSM, EDX, PEI probing	Cell culture scaffold, Synthetic ECM model	MTS assay, microscopy (bright-field, CLSM)	59, 60
	PEGDA	PLL	PAA graft, EDC/NHS	CLSM	GFP lentivirus delivery	SEM, CLSM, live/dead staining, Flow cytometry	110

Functional monomers like GMA or AGE are used to prepare epoxide-bearing cryogel surfaces to exploit their high reactivity towards subsequent modifications of the prepared cryogels. Besides the direct coupling with nucleophiles like  $\beta$ -cyclodextrin<sup>107</sup> (Figure 18B), diamine spacers such as 1,6-hexanediamine<sup>77-79</sup> or ethylenediamine<sup>64</sup> can react with the epoxide groups before the ligand is covalently attached by reductive amination using glutaraldehyde (Figure 18C). The formation of spacer arms enables the reduction of potential steric hindrance effects with the polymeric backbone.<sup>142</sup>

Apart from the qualitative evaluation of sugar functionalization by FTIR, da Silva *et al.* quantified the amount of immobilized *N*-acetyl glucosamine on p(AGE-AAm) cryogels spectrophotometrically by the use of the dinitrosalicylic acid method.<sup>64</sup> 160.39 mg g<sup>-1</sup> of *N*-acetyl glucosamine were attached which was the highest ever reported amount so far also enabling to adsorb 7.79 mg g<sup>-1</sup> lectin from a barley derived raw protein extract.

The functionalization of p(AGE-AAm) cryogels with nitrogen-containing ligands such as amino acids (Trp, Phe) can easily be quantified by the use of the Kjeldahl method.<sup>77-79</sup> Such modified cryogels were applied for the isolation of enzymes<sup>77, 79</sup> or proteins<sup>78</sup> by hydrophobic interaction chromatography. The functionalization of 380.51 mg g<sup>-1</sup> tryptophan (Trp) enabled the adsorption of 58.03 mg g<sup>-1</sup> lysozyme,<sup>77</sup> superior to previous systems based on p(HEMA-MATrp)<sup>145</sup> and p(HEMA-MAPhe).<sup>146</sup> Using a slightly higher initial ligand concentration for the functionalization, 458.65 mg g<sup>-1</sup> Phe were immobilized onto p(AGE-AAm) cryogels.<sup>79</sup> In this recent work, spectrophotometry was utilized to determine the density of cryogel epoxide groups. By the use of excess CuSO<sub>4</sub> solution, the gels were saturated with Cu<sup>2+</sup> ions which were eluted by complexation with EDTA. The amount of the eluted Cu<sup>2+</sup>-EDTA complex was found to be 369.17  $\mu$ mol g<sup>-1</sup>, as determined spectrophotometrically at 730 nm. The authors claimed that this amount is equimolar to the amount of epoxide groups. The higher amount of immobilized ligand resulted also in a higher amount of adsorbed lysozyme (67.65 mg g<sup>-1</sup>).



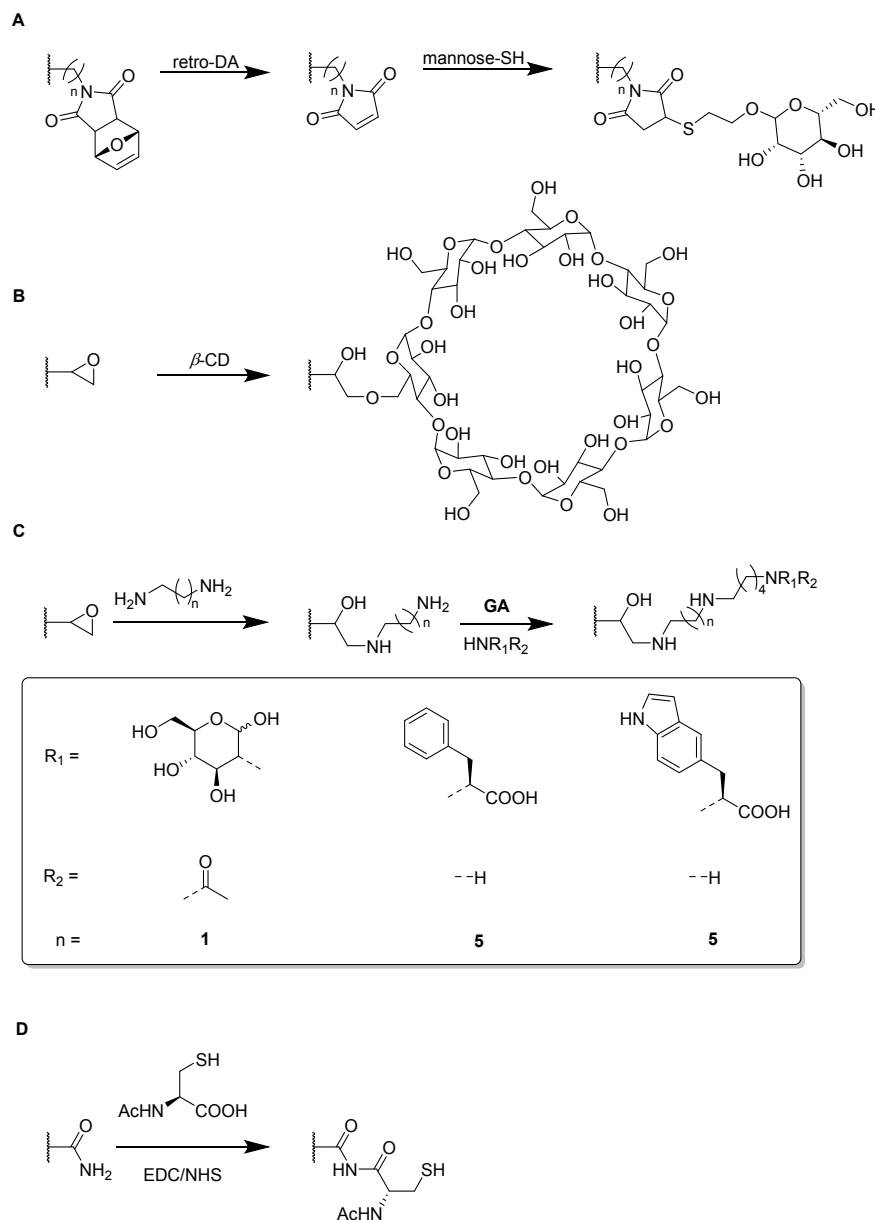


Figure 18 Schematic representation of various strategies for the functionalization of synthetic polymer based cryogels with sugars and amino acids. Thiol-maleimide click reaction for the introduction of mannose-thiol after retro-Diels Alder (retro-DA) reaction (A). Direct coupling of nucleophiles such as cyclodextrin (CD) to epoxide cryogel surfaces (B), coupling of nucleophiles using the glutaraldehyde method *via* spacer formation (C) and EDC/NHS coupling (D).

Both functionalizing ligands (Trp, Phe) were compared for the adsorption of *ora-pro-nobis* proteins.<sup>78</sup> The amounts of immobilized Trp and Phe were found to be lower as reported earlier, with about 128.01 mg g<sup>-1</sup> and 165.85 mg g<sup>-1</sup>, respectively. Although no explanation was given on such low ligand functionalizations, it might be assumed that this was due to the reduced amount of initial ligand concentration which was 5 mg mL<sup>-1</sup> instead of 8.225 mg mL<sup>-1</sup> for Trp or 10 mg mL<sup>-1</sup> for Phe as previously reported. The disappearance of the epoxide band (1242 cm<sup>-1</sup>),<sup>77</sup> together with the presence of the aromatic C=C stretching vibrations (1510 to 1542 cm<sup>-1</sup>),<sup>78</sup> and the carboxylic acid bands (1396 cm<sup>-1</sup> and 1716 cm<sup>-1</sup>) in the FTIR spectra also

confirmed the successful ligand attachment.<sup>78, 79</sup> The appearance of the band at 756 cm<sup>-1</sup> which is characteristic for Trp (pyrrole ring torsion vibration) served also as indication.<sup>77</sup> Phe functionalization enabled a higher protein adsorption with 92.53 mg g<sup>-1</sup> compared to Trp containing cryogels which exhibited a maximum adsorption capacity of 62.76 mg g<sup>-1</sup>.

EDC/NHS coupling was used to attach *N*-acetylated cysteine as coordinating ligand for the removal of heavy metal ions (Figure 18D).<sup>52</sup> The amount of immobilized ligand was determined by EDX considering sulfur stoichiometry which was



found to be  $180.88 \mu\text{mol g}^{-1}$ . This functionalization significantly increased the adsorption of heavy metals onto p(AAm-MMA) cryogels, with adsorption rates of 98.33% ( $\text{Zn}^{2+}$ ), 90.74% ( $\text{Cd}^{2+}$ )

and 96.19% ( $\text{Pb}^{2+}$ ) whereas unmodified p(AAm-MMA) cryogels removed less than 1% of each ion. DOI: 10.1039/D4MH00315B

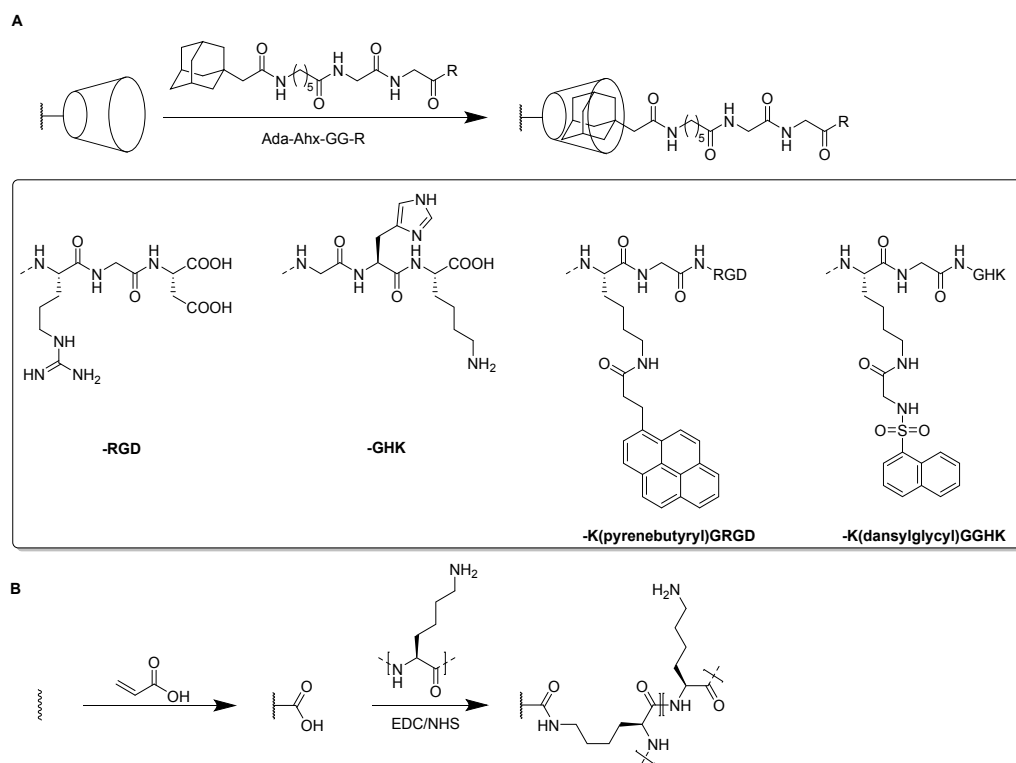


Figure 19 Schematic representation of various strategies for the functionalization of synthetic polymer based cryogels with peptides. Functionalization of  $\beta$ -CD containing cryogels via host-guest interaction with adamantyl-coupled peptide sequences (A). Introduction of acid groups by photo-induced graft polymerization followed by p(L-lysine) attachment (B).

For the introduction of peptides like RGD or GHK, host-guest interactions between adamantane and  $\beta$ -cyclodextrin can be exploited.<sup>59, 60</sup> Thus, cyclodextrin containing cryogels were prepared using acryloyl  $\beta$ -CD as functional monomer followed by the reaction with adamantane functionalized RGD and GHK peptide sequences (Figure 19A). Saturation of the CD groups on the cryogels with toluidine blue O followed by elution with methanol enabled their indirect quantification by spectrophotometry as the amount eluted dye would be equimolar to the number of CD groups. Fluorescence analysis revealed the successful peptide functionalization due to a three to five increase in the fluorescence signal which remained stable for 30 days. Both peptide sequences were found to increase the proliferation of 3T3 and PC-12 cells individually but the highest increases (four times each) were observed for a dual peptide functionalization of RGD and GHK present in the same cryogel (Figure 20). CLSM images of cross-sectioned peptide functionalized cryogel samples revealed an even distribution of peptides into deep areas of the gel slices.<sup>60</sup> With additional  $\text{Cu}^{2+}$  binding towards the GHK motif ( $1.92 \text{ wt}\%$  for  $0.18 \text{ mg mL}^{-1}$  GHK and  $3.79 \text{ wt}\%$  for  $0.36 \text{ mg mL}^{-1}$  GHK), human umbilical vein endothelial cells revealed different cellular morphologies and were more elongated (Figure 21). These gels demonstrated a significant upregulation of cytokines (MCP-1, IL6, IL8) as well as growth factors (VEGF, GF-2) indicating the stimulation of angiogenic cell differentiation for the first time.

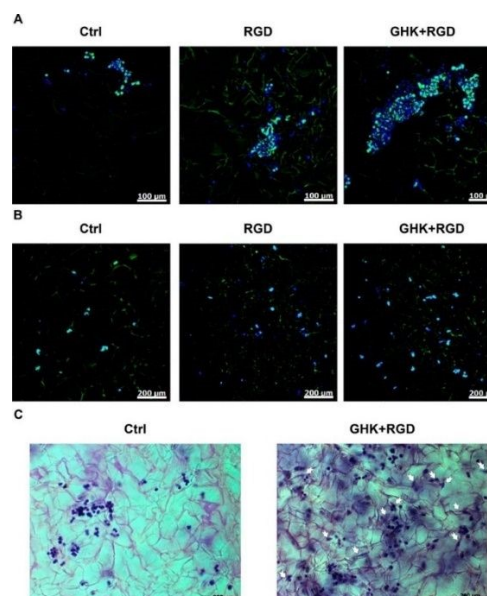


Figure 20 Microscopic visualization of 3T3 and PC-12 cells in peptide-functionalized cryogels at day 3. CLSM of 3T3 cells (A) and PC-12 cells (B). Bright-field microscopy of PC-12 cells (C). Arrows indicate some PC-12 cells with distinct morphological changes. The matrices were stained with Celltracker Green CMFDA and DAPI (CLSM) or cresyl violet (bright-field microscopy). Reproduced with permission.<sup>59</sup> Copyright 2019, American Chemical Society.



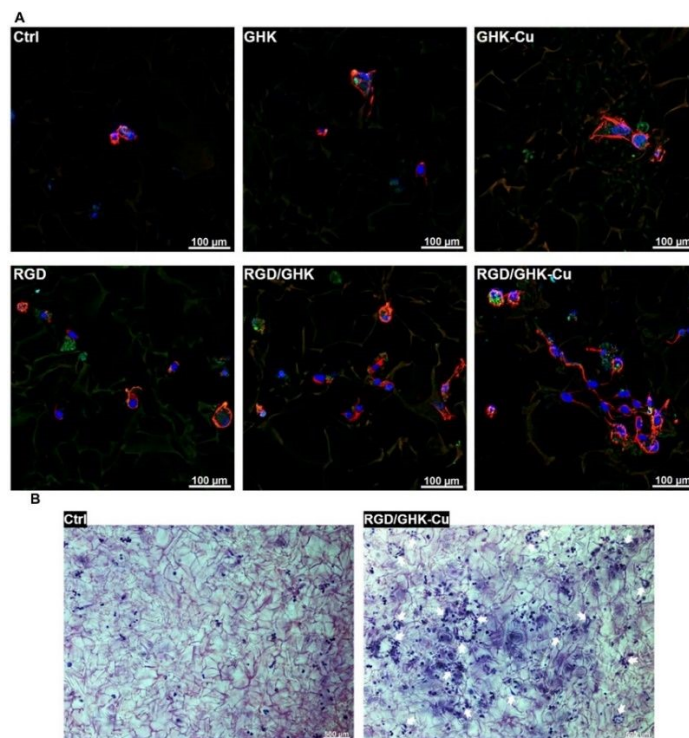


Figure 21 Representative CLSM images of HUVECs grown in peptide-functionalized pHEMA- $\beta$ -CD cryogels at 48 h post-seeding (A). Cells were stained with phalloidin CruzFluor™ 647 conjugate for F-actin (red) and DAPI for nuclei (blue). Representative bright-field microscopy images of HUVECs stained with cresyl violet at 48 h post-seeding in peptide free (Ctrl) and (RGD/GHK-Cu)-functionalized pHEMA- $\beta$ -CD cryogels (B). Reproduced with permission.<sup>60</sup> Copyright 2020, Elsevier B.V.

### 3.2.3 Modification with biopolymers

For the functionalization of cryogel surfaces with biopolymers, epoxide functionalities are commonly used as reactive binding sites (Table 7). Typically, glycidyl methacrylate (GMA) or epoxy hexene (EH) serve as functional monomers for the introduction

of reactive epoxide groups on cryogel surfaces. As for the functionalization with small molecules, biopolymers can either be attached directly to epoxide bearing cryogels (Figure 22A) or *via* amination followed by treatment with glutaraldehyde which acts as a spacer and connects the amine groups with the biopolymer (Figure 22B).

Table 7 Modification of synthetic polymer based cryogels with biopolymers *via* coupling towards reactive epoxide groups on cryogel surfaces.

Composition	Modification	Coupling strategy	Proof of functionalization	Application	Proof of application	Ref.
GMA, HEMA, MBAAm	Horseradish peroxidase	Epoxide	Pyridine-HCl method Spectrophotometry (Bradford method), FTIR	Dye degradation (Direct Blue-6)	Spectrophotometry GC-MS	66
	L-ASNase		Spectrophotometry (Bradford method) EDX, FTIR	Enzyme stability studies	Enzyme activity assay	49
EH, HEMA, MBAAm	Lysozyme		Spectrophotometry	Bacterial removal	Optical microscopy (methylene blue staining)	67
GMA, HEMA, EGDMA	Anti-transferrin		Spectrophotometry (Bradford method) FTIR, Raman	Purification of hTf	Spectrophotometry (Bradford method)	69
GMA EGDMA, MBAAm	ConA	Amination of epoxides, GA	Spectrophotometry EDX, FTIR	Adsorption of amyloglucosidase	Spectrophotometry	50

The covalent immobilization of biopolymers such as horseradish peroxidase, L-asparaginase, lysozyme, anti-transferrin or concanavalin A is most commonly indirectly quantified by spectrophotometry.<sup>49, 50, 66, 67, 69</sup> The presence of protein characteristic bands in the IR or Raman spectra for amide I

(1700 to 1600  $\text{cm}^{-1}$ , CO stretching), amide II (1510 to 1580  $\text{cm}^{-1}$ , C-N stretching, NH vibration) or amide III (1250 to 1350  $\text{cm}^{-1}$ ), or additional sulfur peaks in the EDX spectra<sup>49, 50</sup> further confirm the successful biopolymer modification.





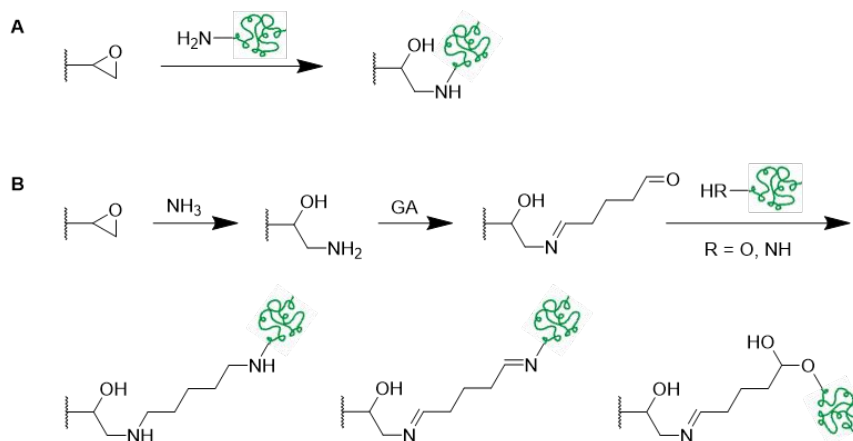


Figure 22 Schematic representation of functionalization strategies of synthetic polymer based cryogels with biopolymers *e.g.* enzymes and antibodies *via* direct coupling to epoxide surfaces (A) or using the glutaraldehyde method after amination of cryogel epoxide groups (B).

Horseshoe peroxidase (HRP) immobilization onto p(GMA-HEMA) cryogels enabled the development of materials for dye degradation.<sup>66</sup> Prior to the functionalization, the amount of cryogel epoxide was determined by the use of the pyridine-HCl method which was found to be 1.73 mmol g<sup>-1</sup>. The immobilization of 87.6 mg HRP per gram cryogel enabled an increased enzymatic stability among a wider range of pH values and temperature range and also revealed excellent long-term stability due to the preservation of 78% of its initial activity after eight weeks. The immobilized enzyme was able to degrade 98.5% of the dye Direct Blue-6 after 2 h, whereas in case of the free enzyme only 78.3% were degraded.

Similarly, Noma *et al.* investigated the stability of L-asparaginase immobilized onto p(GMA-HEMA).<sup>49</sup> 68.8% of the initially used enzyme was attached as determined by spectrophotometry. The immobilized enzyme revealed an improved stability in different media and at temperatures up to 70 °C in comparison with the free enzyme. After four weeks at 25 °C, 54% of the activity of the immobilized enzyme were still remaining whereas the activity of the free enzyme was found to be 28% by this time. Reusability investigations revealed 52% remaining activity of the immobilized enzyme after ten cycles. Gunay *et al.* reported the covalent immobilization of 43.56 mg g<sup>-1</sup> lysozyme onto p(EH-HEMA) cryogels for the first time while also studying the enzymatic stability and reusability of the system.<sup>67</sup> The cryogel was able to preserve 87% of the enzymatic activity after storage for 30 days at 4 °C. Optical microscopy revealed the antimicrobial activity of the immobilized lysozyme towards methylene blue stained bacteria (*Micrococcus lysodeikticus*) which lost their integrity resulting in a color decrease. These examples show that immobilization is significantly improving the enzymatic activity whilst also preserving its stability to harsher conditions such as high or low pH values or high temperatures. The excellent reusability and longtime storage was demonstrated which makes these systems very promising for biotechnological applications.

p(GMA-HEMA) cryogels were also modified with anti-transferrin antibody for the adsorption of human serum transferrin (hsTf).<sup>69</sup> The immobilization of 3.18 mg g<sup>-1</sup> anti-transferrin enabled the adsorption of 9.82 mg g<sup>-1</sup> hsTf after 60 min at pH 6 whereas the unspecific adsorption towards unmodified cryogels was negligibly low at all tested pH values. 80% of the adsorption capacity was still remaining after ten adsorption-desorption cycles, with desorption efficiencies of >88% after each cycle using glycine HCl as desorbing agent. Isolated hsTf from artificial plasma was obtained with 84% purity, as confirmed by FPLC and SDS-PAGE, and 82% yield after a contact time of only 7 min.

Recently, Con A was covalently attached onto p(GMA-HEMA) cryogels upon amination followed by glutaraldehyde treatment for the adsorption of amyloglucosidase (Figure 22B).<sup>50</sup> The amount of immobilized Con A was found to be 53.22 mg g<sup>-1</sup> as determined by spectrophotometry. The successful incorporation was further confirmed by the presence of sulfur peaks in the EDX spectrum and the presence of the characteristic amide I (1660 cm<sup>-1</sup>) and amide II (1530 cm<sup>-1</sup>) bands in the IR spectrum. Spectrophotometry revealed the maximum amount of adsorbed amyloglucosidase as 30.5 mg g<sup>-1</sup> at pH 5 and an initial enzyme concentration of 0.7 mg mL<sup>-1</sup>. 98.8% of the adsorbed enzyme were recovered by desorptive treatment with methyl α-D-mannopyranoside with 90% of its initial activity remaining. After 30 consecutive adsorption-desorption cycles, ConA-cryogel still retained 89% of its initial adsorption capacity which demonstrated the excellent reusability of this system.

Alternative strategies for the functionalization of synthetic polymer based cryogels with biopolymers such as horseradish peroxidase,<sup>51</sup> fibronectin<sup>63</sup>, heparin<sup>65</sup>, alginate,<sup>72</sup> RGD<sup>72</sup> or pectinase<sup>68</sup> include the use of EDC/NHS coupling (Figure 23A and 23B),<sup>51, 63</sup> the activation of hydroxy groups using cyanogen



bromide (CNBr) (Figure 23C)<sup>65, 72</sup> or by amino-yne click reaction (Figure 23D) (Table 8).

View Article Online  
DOI: 10.1039/D4MH00315B

Table 8 Overview about of alternative coupling strategies for the subsequent modification of synthetic polymer based cryogels with biopolymers.

Composition	Modification	Coupling strategy	Proof of functionalization	Application	Proof of application	Ref.
AAm, MBAAm	Horseradish peroxidase	EDC/NHS	Spectrophotometry EDX, FTIR	Removal of phenolic compounds	Spectrophotometry	51
AES, MAG DMAAm MBAAm ARhoB	Fibronectin-FITC	EDC/NHS	Fluorescence spectroscopy	3D cell culture of L929 cells	CLSM, fluorescence microscopy	63
HEMA, MBAAm	Heparin	CNBr activation	Spectrophotometry FTIR	Cholesterol removal	Homogenous enzymatic colorimetric assay	65
HEMA, MBAAm or PEGDA	i) Alginate ii) RGD	i) Glutar-aldehyde ii) CNBr activation	FTIR Spectrophotometry	Bioartificial liver	Live/dead assay, MTT assay	72
PEI, PEGDGE	Propiolate pectinase	Amino-yne click reaction	Bradford assay	Enzyme stability studies	Enzyme activity assay	68

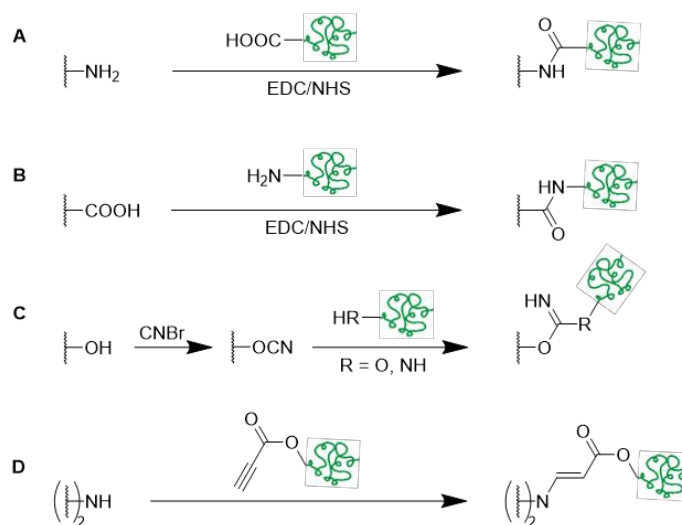


Figure 23 Schematic representation of alternative functionalization strategies of synthetic polymer based cryogels with biopolymers *e.g.* enzymes, proteins and polysaccharides via EDC coupling (A and B), cyanogen bromide activation (C) of cryogel hydroxy groups or using amino-yne click reaction (D).

For example, p(AAm) cryogels were functionalized with peroxidase by EDC/NHS coupling in order to remove phenolic compounds (Figure 23A).<sup>51</sup> 127.30 mg g<sup>-1</sup> peroxidase were immobilized as determined by spectrophotometry at 280 nm which was further confirmed by the presence of characteristic enzyme signals in the IR spectrum (1650 cm<sup>-1</sup>, amide I, CO stretching; 1550 to 1530 cm<sup>-1</sup>, amide II, N-H bending and C-N stretching), together with the presence of sulfur and iron peaks in the EDX spectrum. The immobilization helped to preserve the enzymatic activity after high temperature treatment *e.g.* by maintaining 58% of the initial activity after 5 h at 55 °C. After ten successive tests at 25 °C, the immobilized enzyme demonstrated 68% of its initial activity which is superior to the reported loss of 50% activity after the fifth reuse of peroxidase immobilized chitosan-holloysite hybrid nanotubes by Zhai *et al.*<sup>147</sup> Among five tested model phenolics (guaiacol, phenol, pyrogallol, bisphenol A, catechol) the engineered cryogel revealed excellent phenol removal capacities with 79.66%, 96.32%, 64.94%, 75.8% and 70.98%, respectively.

An alternative strategy for the covalent immobilization of biopolymers utilizes cyanogen bromide as activation agent of p(HEMA) cryogels designed to remove low-density lipoprotein-cholesterol (LDL-C) from hypercholesterolemic human plasma (Figure 23C).<sup>65</sup> The amount of immobilized heparin determined by spectrophotometry correlated with increasing incubation time and initial heparin concentration and was found to be 35.42 mg g<sup>-1</sup> using optimized conditions. Non-covalent immobilization was negligible with an amount of 0.94 mg g<sup>-1</sup> when using non-activated p(HEMA) cryogels. Heparin modification enabled the adsorption of 26.7 mg g<sup>-1</sup> LDL-C from human plasma whereas only 1.67 mg g<sup>-1</sup> were adsorbed onto unmodified p(HEMA) cryogels. No significant losses of the adsorption capacity and desorption ratio were observed after ten adsorption-desorption cycles when using 0.04 M citric acid and 0.02 M dibasic sodium phosphate as desorbing agent. Compared to immunoaffinity chromatography utilizing expensive antibody functionalization, or molecular imprinting, which might be limited when using biomacromolecules due to



their structure, size and conformational stability, the reported cryogel system demonstrated its superiority.

Amino-yne click reaction enabled the covalent immobilization of propionic acid-modified pectinase onto PEI cryogels with high immobilization efficiencies of 88% to 90% as determined by the Bradford assay (Figure 23D).<sup>68</sup> Presence of the characteristic band for triple bonds at  $2327\text{ cm}^{-1}$  confirmed the successful pectinase modification. Cryogel immobilization enabled improved enzymatic stability at higher temperatures and a wider range of pH values by preserving its maximum activity at pH 6.5 and  $55\text{ }^{\circ}\text{C}$ . The storage stability was also improved, as the immobilized enzyme still retained 71% of its activity after 60 days which was almost double the amount compared to the free enzyme after the same time.

In brief, biopolymers are most commonly attached to synthetic polymer based cryogels bearing epoxide groups directly or *via* amination followed by glutaraldehyde treatment and reductive amination. Alternative synthetic strategies include EDC/NHS coupling, cyanogen bromide activation or amino-yne click

reactions. For all modification methods, spectrophotometry typically enables the quantification of the cryogel functionalization.

#### 4. Functional cryogels based on biopolymers

In comparison with synthetic polymers, biopolymers offer a wide range of advantages such as their excellent biocompatibility, high bioactivity and low toxicity. In particular for biological applications, biopolymers are highly favorable since they are commonly part of natural extracellular matrices and exhibit cell-adhesive domains. The preparation of functional biopolymer based cryogels can be realized using modified functional biopolymers for radical cross-linking polymerization (Figure 24A), by cross-linking of functional biopolymers (Figure 24B) or *via* the subsequent modification of biopolymer networks with functional biopolymers (Figure 24C) (Table 9 and 10).

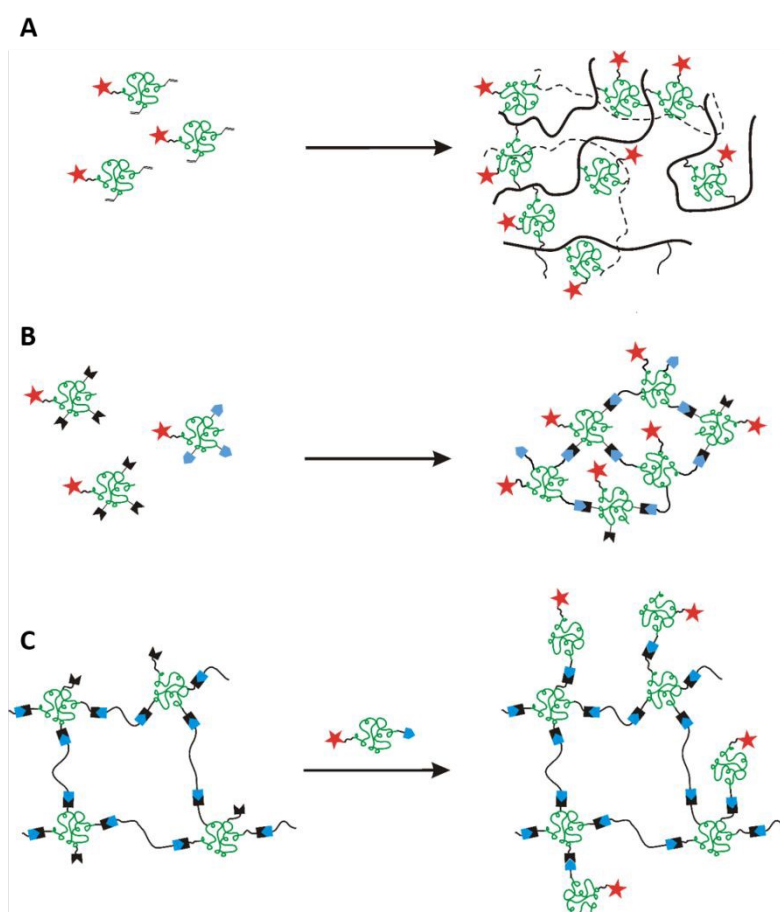


Figure 24 Schematic representation of different strategies for the preparation of functional biopolymer based cryogels. Functionalities of interest (red stars) are incorporated by cross-linking polymerization of macromonomeric precursors bearing functional groups (A), cross-linking of functional biopolymers (B) or the subsequent modification of biopolymer based cryogels with functional biopolymers (C).



Table 9 Overview about the preparation of biopolymer based cryogels by functional polymerizable macromonomers (Figure 24A).

View Article Online

DOI: 10.1039/D4MH00315B

Composition	Biopolymer	Special features/ Proof of functionalization	Application	Proof of application	Ref.
KefMA	Methacrylated kefiran	Biocompatible, elastic, robust	Tissue engineering	Alamar blue assay	116
GelMA, GelUPY	Modified gelatin	Degradable, shape recovery	Osteochondral regeneration	WST-8 assay fluorescence microscopy	74
HA-MA	Methacrylated hyaluronic acid	Shape-memory	Gene delivery for tissue engineering	CLSM, RT-PCR, histological and immunochemical analysis	148
GelMA, HA-MA	Methacrylated gelatin, methacrylated hyaluronic acid	Mechanically robust, cell-responsive, injectable	Tissue engineering	Fixable dead cell assay	135
GelMA + HA-MA/CS-MA	Methacrylated gelatin, methacrylated hyaluronic acid or chondroitin sulfate	Supporting formation of cartilage tissue	Cartilage tissue engineering	Live/dead staining	131
GelMA, Dex-MA	Methacrylated gelatin, methacrylated dextran	Shape recovery, compression resistant	Tissue regeneration	AlamarBlue assay	118
Dex-MA/HA-MA	Methacrylated dextran or hyaluronic acid	Prepared by electron-beam assisted cross-linking	Tissue regeneration	Live/dead staining	134
EPL-A, GCMA	Methacrylated glycol chitosan, acrylated p( $\epsilon$ -L-lysine)	/	Antibacterial wound dressing	Histological imaging, MTT assay	124

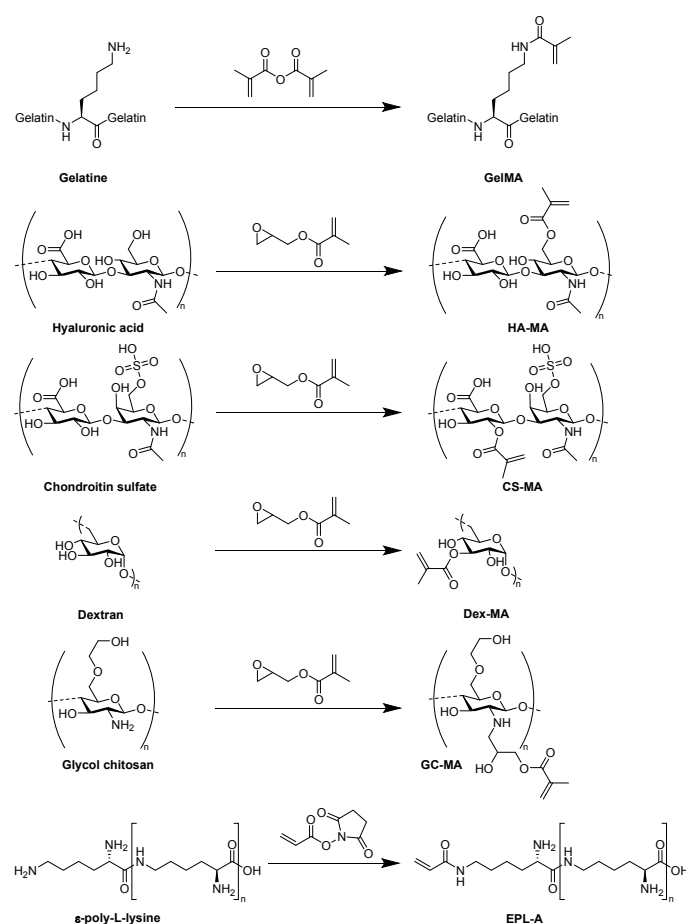


Figure 25 Schematic representation of the synthesis of modified biopolymers for the preparation of functional biopolymer based cryogels. The chemical structures are presented as proposed by the respective authors, except for dextran.

The chemical modification of biopolymers such as kefiran,<sup>116</sup> hyaluronic acid,<sup>131, 134, 135, 148</sup> chondroitin sulfate,<sup>131</sup> dextran,<sup>118, 134</sup> glycol chitosan,<sup>124</sup> gelatin<sup>74, 118, 131, 135</sup> or  $\epsilon$ -poly-L-lysine<sup>124</sup> by the incorporation of polymerizable units enables a facile/simplified preparation of cryogels. The macromonomeric precursors can subsequently be polymerized *via* free radical cross-linking polymerization at sub-zero temperatures. Typically, methacrylic anhydride or glycidyl methacrylate are utilized for biopolymer modification (Figure 25).

In a few cases, the degree of methacrylation is determined by <sup>1</sup>H NMR,<sup>135, 148</sup> by the use of an internal standard,<sup>116, 118</sup> or using the Habeeb assay.<sup>74</sup> Unfortunately, the successful incorporation of the functional precursors into the cryogel was not evaluated. Radhouani *et al.* reported recently the preparation of cryogels based on methacrylated kefiran for tissue engineering applications for the first time.<sup>116</sup> Culture experiments with L929 cells revealed no significant cytotoxicity of the kefiran cryogel according to the AlamarBlue assay. Thus, it was demonstrated, that the modification of kefiran by the attachment of the methacryloyl group didn't change the biocompatibility of the material.

Another recent example for the preparation of functional biopolymer based cryogels *via* cross-linking polymerization is given by Wu *et al.* who utilized different modified gelatin derivatives, namely methacrylated gelatin (GelMA) and 2-ureido-4[1H]-6-methyl-pyrimidinone functionalized gelatin (GelUPY) to create materials for osteochondral regeneration (Figure 26).<sup>74</sup>



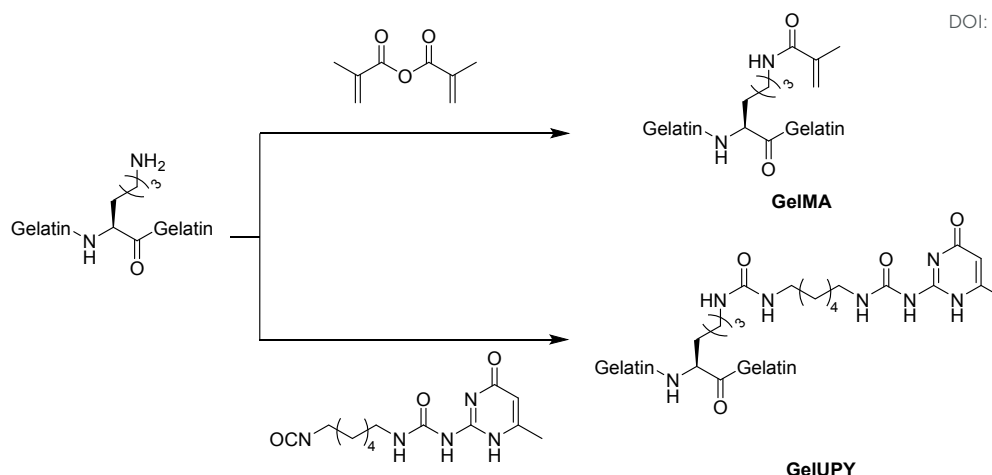


Figure 26 Schematic representation of two modified gelatin-based macromonomers: Methacrylated gelatin (**GelMA**) and 2-ureido-4[1H]-6-methyl-pyrimidinone functionalized gelatin (**GelUPY**).

The prepared GelMA/GelUPY gels were able to recover their shape after compression and exhibited an enhanced toughness in comparison to sole GelMA gels, due to additional non-covalent cross-linking through hydrogen bond formation of the UPY moieties. No significant cytotoxic effects towards SW1353 cells were observed according to the WST-8 assay. The successful cellular migration into the gel was confirmed by fluorescence microscopy after Hoechst staining of the nuclei. *In vivo* experiments revealed the capability of the gels for tissue regeneration in rabbit knees.

Cryogels consisting of methacrylated dextran and methacrylated hyaluronic acid were prepared the first time using electron-beam initiated cross-linking which up until this point had not been applied for the initiator and cross-linker free preparation of polysaccharide cryogels.<sup>134</sup> Stable materials were obtained after short reaction times (10 min) with pore sizes in the range of 70  $\mu\text{m}$  in average as observed by SEM. The excellent cytocompatibility was demonstrated by live/dead staining in combination with CLSM upon seeding 3T3 mouse fibroblast cells.

Table 10 Overview about the preparation of biopolymer based cryogels by cross-linking of functional biopolymers (**Figure 24B**) or *via* subsequent modification of biopolymer based cryogels (**Figure 24C**).

Composition	Biopolymer/ Functionalization	Special features/ Proof of functionalization	Application	Proof of application	Ref.
HA, EGDGE	Hyaluronic acid	Systemic study	Tissue engineering	n/a	149
GELox, HAa, ox-PHSRN-RGDSP	Gelatin-oxyamine, hyaluronan-aldehyde	Artificial tumor micro- environment	Macrophage culture	CLSM Live/dead staining	130, 137
HA-Tz, HA-Nb	Hyaluronic acid modified with tetrazine (Tz) and norbornene (Nb)	Biodegradable, immune- responsive	Vaccine delivery, neutrophil regeneration	Micro BCA, OliGreen Assay, flow cytometry	150, 151
Carboxymethyl cellulose	Laminin, collagen IV, fibronectin	Fluorescence spectroscopy	Neural transplantation	Alamar blue assay Live/dead staining CLSM	117
Albumin-MA	Collagen I, fibronectin	FTIR, immunofluorescence microscopy	3D cell culture and drug screening	Live/dead staining WST-8 assay SEM	61

Functionalized biopolymer-based cryogels can also be obtained by the cross-linking of functional biopolymers at temperatures below the freezing point of the reaction solvent, so called cryo-cross-linking. These cryogels can be applied for the controlled delivery of bioactive compounds<sup>152</sup> or vaccines,<sup>151</sup> as tissue engineering scaffolds<sup>149, 150</sup> or as materials for macrophage culture.<sup>130, 137</sup> For the investigation of the local elastic and viscous gel properties which directly influence cellular

adhesion, morphology, migration and proliferation, multiple particle tracking based optical microrheology represents a helpful tool recently reported by Oelschlaeger *et al.*<sup>149</sup> Herein, the movement of green fluorescent polystyrene microspheres through hyaluronic acid based cryogels was tracked, which were either injected into the gel or included in the initial gel preparing solution before freezing. The promising results of this study strongly suggest these cryogels as potential tissue



engineering materials. Cross-linking of modified biopolymers by click chemistry represents an interesting synthetic strategy in the preparation of functionalized cryogels. The utilization of oxime click chemistry enabled the preparation of gelatin-hyaluronic acid based cryogels as model materials for the investigation of tumor-associated macrophage invasion.<sup>130</sup> As precursors, gelatin-oxymamine (GELox), hyaluronan-aldehyde (HAa) and an oxyamin-modified, fibronectin derived peptide sequence (oxHSRN-RGSP) for enhanced cellular adhesion were utilized (**Figure 27** and **28**). Biopolymer modification with clickable groups was evaluated by <sup>1</sup>H NMR using an internal standard, DOSY NMR and ESI-MS. Pore size distributions became narrower and were shifted to lower pore sizes when increasing the HAa content in the gel formulations. A significantly higher number of CD14<sup>+</sup> macrophages in deeper gel regions was observed in case of cryogels with the least HAa content. Incorporation of ox-PHSRN-RGDSP revealed a significant increase in the cellular invasion from 13.0 ± 9.2 μm to 27.1 ± 8.7 μm. Unlike commonly applied Matrigel or collagen I based scaffolds, the cryogel system contains the two most abundant components of natural tumor microenvironments and exhibits excellent tunability. Accordingly, it represents a promising candidate to fill the gap for the targeting of macrophage infiltration and polarization. In a more recent study, the same cryogel system was used to model the invasion of tumor-associated macrophages in Hodgkin lymphoma and for the targeted screening of potentially anti-invasive drugs for

the very first time.<sup>137</sup> Among 25 drugs tested, marimastat, batimastat, AS1517499, PD-169316 and paxlitinib significantly reduced macrophage invasion. Additionally, a platform for the rapid and high-content evaluation of dose response invasion assays was created which enabled high reproducibility and also demonstrated the scalability of the assay.

Biodegradable, injectable cryogels have recently been prepared by click chemistry utilizing norbornene and triazine modified hyaluronic acid precursors, for neutrophil regeneration (**Figure 29**).<sup>150, 151</sup> Functionalization of the carboxylic acid groups with benzylamino tetrazine or norbornene methylamine was realized by the use of EDC/NHS. The interconnectedness of the cryogel pores was demonstrated by CLSM after incubation with FITC labelled melamine resin particles which remained unchanged even after the injection. 1 μg of Cy5 labelled granulocyte colony stimulating factor (GCSF) was encapsulated into the cryogels.<sup>150</sup> IVIS fluorescence microscopy revealed a sustained release of GCSF from implanted cryogels into mice tissue of 20% after 12 days which enabled a higher peripheral blood neutrophil concentration. The simultaneous delivery of ovalbumin, granulocyte macrophage-colony stimulating factor and CpG-ODN 1826 from this cryogel system for the treatment of murine cancer enabled a significant reduction of the tumor growth rate with increased survival times.<sup>151</sup>

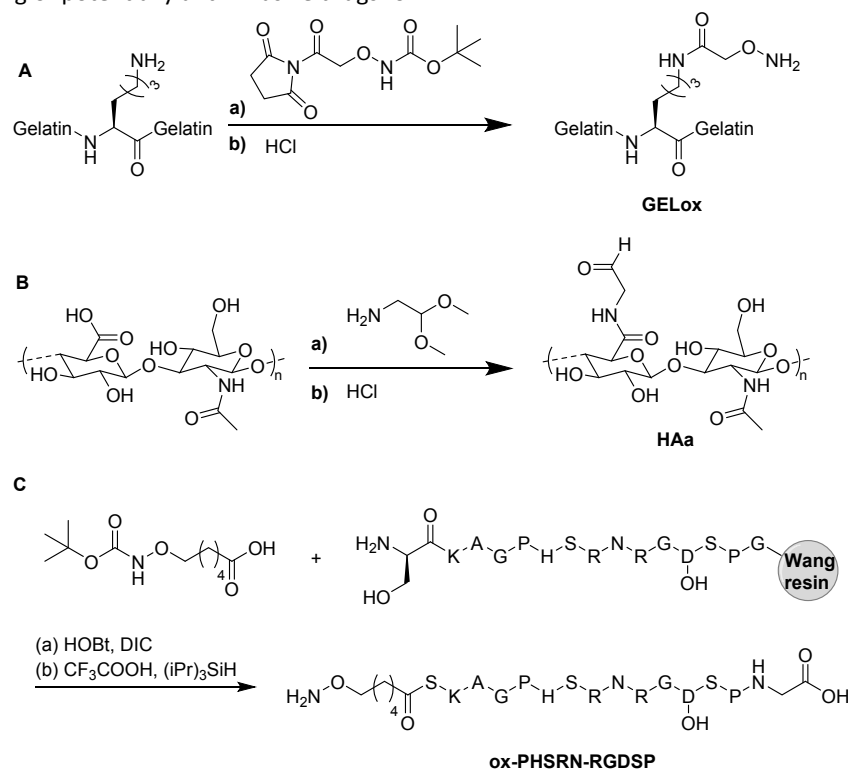


Figure 27 Schematic representation of the preparation of the functional biopolymer based building blocks GELox (oxyamine modified gelatin, **A**), HAa (hyaluronan-aldehyde, **B**) and ox-PHSRN-RGDSP (oxyamine-functionalized peptide sequence, **C**) for cryogel preparation by oxime-click chemistry.



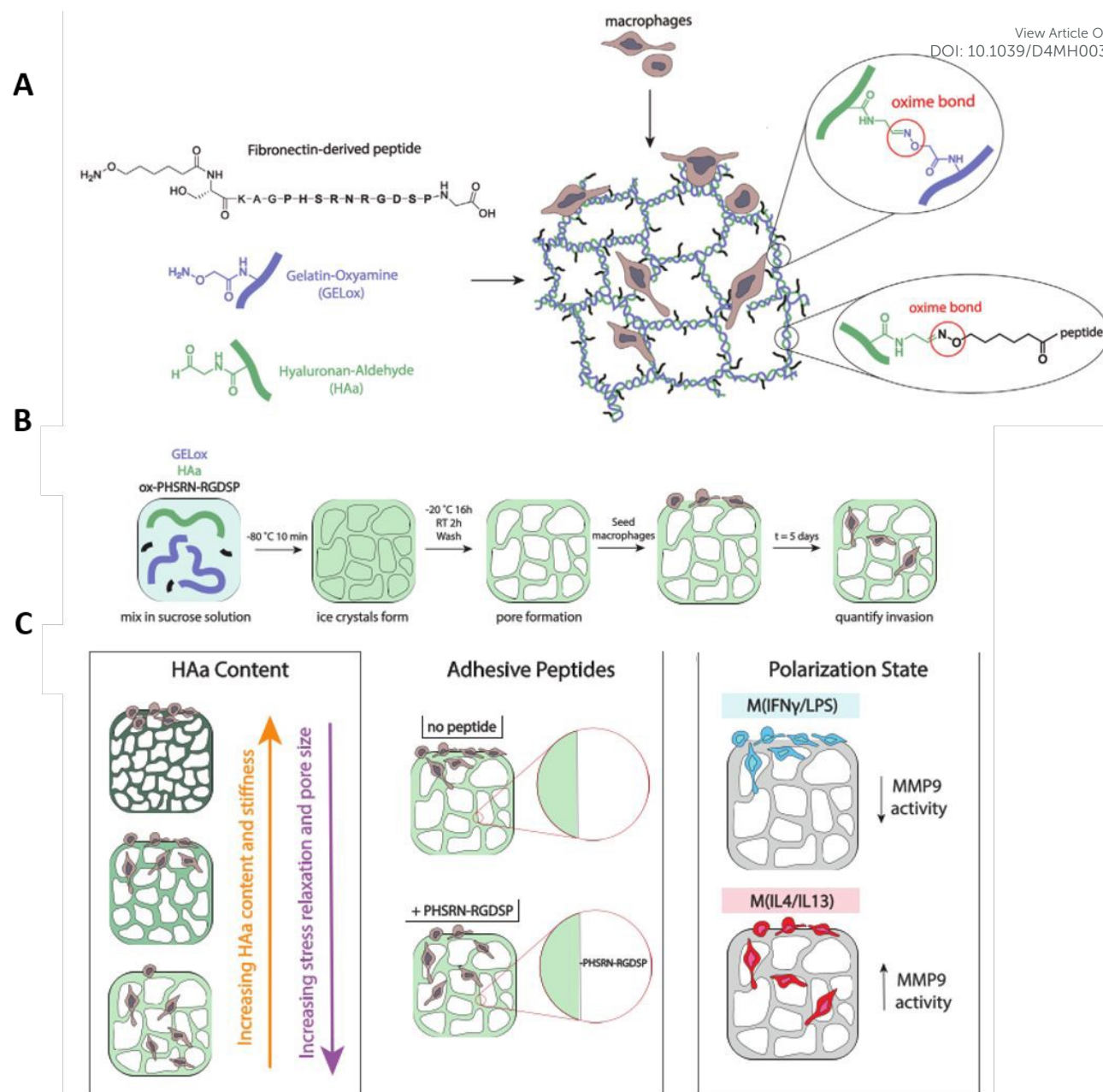


Figure 28 Schematic representation of the preparation of gelatin-HA oxime-cross-linked cryogels (GELox-HAa) with oxime immobilized peptide for primary macrophage invasion studies (A). Cryogels are formed via oxime chemistry by mixing gelatin-oxyamine (GELox), hyaluronan-aldehyde (HAa), and oxyamine-modified fibronectin-derived peptide, ox-PHSRN-RGDSP, together and freeze-thawing in a sucrose solution (B). Macrophage invasion is studied over five days as a function of HAA content, adhesive peptide content, and polarization (C). Reproduced and adapted with permission.<sup>130</sup> Copyright 2021, Wiley-VCH GmbH.

Another method for the preparation of functionalized cryogels based on biopolymers utilizes the subsequent modification of cryogels with biopolymers (Figure 24C). The attachment of ECM-like proteins such as laminin, collagen IV and fibronectin onto carboxymethylcellulose based cryogels using EDC enabled their use as carrier materials for the transplantation of neural cells which might represent a new perspective regarding the treatment of Parkinson's disease.<sup>117</sup> The coupling efficiency at various pH values was determined by fluorescence spectroscopy upon protein labelling with rhodamine B isothiocyanate followed by the dissolution of the gel network with 1 M NaOH. At pH 4 the amount of bound collagen IV,

fibronectin and laminin was approx. 0.74  $\mu\text{g}$  per gel, 1.79  $\mu\text{g}$  per gel and 1.89  $\mu\text{g}$  per gel as determined by the authors, respectively. In contrary to unfunctionalized cryogels as well as gels containing fibronectin and collagen IV, the highest number of LUHMES neurites was observed in case of laminin functionalization in the absence of cell aggregates. Laminin-functionalized cryogels loaded with human embryonic stem cells which were injected into the striatum of immunosuppressed mice were still intact after one month and indicated the ability to preserve the cellular integrity.



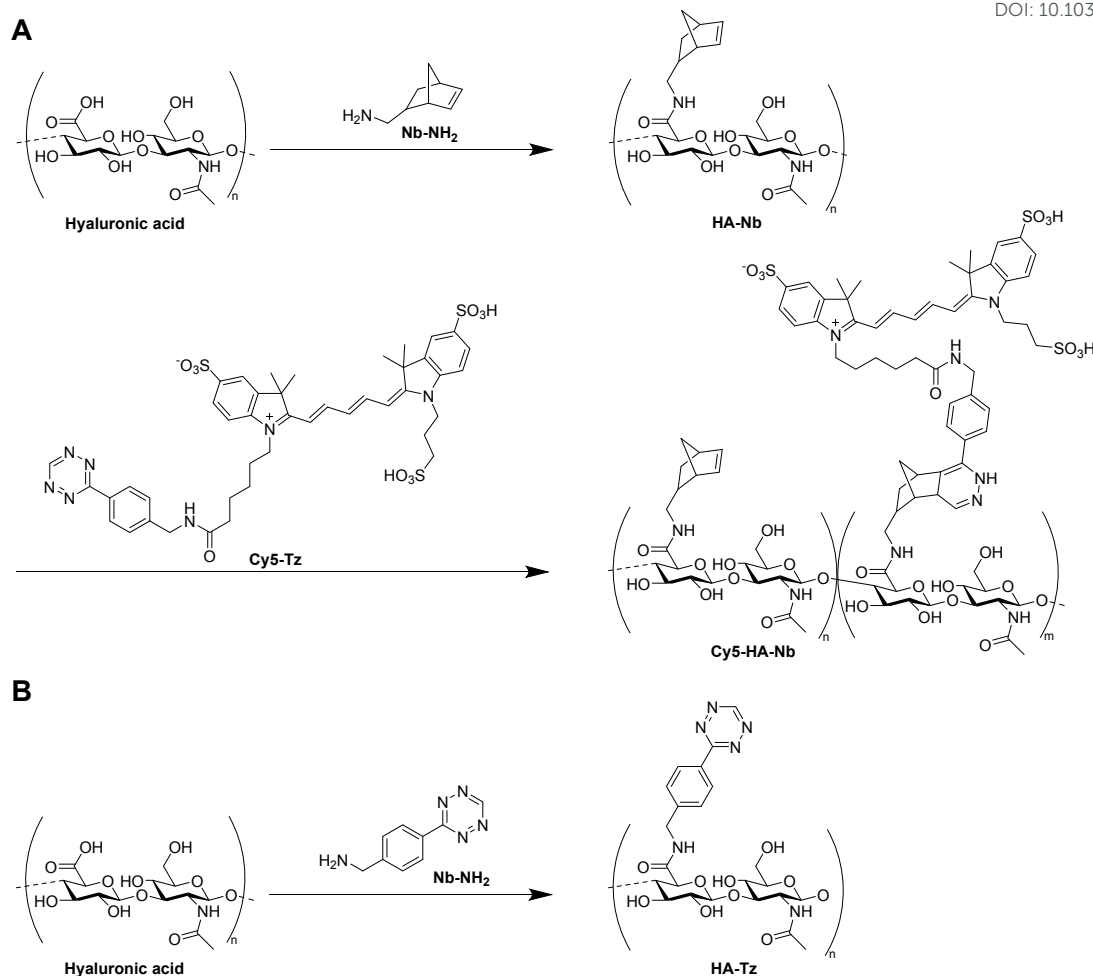


Figure 29 Schematic representation of the preparation of hyaluronic acid based precursors with norbornene and partial Cy5 modification (A) and tetrazine functionalization (B).

Very recently, methacryloyl albumine based cryogels were functionalized with collagen I and/or fibronectin using EDC as artificial liver model for the 3D cultivation of HepG2 cells and screening of drugs.<sup>61</sup> The degree of methacrylation was determined by the Habeeb assay which was found to be 93%. Immunofluorescence microscopy visualized the homogenous distribution of collagen I and fibronectin on the cryogel surfaces upon staining with DyLight488 or DyLight594, respectively. An increase of the signals belonging to amide I (stretching vibration of C=O, 1648  $\text{cm}^{-1}$ ), amide II (stretching vibration of N-H, 1529  $\text{cm}^{-1}$ ) and amide III (1229  $\text{cm}^{-1}$ ) in combination with the presence of a new broad band at 3118 to 3490  $\text{cm}^{-1}$  (stretching frequency of  $\text{NH}_2$  groups) further confirmed the successful modification. Protein modification increased the density of HepG2 cells and their migration into the cryogels as well as the upregulation of hepatocyte specific genes, most significantly in case of the dual-protein functionalization. This indicates the advantage and suitability of a dual functionalization strategy for a better liver ECM mimicking.

In conclusion, functional biopolymer based cryogels are most commonly prepared by the use of polymerizable macromonomeric precursors. Although the degree of modification is typically determined by NMR or the Habeeb assay, the successful incorporation of the precursors into the cryogel polymeric network is not evaluated. Cryo-cross-linking represents another preparation approach which utilizes tetrazine-norbornene or oxyamine click chemistry. The attachment of the clickable groups can be confirmed by NMR or ESI-MS. Nevertheless, no evaluation of the successful incorporation was carried out by now. A third approach is based on the subsequent modification of biopolymer based cryogels with ECM-like proteins utilizing EDC chemistry. Fluorescence spectroscopy enables the determination of the coupling efficiency. The recent development of multiple particle tracking microrheology enabled the determination of local elastic and viscous properties of hyaluronic acid based cryogels. Due to the impact on the cellular adhesion, morphology, migration and proliferation, their determination is of tremendous importance with regard to potential biological applications. With respect to new fabrication techniques, the development of electron-beam initiated cross-linking enabled an initiator and cross-linker free formulation with short reaction times.





## 5. Functional cryogels based on hybrid systems of modified biopolymers and synthetic polymers

### 5.1 Functional polymerizable building blocks based on synthetic polymers and modified biopolymers

Contrary to synthetic polymer based cryogels typically used as adsorbent materials, hybrid cryogels comprised of synthetic polymers and modified biopolymers can be used in a variety of biomedical applications due to their excellent biocompatibility induced by the modified biopolymers (Table 11 and 12). The combined use of biopolymers with synthetic polymers enables sufficient mechanical properties, in comparison with

sole biopolymer based systems. The modification of biopolymers such as hyaluronic acid,<sup>118, 119, 120, 121, 122, 123, 124, 125, 126, 127, 128, 129, 130, 131, 132, 133, 134, 135, 136, 137, 138, 139, 140, 141, 142, 143, 144, 145, 146, 147, 148, 149, 150, 151, 152, 153, 154, 155, 156, 157, 158, 159, 160, 161, 162, 163, 164, 165, 166, 167, 168, 169, 170, 171, 172, 173, 174, 175, 176, 177, 178, 179, 180, 181, 182, 183, 184, 185, 186, 187, 188, 189, 190, 191, 192, 193, 194, 195, 196, 197, 198, 199, 200, 201, 202, 203, 204, 205, 206, 207, 208, 209, 210, 211, 212, 213, 214, 215, 216, 217, 218, 219, 220, 221, 222, 223, 224, 225, 226, 227, 228, 229, 230, 231, 232, 233, 234, 235, 236, 237, 238, 239, 240, 241, 242, 243, 244, 245, 246, 247, 248, 249, 250, 251, 252, 253, 254, 255, 256, 257, 258, 259, 260, 261, 262, 263, 264, 265, 266, 267, 268, 269, 270, 271, 272, 273, 274, 275, 276, 277, 278, 279, 280, 281, 282, 283, 284, 285, 286, 287, 288, 289, 290, 291, 292, 293, 294, 295, 296, 297, 298, 299, 300, 301, 302, 303, 304, 305, 306, 307, 308, 309, 310, 311, 312, 313, 314, 315, 316, 317, 318, 319, 320, 321, 322, 323, 324, 325, 326, 327, 328, 329, 330, 331, 332, 333, 334, 335, 336, 337, 338, 339, 340, 341, 342, 343, 344, 345, 346, 347, 348, 349, 350, 351, 352, 353, 354, 355, 356, 357, 358, 359, 360, 361, 362, 363, 364, 365, 366, 367, 368, 369, 370, 371, 372, 373, 374, 375, 376, 377, 378, 379, 380, 381, 382, 383, 384, 385, 386, 387, 388, 389, 390, 391, 392, 393, 394, 395, 396, 397, 398, 399, 400, 401, 402, 403, 404, 405, 406, 407, 408, 409, 410, 411, 412, 413, 414, 415, 416, 417, 418, 419, 420, 421, 422, 423, 424, 425, 426, 427, 428, 429, 430, 431, 432, 433, 434, 435, 436, 437, 438, 439, 440, 441, 442, 443, 444, 445, 446, 447, 448, 449, 450, 451, 452, 453, 454, 455, 456, 457, 458, 459, 460, 461, 462, 463, 464, 465, 466, 467, 468, 469, 470, 471, 472, 473, 474, 475, 476, 477, 478, 479, 480, 481, 482, 483, 484, 485, 486, 487, 488, 489, 490, 491, 492, 493, 494, 495, 496, 497, 498, 499, 500, 501, 502, 503, 504, 505, 506, 507, 508, 509, 510, 511, 512, 513, 514, 515, 516, 517, 518, 519, 520, 521, 522, 523, 524, 525, 526, 527, 528, 529, 530, 531, 532, 533, 534, 535, 536, 537, 538, 539, 540, 541, 542, 543, 544, 545, 546, 547, 548, 549, 550, 551, 552, 553, 554, 555, 556, 557, 558, 559, 560, 561, 562, 563, 564, 565, 566, 567, 568, 569, 570, 571, 572, 573, 574, 575, 576, 577, 578, 579, 580, 581, 582, 583, 584, 585, 586, 587, 588, 589, 590, 591, 592, 593, 594, 595, 596, 597, 598, 599, 600, 601, 602, 603, 604, 605, 606, 607, 608, 609, 610, 611, 612, 613, 614, 615, 616, 617, 618, 619, 620, 621, 622, 623, 624, 625, 626, 627, 628, 629, 630, 631, 632, 633, 634, 635, 636, 637, 638, 639, 640, 641, 642, 643, 644, 645, 646, 647, 648, 649, 650, 651, 652, 653, 654, 655, 656, 657, 658, 659, 660, 661, 662, 663, 664, 665, 666, 667, 668, 669, 670, 671, 672, 673, 674, 675, 676, 677, 678, 679, 680, 681, 682, 683, 684, 685, 686, 687, 688, 689, 690, 691, 692, 693, 694, 695, 696, 697, 698, 699, 700, 701, 702, 703, 704, 705, 706, 707, 708, 709, 710, 711, 712, 713, 714, 715, 716, 717, 718, 719, 720, 721, 722, 723, 724, 725, 726, 727, 728, 729, 730, 731, 732, 733, 734, 735, 736, 737, 738, 739, 740, 741, 742, 743, 744, 745, 746, 747, 748, 749, 750, 751, 752, 753, 754, 755, 756, 757, 758, 759, 760, 761, 762, 763, 764, 765, 766, 767, 768, 769, 770, 771, 772, 773, 774, 775, 776, 777, 778, 779, 780, 781, 782, 783, 784, 785, 786, 787, 788, 789, 790, 791, 792, 793, 794, 795, 796, 797, 798, 799, 800, 801, 802, 803, 804, 805, 806, 807, 808, 809, 810, 811, 812, 813, 814, 815, 816, 817, 818, 819, 820, 821, 822, 823, 824, 825, 826, 827, 828, 829, 830, 831, 832, 833, 834, 835, 836, 837, 838, 839, 840, 841, 842, 843, 844, 845, 846, 847, 848, 849, 850, 851, 852, 853, 854, 855, 856, 857, 858, 859, 860, 861, 862, 863, 864, 865, 866, 867, 868, 869, 870, 871, 872, 873, 874, 875, 876, 877, 878, 879, 880, 881, 882, 883, 884, 885, 886, 887, 888, 889, 890, 891, 892, 893, 894, 895, 896, 897, 898, 899, 900, 901, 902, 903, 904, 905, 906, 907, 908, 909, 910, 911, 912, 913, 914, 915, 916, 917, 918, 919, 920, 921, 922, 923, 924, 925, 926, 927, 928, 929, 930, 931, 932, 933, 934, 935, 936, 937, 938, 939, 940, 941, 942, 943, 944, 945, 946, 947, 948, 949, 950, 951, 952, 953, 954, 955, 956, 957, 958, 959, 960, 961, 962, 963, 964, 965, 966, 967, 968, 969, 970, 971, 972, 973, 974, 975, 976, 977, 978, 979, 980, 981, 982, 983, 984, 985, 986, 987, 988, 989, 990, 991, 992, 993, 994, 995, 996, 997, 998, 999, 1000</sup> includes the attachment of a polymerizable group prior to radical polymerization. This is typically realized by the reaction with methacrylic anhydride,<sup>110, 122, 123, 125, 126, 133, 136</sup> glycidyl methacrylate,<sup>113-115, 119, 121, 122, 129, 132, 133, 153</sup> 2-aminoethyl methacrylate hydrochloride,<sup>93, 120, 156</sup> *N*-(3-aminopropyl) methacrylamide,<sup>120</sup> acryloyl chloride<sup>96</sup> or *p*-vinylbenzyl chloride<sup>96</sup> (Figure 25 and Figure 30).

Table 11 Overview about cryogels containing polysaccharides based on both, biopolymers and synthetic polymers using functional polymers/macromonomers.

Composition	Biopolymer	Application	Proof of application	Ref.
HA-MA, DMAAm	Methacrylated hyaluronic acid	Potential biomedical applications	Rheological measurements, compression tests	153
HA-MA, PEGDA		Cell transplantation	CLSM	113
Acrylate-PEG-G <sub>4</sub> RGDSP HA-MA, (mPEGA)		Breast tumor model, tissue engineering	Live/dead staining AlamarBlue assay	114, 115
Acrylate-PEG-YRGDS/YRDGS, CS-MA, PEGDA	Methacrylated chondroitin sulfate	Tissue engineering	CLSM, PrestoBlue assay	121
DexMA, PEGDA	Methacrylated dextran	Drug delivery	HPLC MTS assay	129
HEMA-lactate-dextran, MBAAm, (NiPAAm)	Modified dextran	Bone regeneration, controlled drug release	Differentiation assays, histological staining, HPLC	154, 155
C-MA, CS-MA PEGDA	Methacrylated chitosan, methacrylated chondroitin sulfate	Growth factor release for neovascularization	ELISA Live/dead assay PrestoBlue assay	122
CS-MA or HA-MA, PEGDA	Methacrylated chondroitin sulfate or hyaluronic acid	Cartilage tissue engineering	Live/dead assay, AlamarBlue assay	119
HA-MA, GelMA, 4arm-PEG-acrylate	Methacrylated hyaluronic acid, methacrylated gelatin	Adipose tissue engineering, nerve regeneration	Live/dead assay, MTT assay, histological evaluation	125, 126
Alg-MA, 4arm-PEG-acrylate	Methacrylated alginate	Biomolecule release for stem cell transplantation	ELISA	156
Hep-MA, Alg-MA, acrylate-PEG-RGD	Methacrylated heparin, methacrylated alginate	Gene delivery	AlamarBlue assay, CLSM	120
Alg-MA sodium <i>p</i> -styrenesulfonate	Methacrylated alginate	Removal of methylene blue	Spectrophotometry	93
Acryloyl-CD or styrene-CD HEMA, MBAAm	Modified cyclodextrin	Controlled drug delivery	Spectrophotometry EDX	96

Table 12 Overview about cryogels containing polypeptides or proteins based on both, biopolymers and synthetic polymers using functional polymers/macromonomers

Composition	Biopolymer	Application	Proof of application	Ref.
GelMA, PEGDA	Methacrylated gelatin	Spheroid formation, anti-cancer drug screening, and gene delivery	CLSM, SEM Live/dead staining, MTT assay	110, 123, 136
mPGA, HEMA, PEGDA	Methacrylated poly( $\gamma$ -glutamic acid)	Bone tissue engineering	Live/dead assay	132
HA-MA or GelMA, Dopa-acrylate or PEG-Dopa-acrylate	Methacrylated hyaluronic acid or gelatin	Bioadhesive materials	Live/dead staining, mechanical tests	133



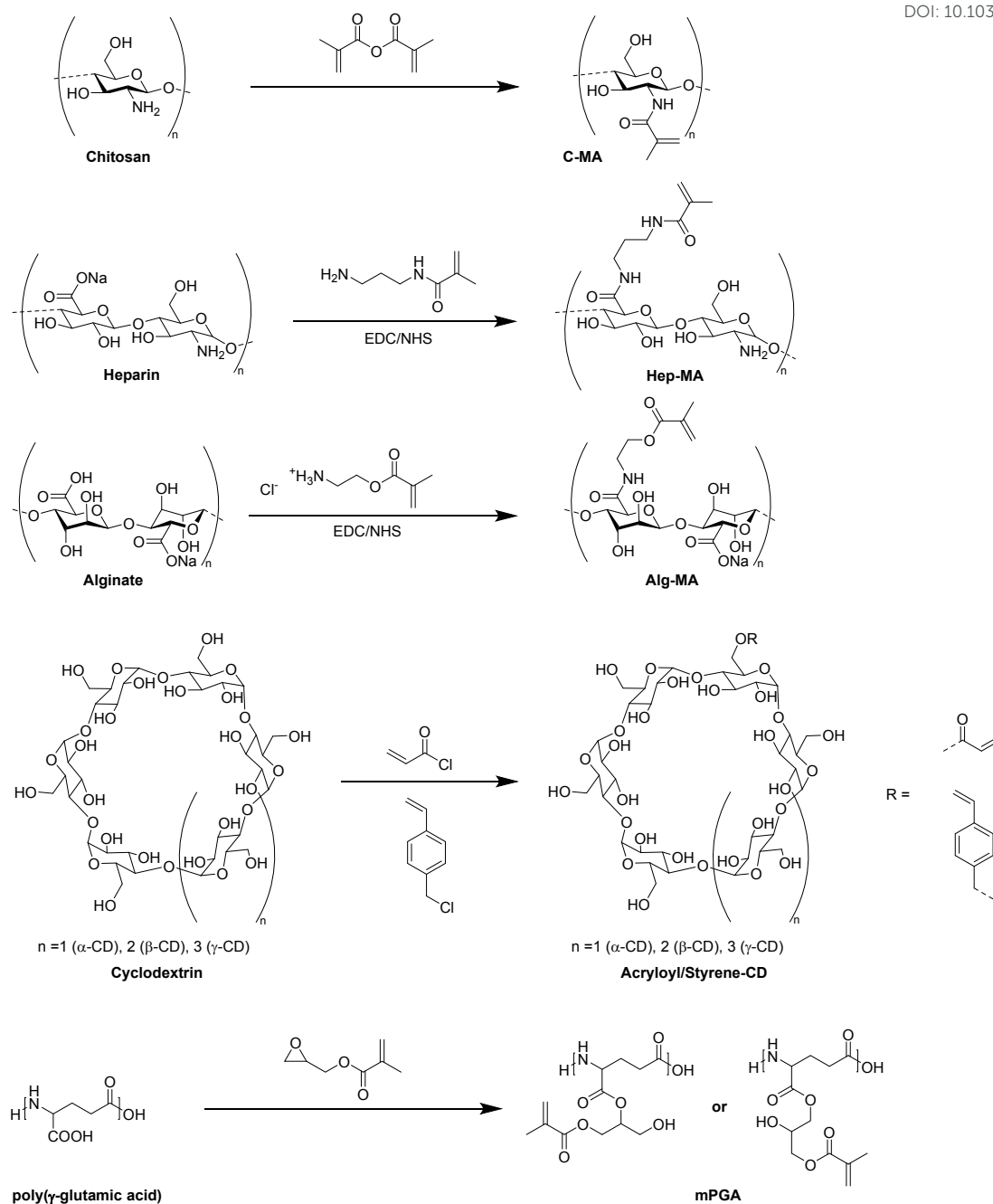


Figure 30 Schematic representation of the synthesis of modified biopolymers for the preparation of hybrid polymer based cryogels. The chemical structures are presented as proposed by the respective authors or reported elsewhere.

Additionally, HEMA-lactate-dextran was prepared by the attachment of imidazolyl carbamate modified HEMA-lactate (Figure 31).<sup>154, 155</sup> The successful modification can be confirmed by <sup>1</sup>H NMR.<sup>157</sup> Incorporation within cryogels can be evaluated by FTIR due to the presence of signals at 1760 cm<sup>-1</sup> (ν<sub>st</sub> (C=O)), 1018 cm<sup>-1</sup> (ν<sub>st</sub> (C-OH)). Copolymerization with NiPAAm enabled the preparation of degradable and thermoresponsive cryogels for simvastatin delivery.<sup>154</sup> In a few cases the degree of modification (DM) was evaluated by the use of <sup>1</sup>H NMR which is

typically expressed as the ratio of the double bond proton integrals in relation to the integral of a reference signal.<sup>96, 110, 121, 153</sup> Dextran methacrylation was determined from the ratio of the integrals of the methacrylic groups (5.67 to 6.09 ppm) divided by the integrals of the backbone protons of dextran (3.5 to 4 ppm).<sup>129</sup> In the cases of hyaluronic acid and chondroitin sulfate which both contain *N*-acetyl groups, the degree of modification was calculated by the ratio of the double bond integrals (5.65 to 6.1 ppm) to the integrals of the methyl group



(1.8 to 1.9 ppm).<sup>121, 126, 133, 158, 159</sup> For the modification of gelatin, the DM is calculated from the loss of the lysine CH<sub>2</sub> peak at 2.8 to 2.9 ppm which is in vicinity to the ε-amine group.<sup>110, 160</sup> For the modification of alginate, no DM determination was carried out although literature examples report the calculation of the DM based on the integral of the methylene group located next to the methacrylamido group,<sup>161</sup> or based on the integration of the alginate protons between 3.5 and 4.0 ppm as

reference signal,<sup>162</sup> respectively. The successful incorporation of the functional building blocks in the cryogel network is mostly not evaluated. In a very few cases, FTIR provides qualitative proof of functionalization with proteins such as gelatin or poly(γ-glutamic acid) by the presence of characteristic bands at 1650 cm<sup>-1</sup> or 1550 cm<sup>-1</sup> representing the amide I bending and amide II bending (N-H) of secondary and primary amides, respectively.<sup>110, 132</sup>

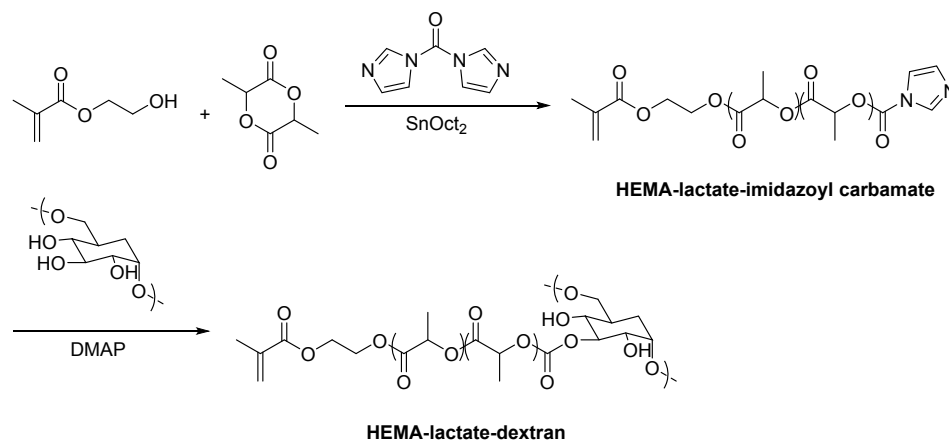


Figure 31 Schematic representation of the preparation of HEMA-lactate-dextran. Ring-opening polymerization initiated by HEMA followed by modification with carbonyldiimidazole (CDI) prior to the functionalization of dextran.

Regarding synthetic polymers, *N,N*-dimethylacrylamide (DMAAm),<sup>153</sup> poly(ethylene glycol) diacrylate (PEGDA),<sup>110, 113, 119, 122, 123, 129, 132, 136</sup> methoxy-poly(ethylene glycol) acrylate (mPEGA),<sup>115</sup> *N,N'*-methylenebisacrylamide (MBAAm),<sup>96, 154, 155</sup> *N*-isopropylacrylamide (NiPAAm),<sup>154</sup> 4arm-PEG-acrylate,<sup>125, 126, 156</sup> sodium *p*-styrene sulfonate (SPS),<sup>93</sup> or 2-hydroxyethyl methacrylate (HEMA)<sup>96, 132</sup> are typically used commercially available precursors (Figure 32). Polymerizable dopamine derivatives Dopa-acrylate and Dopa-PEG-acrylate were synthesized by the modification with NHS-acrylate or NHS-PEG-acrylate, respectively.<sup>133</sup> The incorporation of Dopa-acrylate

into gelatin or hyaluronic acid based cryogels improved the adhesive strength towards porcine skin in comparison with the Dopa-free analogues. By the use of Dopa-PEG-acrylate instead, the adhesion strengths were increased by almost three times up to 14.7 kPa and 15.5 kPa for hyaluronic acid and gelatin, respectively, which is expected to be due to minimized sterical hindrance effects and thus, increased tissue binding by the presence of the PEG spacer. Adhesion properties were similar or higher in comparison with commercially available surgical adhesives.

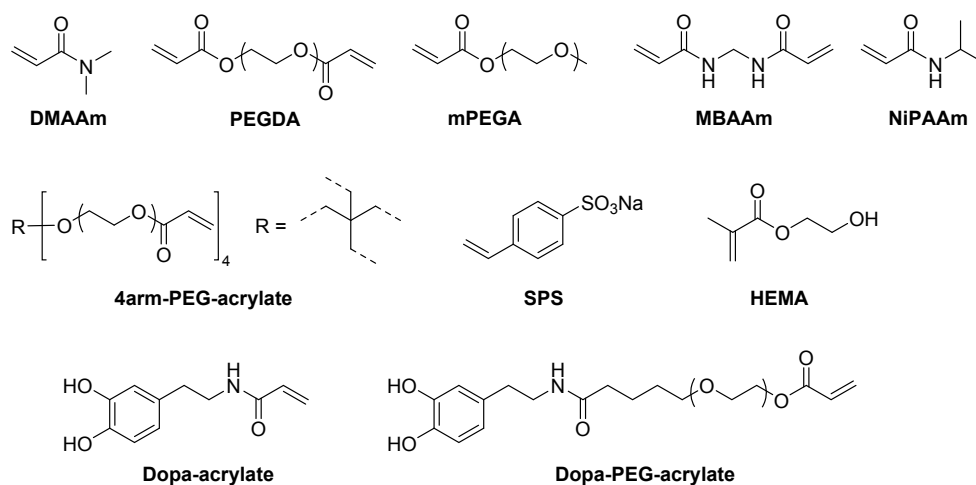


Figure 32 Schematic representation of synthetic polymer precursors for the preparation of hybrid cryogels.



A new cryogel formulation containing methacrylated dextran and poly(ethylene glycol) dimethacrylate (PEGDMA) was prepared for potential drug delivery applications.<sup>129</sup> The incorporation of PEGDMA into the polymer network enabled improved physical and mechanical properties. The excellent cytocompatibility was demonstrated by the cultivation of human adipose derived stem cells using the MTS assay.

Additionally, the polymerization of peptide sequences such as G4RGDSP, YRGDS, YRDGS or RGD from modified precursors is possible by their functionalization with PEG acrylate containing a terminal active ester unit (**Figure 33**). The degree of peptide conjugation can be determined by <sup>1</sup>H NMR from the number of aromatic protons of tyrosine divided by the number of double bond protons.<sup>121</sup>

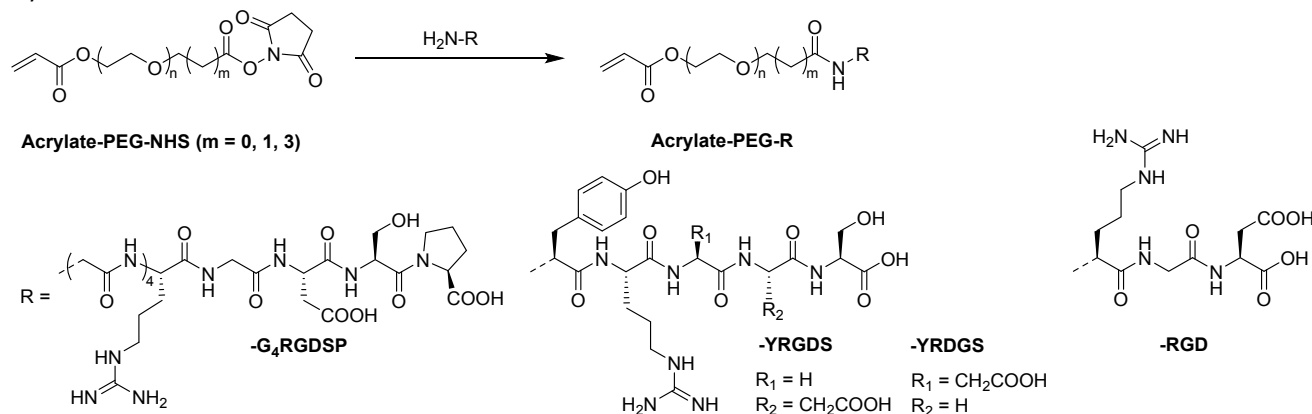


Figure 33 Schematic representation of the synthesis of acrylate-PEG functionalized peptide sequences.

Both the determination of the DM of the modified building blocks and the evaluation of the successful incorporation into the cryogel network is rarely reported in literature. In one of the few examples, cryogels were prepared from acrylated or styrene-modified  $\alpha$ -,  $\beta$ - and  $\gamma$ -cyclodextrin (CD) in the presence of HEMA and MBAAm for controlled drug delivery in wound healing applications.<sup>96</sup> The degree of modification determined by <sup>1</sup>H NMR and MALDI-ToF was found to be 3 for the acrylation, whereas in the case of styrene-functionalized analogues the DM varied depending on the type of CD. The presence of characteristic bands in the IR spectrum confirmed the successful incorporation of CD into the cryogels. Compared with sole p(HEMA) cryogels, a higher loading efficiency of lomefloxacin in the CD functionalized cryogels was observed as determined by

spectrophotometry. Cryogels prepared with styrene-modified CD revealed higher loading efficiencies compared to the acrylate analogues which is most likely to the increased number of  $\pi$ - $\pi$  interactions with the drug molecules (**Figure 34A**). An increased drug release was observed in case of cryogels with styrene-modified CD incorporation due to the formation of hydrogen bonds in contrary to the acrylate derivatives preventing the drug release (**Figure 34B and 34C**). Drug release kinetics revealed a burst release within the first 3 to 5 hours for all the systems and a continuous release of small doses of drugs in case of cryogels containing acrylate-CD. The cryogels did not reveal an induction of cytotoxic effects towards human dermal fibroblasts according to cell viability determinations based on the MTT assay which were found to be >90%.

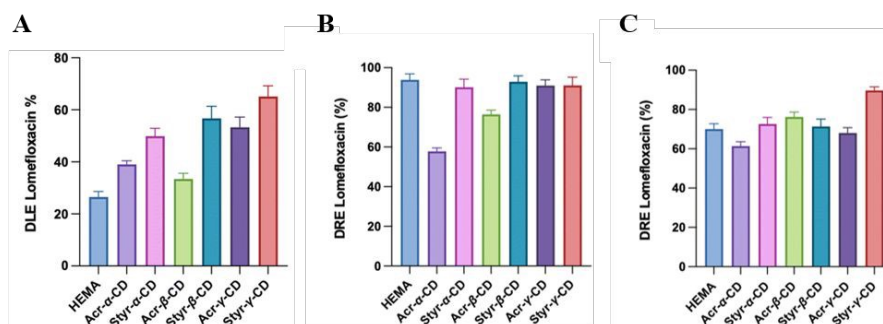


Figure 34 Drug loading efficiency (DLE) after 24 h of adsorption of HEMA and CD-HEMA cryogels for lomefloxacin (A). Drug release efficiency (DRE) after 24 h in acidic solution (pH = 3, B) and a saline buffer (pH = 7.4, C) of HEMA and CD-HEMA cryogels for lomefloxacin. Reproduced with permission.<sup>96</sup> Copyright 2023, The Royal Society of Chemistry and the Chinese Chemical Society.



In short, the preparation of cryogels based on a combination of synthetic polymers and biopolymers most commonly utilizes polymerizable precursors. In case of the synthetic polymers, these are typically commercially available whereas in case of biopolymer precursors the attachment of a polymerizable unit is required. The degree of modification is typically determined by the use of  $^1\text{H}$  NMR. The successful incorporation of the precursors into the cryogel polymeric structure is unfortunately only evaluated by the use of FTIR.

## 5.2 Functional cryogels via modification of hybrid cryogels

For the modification of hybrid cryogels based on synthetic polymers and biopolymers, the high reactivity of epoxide groups is most commonly exploited (Table 13). By the use of AGE as functional monomer, epoxide containing cryogels can directly be functionalized with affinity ligands such as IDA<sup>70, 71</sup> or ortho-phospho-L-tyrosine<sup>73</sup> (Figure 35A). Alternatively, epoxide groups can be introduced subsequently by the reaction of cryogel hydroxy groups with 1,4-butanedioldiglycidylether<sup>48</sup> or epichlorohydrin<sup>73</sup> (Figure 35B and 35C). Furthermore, peptides such as cyclo(Arg-Gly-Asp-D-Tyr-Lys) can be coupled towards carboxylic acid groups on cryogel surfaces using EDC and sulfoNHS (Figure 35D).

Table 13 Overview about the subsequent modification of cryogels based on both biopolymers and synthetic polymers.

Composition	Modification	Coupling strategy	Proof of functionalization	Application	Proof of application	Ref.
AGE, AAm MBAAm alginate	IDA $\text{Cu}^{2+}$ , $\text{Ni}^{2+}$	Epoxide	FTIR Spectrophotometry	Adsorption of IgG	Spectrophotometry (Bradford method)	70
AGE, AAm, MBAAm chitosan, GA	IDA $\text{Cu}^{2+}$ , $\text{Ni}^{2+}$	Epoxide	FTIR Spectrophotometry	Isolation of IgG from human serum	Spectrophotometry (Bradford method)	71
Alginate, AAm MBAAm	Ortho-phospho-L-tyrosine	Bisoxirane activation (BDDGE)	FTIR, EA	Purification of IgG	Spectrophotometry (Bradford method)	48
AAm, alginate (AGE), MBAAm	Ortho-phospho-L-tyrosine	A) Epoxide or B) ECH activation	Spectrophotometry	Isolation of IgG from human serum	Spectrophotometry (Bradford method)	73
Heparin/ starPEG-COOH starPEG-NH <sub>2</sub>	Cyclo(Arg-Gly-Asp-D-Tyr-Lys)	EDC/sulfo-NHS	/	Delivery of signaling proteins	ELISA	109

The functionalization of p(AGE-AAm-alginate) cryogels with iminodiacetic acid (IDA) enabled the adsorption of bovine immunoglobulin G (bIgG) by immobilized metal affinity chromatography (IMAC) via the complexation of copper and nickel ions (Figure 35A).<sup>70</sup> The amount of immobilized IDA ligand was determined by stoichiometric  $\text{Cu}^{2+}$  chelation in combination with spectrophotometry. After saturation, the amount of  $\text{Cu}^{2+}$  ions adsorbed by the IDA ligands was determined spectrophotometrically at 733 nm upon elution with EDTA which were found to be 267.67  $\mu\text{mol g}^{-1}$ . The increase of the signal intensities at 1655  $\text{cm}^{-1}$  and 1609  $\text{cm}^{-1}$  (C=O stretching) and between 1190 to 1114  $\text{cm}^{-1}$  (C-O stretching vibration), as well as the presence of signals at 1563 to 1552  $\text{cm}^{-1}$  (asymmetrical COO vibration) and at 1401 to 1399  $\text{cm}^{-1}$  (CH<sub>2</sub>-N group, symmetrical COO vibration) confirmed the successful cryogel modification with IDA.<sup>70, 71</sup> The  $\text{Cu}^{2+}$  immobilized cryogel exhibited 3.7 times higher adsorption capacities of IgG compared to the nickel analogue, with a total of 148.09 mg  $\text{g}^{-1}$ . The adsorption capacities remained unchanged after 20 adsorption-desorption cycles using imidazole containing buffer solutions as desorbing agent, which demonstrates the excellent stability and reusability of these systems.

Very recently, the use of a similar cryogel for the isolation of human IgG from human serum was reported in which alginate has been replaced by chitosan.<sup>71</sup> The functionalization with 472.66  $\mu\text{mol g}^{-1}$   $\text{Cu}^{2+}$  ions was found to be very unselective regarding the adsorption of IgG from human serum due to the presence of additional lanes in the SDS-PAGE of the eluted protein fraction. On the other hand, the functionalization with 33.71  $\mu\text{mol g}^{-1}$   $\text{Ni}^{2+}$  functionalization allowed to recover 55.6% of IgG with 88.6% purity.

Besides spectrophotometry, elemental analysis was applied for the determination of ligand functionalization, for instance ortho-phospho-L-tyrosine (Figure 35A).<sup>48</sup> The amount of immobilized ligand on p(AAm-Alg) cryogels was found to be 7.43  $\mu\text{mol g}^{-1}$  based on the phosphorous content. The increase of the signal at 1655  $\text{cm}^{-1}$  (amide) and the appearance of a signal 1609  $\text{cm}^{-1}$  (C=C bond) in the FTIR spectrum confirmed the ligand functionalization. The tyrosine ligand functionalization had no influence on the purity of adsorbed IgG from buffer solutions as both modified and unmodified cryogels were able to obtain comparably pure IgG. Nevertheless, p(AAm-Alg)-Tyr exhibited 13.4 times higher dynamic adsorption capacities. Additionally, no reduction of the adsorption capacity was observed after 10 adsorption-desorption cycles using different adsorption buffers as desorbing agents containing 1 M NaCl.



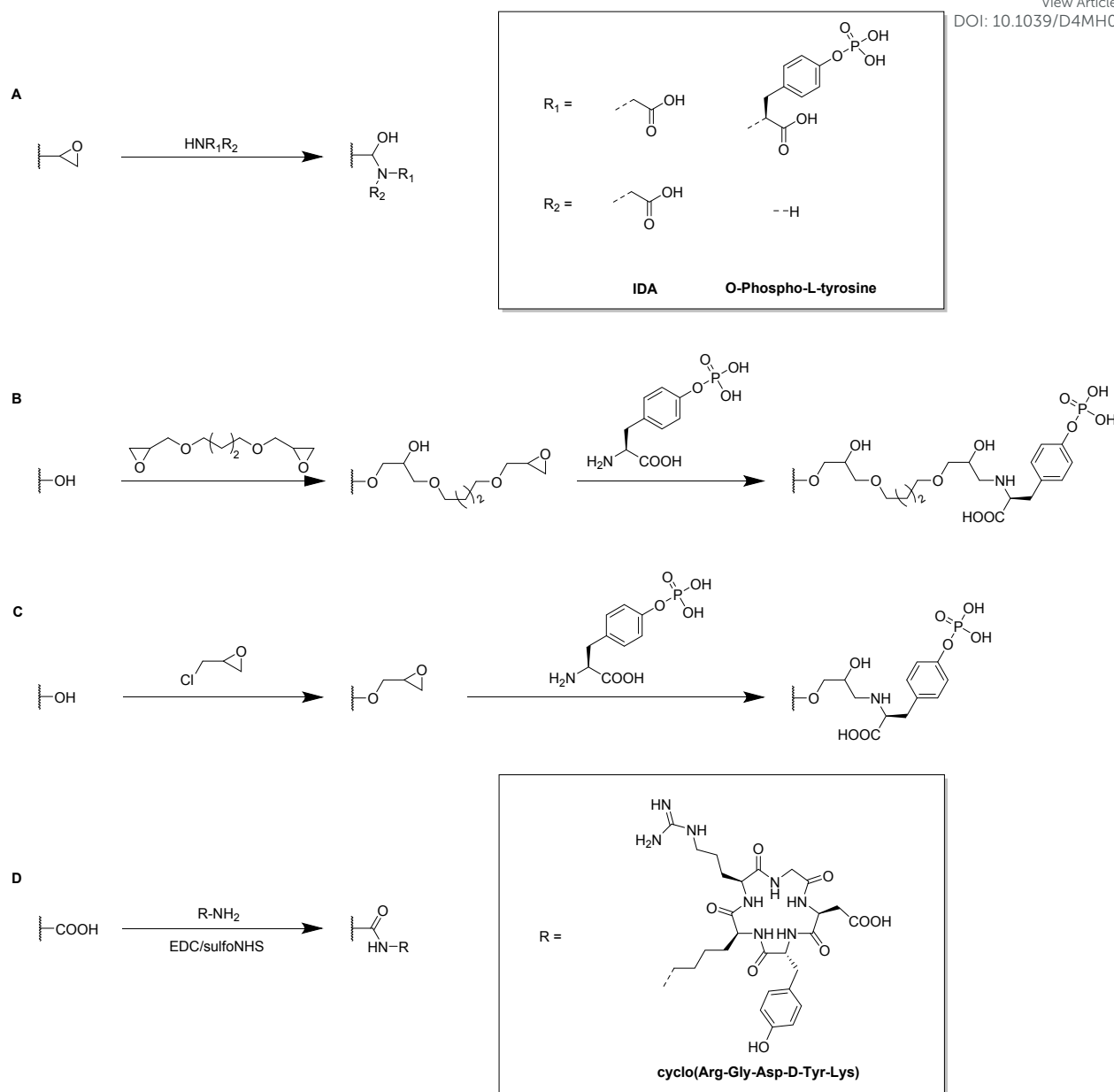


Figure 35 Schematic representation of the subsequent modification of hybrid cryogels by the direct functionalization of epoxide groups with amines such as IDA or o-phospho-L-tyrosine (A), or *via* the modification of hydroxy groups by the introduction of epoxy groups using 1,4-butanedioldiglycidyl ether (B) or epichlorohydrin (C). Alternative strategies include the attachment of peptides such as cyclo(Arg-Gly-Asp-D-Tyr-Lys) *via* EDC/sulfoNHS coupling towards cryogel carboxylic acid groups (D).

p(AAm-Alg) cryogels were functionalized with ortho-phospho-L-tyrosine by two different approaches for the purification of immunoglobulin G (IgG) from human serum.<sup>73</sup> Epoxide containing p(AAm-Alg-AGE) cryogels were directly functionalized with ortho-phospho-L-tyrosine (Tyr) (Figure 35B). Alternatively, epichlorohydrin activation of the alginate hydroxy groups within p(AAm-Alg) cryogels resulted in the introduction of reactive epoxide groups (p(AAm-Alg-ECH)) which were then directly modified with Tyr (Figure 35C). By the use of spectrophotometry, the tyrosine ligand density for both types of cryogels was indirectly determined based on the binding of copper ions towards Tyr assuming the formation of an equimolar complex. The amount of eluted  $\text{Cu}^{2+}$  from Tyr

functionalized cryogels by EDTA relatively to the amount of eluted  $\text{Cu}^{2+}$  from unmodified p(AAm-Alg) cryogels was quantified at 733 nm. An increased amount of Tyr ligand immobilization was found in case of the ECH activated p(AAm-Alg-ECH) cryogels ( $1070 \mu\text{mol g}^{-1}$ ) compared to p(AAm-Alg-AGE) ( $52.72 \mu\text{mol g}^{-1}$ ) resulting in a higher swelling ratio of  $27.79 \text{ g g}^{-1} \text{ H}_2\text{O}$  which was almost twice the amount for p(AAm-Alg-AGE)-Tyr cryogels. The dynamic adsorption capacity of IgG was found to be  $262.97 \text{ mg g}^{-1}$  which was 9.2 times higher compared to the p(AAm-Alg-AGE)-Tyr cryogels and even higher than the p(AAm-Alg)-bisoxirane-Tyr cryogels reported by Mourao *et al.*<sup>48</sup> No reduction of the protein adsorption capacities after 20 adsorption-desorption cycles was observed for both cryogel



types using different adsorption buffers containing 0.5 M NaCl as desorbing agents.

An outstanding modular cryogel platform based on heparin and starPEG-NH<sub>2</sub> with additional functionalization by cyclo(Arg-Gly-Asp-D-Tyr-Lys) for the delivery of signaling proteins was recently reported (Figure 36).<sup>109</sup> Human vascular endothelial growth factor (VEGF), stromal cell-derived factor 1 $\alpha$  (SDF-1) and human neuronal growth factor (NGF) were loaded into the starPEG-heparin cryogels with high efficiencies of 80% (1600 ng per scaffold), 90% (400 ng per scaffold) and 98% (700 ng per scaffold), respectively, which was quantified by ELISA. StarPEG-NH<sub>2</sub> cryogels without protein-affinity mediating heparin revealed low loading efficiencies of VEGF and SDF-1 of 20 and 30%, respectively.

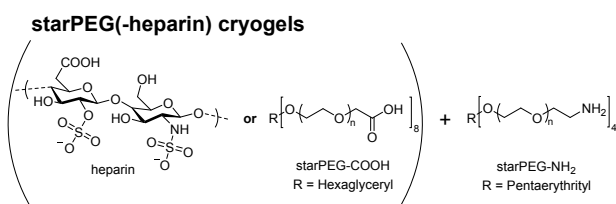


Figure 36 Schematic representation of the different components for the preparation of starPEG(-heparin) cryogels.

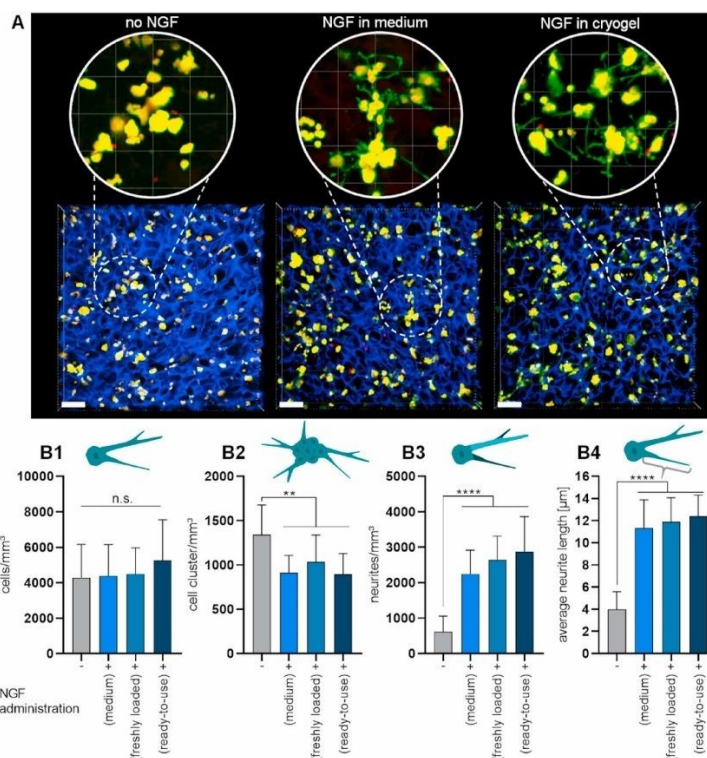


Figure 37 NGF-induced neuronal differentiation of PC-12 cells cultured in cRGD peptide-functionalized starPEG-heparin cryogels (3.9 mM heparin) for seven days. NGF was either administered from pre-loaded ready-to-use cryogels, released from freshly loaded cryogels, or supplemented to the cell culture medium (100 ng mL<sup>-1</sup>). Confocal microscopy images (maximum intensity projections) of neuronal differentiation of PC-12 cells in dependence of the applied NGF administration strategy (blue: cryogel, green: F-actin, and red: nuclei, scale bars: 80 µm, **A**). Quantification of the cell number and neurite outgrowth (**B**). Total number of cells (**B1**), number of cell clusters (**B2**), number of neurite branches (**B3**) and average neurite length derived from the longest neurite segment of each identified neurite branching structure (**B4**). Reproduced with permission.<sup>[104]</sup> Copyright 2021, Elsevier Ltd



## 6. Conclusions

In cryogel research, a particular attention should be focused to the actual quantification of the cryogel functionalization. This does not only help to ensure certain levels of quality and consistency in cryogel research. It also enables for reproducibility and comparability when using cryogels as adsorbent materials or in cell biological applications. Furthermore, it represents an inevitable tool enabling further developments for the optimization of the amount of functionalization in order to obtain materials with targeted and desired properties. Further improvement regarding their injectability, drug delivery, stimuli responsivity or their ability to replicate new specific tissue-like environments would be enabled. Suitable modification strategies for the preparation of new materials can be selected based on the success of each of the different methods. Unfortunately, FTIR is most commonly reported solely as qualitative proof without determining the actual amount of achieved functionalization. In contrast, EDX, XPS and elemental analysis allow for a direct quantification based on the presence of heteroatomic elements such as sulfur, boron, nitrogen or phosphorous. For the indirect determination, spectrophotometry is most commonly applied, often coupled with colorimetric assays such as the Bradford assay, the Habeeb assay or the DNS assay to determine proteins, amines or reducing sugars, respectively. In the case of nitrogen containing monomers or ligands, the Kjeldahl method can be applied as suitable quantification technique. Depending on the polymer source, different applications are possible. Synthetic polymer based cryogels are commonly used for the adsorption of metal ions, proteins or enzymes due to their favorable mechanical properties. As biopolymers exhibit excellent biocompatibilities, their use as precursor molecules enables applications in tissue engineering and 3D (cell) cultivation. A combination of these two polymer types extends the applications for the resulting materials to both adsorption and cell biological purposes as well as drug delivery. By the additional modification with bioactive molecules such as peptides or proteins, the typical issue of synthetic polymer based cryogels possessing low biocompatibilities can be overcome. Besides the use of (macro-)monomeric precursor molecules, functionalized cryogels can also be obtained by the subsequent modification with certain binding ligands. Each of the two strategies has its advantages and disadvantages. On the one hand, (macro-)monomeric precursors allow for a better control on the amount of functionalization in the material but need to contain an attached polymerizable group which requires certain synthetic steps beforehand. On the other hand, the subsequent modification of cryogels allows for the use of plain, unmodified molecules of choice. This can be beneficial for biomacromolecules in which the modification with a polymerizable group is often rather difficult to quantify. Overall, there is no standard approach for manufacturing and the synthetic strategy has to be carefully selected in dependence on the final cryogel and its foreseen application. Recently, promising studies have shown the potential of cryogels to be used for the simultaneous adsorption of different metal ions as well as the simultaneous loading and release of different drugs. Accordingly, we believe that multifunctional cryogels capable of releasing various compounds such as drugs from the same material at the same time will be in the focus of future research. This would lead to further improvements regarding combination therapies and advanced treatments of diseases.

## Conflicts of interest

The authors declare that there is no conflict of interests.

## Acknowledgements

This work was funded by the Deutsche Forschungsgemeinschaft (DFG, German Research Foundation) under Germany's Excellence Strategy – EXC 2051 – Project-ID 390713860.

## Notes and references

- M. B. Dainiak, I. Y. Galaev, A. Kumar, F. M. Plieva and B. Mattiasson, in *Adv Biochem Eng Biot*, eds. A. Kumar, I. Y. Galaev and B. Mattiasson, Springer-Verlag Berlin, Heidelberg, 1st Edition edn., 2007, DOI: 10.1007/10\_2006\_044, pp. 101-127.
- V. I. Lozinsky, I. Y. Galaev, F. M. Plieva, I. N. Savinal, H. Jungvid and B. Mattiasson, *Trends Biotechnol.*, 2003, **21**, 445-451.
- O. Okay and V. I. Lozinsky, *Adv. Polym. Sci.*, 2014, **263**, 103-157.
- B. M. A. Carvalho, S. L. Da Silva, L. H. M. Da Silva, V. P. R. Minim, M. C. H. Da Silva, L. M. Carvalho and L. A. Minim, *Sep. Purif. Rev.*, 2014, **43**, 241-262.
- W. Wan, A. D. Bannerman, L. Yang and H. Mak, *Adv. Polym. Sci.*, 2014, **263**, 283-321.
- Y. He, C. Wang, C. Wang, Y. Xiao and W. Lin, *Polymers*, 2021, **13**, 2299.
- A. Damania, A. K. Teotia and A. Kumar, in *Supermacroporous Cryogels: Biomedical and Biotechnological Applications*, ed. A. Kumar, CRC Press, Boca Raton, Florida, United States, 1st Edition edn., 2016, DOI: 10.1201/b19676-4, pp. 35-89.
- K. R. Hixon, T. Lu and S. A. Sell, *Acta Biomater.*, 2017, **62**, 29-41.
- I. N. Savina, M. Zoughaib and A. A. Yergeshov, *Gels*, 2021, **7**, 79.
- C. Chircov, A. M. Grumezescu and L. E. Bejenaru, *Rom. J. Morphol. Embryol.*, 2018, **59**, 71-76.
- T. Vishnoi and A. Kumar, in *Supermacroporous Cryogels: Biomedical and Biotechnological Applications*, ed. A. Kumar, CRC Press, Boca Raton, Florida, United States, 1st Edition edn., 2016, pp. 251-276.
- R. Mishra, S. Bhat and A. Kumar, in *Supermacroporous Cryogels: Biomedical and Biotechnological Applications*, ed. A. Kumar, CRC Press, Boca Raton, Florida, United States, 1st Edition edn., 2016, pp. 215-250.
- A. Baimenov, D. A. Berillo, S. G. Pouloupoulos and V. J. Inglezakis, *Adv. Colloid Interface Sci.*, 2020, **276**, 102088.
- L. Oennby, in *Supermacroporous Cryogels: Biomedical and Biotechnological Applications*, ed. A. Kumar, CRC Press, Boca Raton, Florida, United States, 1st Edition edn., 2016, pp. 331-359.
- A. A. Aryee, F. M. Mpatani, R. P. Han, X. X. Shi and L. B. Qu, *J. Environ. Chem. Eng.*, 2021, **9**, 106907.





16. K. N. How, W. H. Yap, C. L. H. Lim, B. H. Goh and Z. W. Lai, *Front. Pharmacol.*, 2020, **11**, 1105.
17. N. Babanejad, K. Mfoafo, E. Zhang, Y. Omid, R. Razeghfard and H. Omidian, *J. Chromatogr. A*, 2022, **1683**, 463546.
18. N. Ganewatta and Z. El Rassi, *Electrophoresis*, 2018, **39**, 53-66.
19. S. Poddar, S. Sharmeen and D. S. Hage, *Electrophoresis*, 2021, **42**, 2577-2598.
20. Z. Li, E. Rodriguez, S. Azaria, A. Pekarek and D. S. Hage, *Electrophoresis*, 2017, **38**, 2837-2850.
21. S. Choudhury, D. Connolly and B. White, *Anal. Methods*, 2015, **7**, 6967-6982.
22. A. Srivastava, S. Singh and A. Kumar, in *Supermacroporous Cryogels: Biomedical and Biotechnological Applications*, ed. A. Kumar, CRC Press, Boca Raton, Florida, United States, 1st Edition edn., 2016, pp. 443-462.
23. G. Erturk and B. Mattiasson, *J. Chromatogr. A*, 2014, **1357**, 24-35.
24. M. Bakhshpour, N. Idil, I. Percin and A. Denizli, *Appl. Sci.*, 2019, **9**, 553.
25. T. M. A. Henderson, K. Ladewig, D. N. Haylock, K. M. McLean and A. J. O'Connor, *J. Mater. Chem. B*, 2013, **1**, 2682-2695.
26. M. Razavi, Y. Qiao and A. S. Thakor, *J. Biomed. Mater. Res. A*, 2019, **107**, 2736-2755.
27. A. Memic, T. Colombani, L. J. Eggermont, M. Rezaeeyazdi, J. Steingold, Z. J. Rogers, K. J. Navare, H. S. Mohammed and S. A. Bencherif, *Adv. Ther.*, 2019, **2**, 1800114.
28. P. A. Shiekh, S. M. Andrabi, A. Singh, S. Majumder and A. Kumar, *Eur. Polym. J.*, 2021, **144**, 110234.
29. E. Jain and A. Kumar, in *Supermacroporous Cryogels: Biomedical and Biotechnological Applications*, ed. A. Kumar, CRC Press, Boca Raton, Florida, United States, 1st Edition edn., 2016, pp. 417-441.
30. I. Jyothilekshmi and N. S. Jayaprakash, *J. Microbiol. Biotechnol.*, 2021, **31**, 349-357.
31. A. Wartenberg, J. Weisser and M. Schnabelrauch, *Molecules*, 2021, **26**, 5597.
32. D. Berillo, A. Al-Jwaid and J. Caplin, *Polymers*, 2021, **13**, 1073.
33. T. Mehrotra, S. Dev, A. Banerjee, A. Chatterjee, R. Singh and S. Aggarwal, *J. Environ. Chem. Eng.*, 2021, **9**, 105920.
34. Y. Petrenko, A. Petrenko, P. Vardi and K. Bloch, in *Supermacroporous Cryogels: Biomedical and Biotechnological Applications*, ed. A. Kumar, CRC Press, Boca Raton, Florida, United States, 1st Edition edn., 2016, pp. 277-305.
35. J. Wang, Q.-M. Wang, L. L. Tian, C. Yang, S.-H. Yu and C. Yang, *Chin. J. Anal. Chem.*, 2015, **43**, 1777-1784.
36. M. Andac, I. Yu Galaev and A. Denizli, in *Biomaterials from Nature for Advanced Devices and Therapies*, ed. R. L. R. N. M. Neves, John Wiley & Sons, Inc., Hoboken, New Jersey, United States, 1st Edition edn., 2016, DOI: 10.1002/9781119126218.ch22, pp. 403-428.
37. N. Bereli, H. Yavuz and A. Denizli, *J. Liq. Chromatogr. Relat. Technol.*, 2020, **43**, 657-670.
38. L. J. Eggermont, Z. J. Rogers, T. Colombani, A. Memic and S. A. Bencherif, *Trends Biotechnol.*, 2020, **38**, 418-431.
39. D. Cimen, M. A. Ozbek, N. Bereli, B. Mattiasson, A. Denizli and P. Gurikov, *Gels*, 2021, **7**, 38.
40. C. Liu, G. Tong, C. Chen, Z. Tan, C. Quan and C. Zhang, *Progr. Chem.*, 2014, **26**, 1190-1201. DOI: 10.1039/D4MH00315B
41. F. M. Plieva, H. Kirsebom and B. Mattiasson, *J. Sep. Sci.*, 2011, **34**, 2164-2172.
42. F. D. Martinez-Garcia, T. Fischer, A. Hayn, C. T. Mierke, J. K. Burgess and M. C. Harmsen, *Gels*, 2022, **8**, 535.
43. B. Mattiasson, *Adv. Polym. Sci.*, 2014, **263**, 245-281.
44. Y. Saylan and A. Denizli, *Gels*, 2019, **5**, 20.
45. E. S. Dragan and M. V. Dinu, *React. Funct. Polym.*, 2020, **146**, 104372.
46. S. P. O. Danielsen, H. K. Beech, S. Wang, B. M. El-Zaatari, X. Wang, L. Sapir, T. Ouchi, Z. Wang, P. N. Johnson, Y. Hu, D. J. Lundberg, G. Stoychev, S. L. Craig, J. A. Johnson, J. A. Kalow, B. D. Olsen and M. Rubinstein, *Chem. Rev.*, 2021, **121**, 5042-5092.
47. F. Behrendt, Y. Deng, D. Pretzel, S. Stumpf, N. Fritz, M. Gottschaldt, G. Pohnert and U. S. Schubert, *Mater. Horiz.*, 2023, **10**, 2412-2416.
48. C. A. Mourao, C. Marcuz, K. Haupt and S. M. A. Bueno, *J. Chromatogr. B*, 2019, **1129**, 121783.
49. S. A. A. Noma, O. Acet, A. Ulu, B. Onal, M. Odabasi and B. Ates, *Polym. Test.*, 2021, **93**, 106980.
50. M. Bayraktaroğlu, H. Orhan, S. Evli, S. Akgöl, D. Aktaş Uygun and M. Uygun, *J. Carbohydr. Chem.*, 2018, **37**, 302-317.
51. F. Akpinar, S. Evli, G. Guven, M. Bayraktaroglu, U. Kilimci, M. Uygun and D. A. Uygun, *Appl. Biochem. Biotechnol.*, 2020, **190**, 138-147.
52. S. Evli, A. A. Karagozler, G. Guven, H. Orhan, M. Uygun and D. A. Uygun, *Bull. Mater. Sci.*, 2020, **43**, 107.
53. M. M. Tonta, Z. M. Sahin, A. Cihaner, F. Yilmaz and A. Gurek, *ChemistrySelect*, 2021, **6**, 12644-12651.
54. M. Daoud-Attieh, H. Chaib, C. Armutcu, L. Uzun, A. Elkak and A. Denizli, *Sep. Purif. Technol.*, 2013, **118**, 816-822.
55. K. Kose, K. Erol and D. A. Kose, *Adsorption*, 2020, **26**, 329-337.
56. B. Erol, K. Erol and E. Gokmese, *Process Biochem.*, 2019, **83**, 104-113.
57. E. Bilgin, K. Erol, K. Köse and D. A. Köse, *Environ. Sci. Pollut. Res.*, 2018, **25**, 27614-27627.
58. H. Zheng, S. Hajizadeh, H. Gong, H. Lin and L. Ye, *J. Agric. Food Chem.*, 2021, **69**, 135-145.
59. T. D. Luong, M. Zoughaib, R. Garifullin, S. Kuznetsova, M. O. Guler and T. I. Abdullin, *ACS Appl. Bio Mater.*, 2020, **3**, 1116-1128.
60. M. Zoughaib, D. Luong, R. Garifullin, D. Z. Gatina, S. V. Fedosimova and T. I. Abdullin, *Mater. Sci. Eng. C*, 2021, **120**, 111660.
61. X. M. Niu, M. A. Lin and B. H. Lee, *Gels*, 2022, **8**, 404.
62. H. Abdul, J.-Y. Wang, H.-J. Li, C.-S. Hu, X.-C. Li and W.-D. He, *Polymers*, 2019, **11**, 1620.
63. F. Behrendt, D. Pretzel, Z. Cseresnyés, M. Kleinstauber, T. Wloka, L. Radosa, M. T. Figge, M. Gottschaldt, A. Brakhage and U. S. Schubert, *J. Polym. Sci.*, 2023, **61**, 3039-3054.
64. J. F. da Silva, D. L. da Silva, R. G. Nascimento, L. A. A. Verissimo, C. M. Veloso, R. C. F. Bonomo and R. D. I. Fontan, *J. Appl. Polym. Sci.*, 2019, **136**, 47956.
65. G. Uzunoglu, D. Cimen, N. Bereli, K. Cetin and A. Denizli, *J. Biomater. Sci. Polym. Ed.*, 2019, **30**, 1276-1290.
66. G. Bayramoglu, A. Akbulut and M. Y. Arica, *Chem. Eng. Res. Des.*, 2021, **165**, 435-444.



67. N. Gunay, U. Kilimci, G. Ozturk, D. A. Uygun and M. Uygun, *Chem. Pap.*, 2023, **77**, 5839-5846.
68. B. Oktay, S. Demir and N. Kayaman-Apohan, *Food Bioprod. Process.*, 2020, **122**, 159-168.
69. K. Cetin and A. Denizli, *J. Chromatogr. B: Anal. Technol. Biomed. Life Sci.*, 2019, **1114-1115**, 5-12.
70. I. F. Fioravante and S. M. A. Bueno, *Process Biochem.*, 2022, **118**, 413-424.
71. H. S. D. R. Hamacek, I. T. L. Bresolin, I. F. Fioravante and S. M. A. Bueno, *Process Biochem.*, 2023, **131**, 199-209.
72. F. Bonalumi, C. Crua, I. N. Savina, N. Davies, A. Habstesion, M. Santini, S. Fest-Santini and S. Sandeman, *Mater. Sci. Eng. C*, 2021, **123**, 111983.
73. C. Marcuz, C. A. Mourao, K. Haupt and S. M. A. Bueno, *J. Chromatogr. B.*, 2021, **1165**, 122530.
74. X. Y. Wu, J. Yang, F. H. Wu, W. B. Cao, T. Zhou, Z. Y. Wang, C. X. Tu, Z. R. Gou, L. Zhang and C. Y. Gao, *Chinese J. Polym. Sci.*, 2023, **41**, 40-50.
75. T. J. Zhang, C. Liu, H. W. Zheng, X. N. Han, H. Lin, L. M. Cao and J. X. Sui, *J. Mol. Recognit.*, 2023, **36**, e2999.
76. J. B. Sumner and V. A. Graham, *J. Biol. Chem.*, 1921, **47**, 5-9.
77. A. C. F. de Oliveira, I. C. O. Neves, J. A. M. Saraiva, M. F. F. de Carvalho, G. A. Batista, L. A. A. Verissimo and J. V. d. Resende, *Sep. Sci. Technol.*, 2020, **55**, 2012-2024.
78. I. C. O. Neves, A. A. Rodrigues, T. T. Valentim, A. Meira, S. H. Silva, L. A. A. Verissimo and J. V. de Resende, *J. Chromatogr. B.*, 2020, **1161**, 122435.
79. A. Meira, R. M. da Silva, I. C. O. Neves, L. A. Minim, L. A. A. Verissimo and J. V. de Resende, *Can. J. Chem. Eng.*, 2023, **101**, 3497-3511.
80. P. Saez-Plaza, T. Michalowski, M. J. Navas, A. G. Asuero and S. Wybraniec, *Crit. Rev. Anal. Chem.*, 2013, **43**, 178-223.
81. G. L. Chaves, P. C. G. Mol, V. P. R. Minim and L. A. Minim, *J. Appl. Polym. Sci.*, 2020, **137**, 48507.
82. L. Sun, X. Feng, T. Zhong and X. Zhang, *J. Sep. Sci.*, 2020, **43**, 3315-3326.
83. L. Sundberg and J. Porath, *J. Chromatogr.*, 1974, **90**, 87-98.
84. Z. P. He, Y. Wang, T. T. Zhao, Z. C. Ye and H. Huang, *Anal. Methods*, 2014, **6**, 4257-4261.
85. B. Eren, O. Zenger, H. I. O. Basegmez and G. B. Pesint, *J. Biotechnol.*, 2023, **364**, 58-65.
86. M. Erzenin, G. B. Pesint, O. Zenger and M. Odabasi, *Polym. Bull.*, 2021, **79**, 1485-1499.
87. T. Zhong, X. Feng, L. Sun, J. Zhang, Y. Tian and X. Zhang, *Polym. Bull.*, 2021, **78**, 5873-5890.
88. W. X. Hou, F. Ma, J. Y. Li, H. R. Tian, G. X. Chen, G. X. Li, L. L. Jing and P. F. Yang, *J. Polym. Environ.*, 2023, **31**, 1656-1667.
89. Z. F. Zhu, J. Y. Li, F. Ma, G. X. Chen, H. R. Tian, J. Li and P. F. Yang, *J. Appl. Polym. Sci.*, 2023, **140**, e53754.
90. H. K. Megbenu, Z. Tauanov, C. Daulbayev, S. G. Poulopoulos and A. Baimenov, *J. Chem. Technol. Biotechnol.*, 2022, **97**, 3375-3384.
91. R. B. J. Ihlenburg, A.-C. Lehen, J. Koetz and A. Taubert, *Polymers*, 2021, **13**, 208.
92. Z. Gun Gok and M. Inal, *J. Polym. Environ.*, 2022, **30**, 151-163.
93. T. Y. Yin, X. Y. Zhang, S. Shao, T. Xiang and S. B. Zhou, *Carbohydr. Polym.*, 2023, **301**, 120356.
94. P. L. F. Tene, A. Weltin, F. Tritz, H. J. D. Soufo, T. Brandstetter and J. R uhe, *Langmuir*, 2021, **37**, 11041-11048.
95. Z. Jing, L. Jie, Q. Sunxiang, N. Haifeng and F. Jie, *J. Mater. Chem. B*, 2023, **11**, 2733-2744.
96. C. Zagni, A. Coco, T. Mecca, G. Curcuruto, V. Patamia, K. Mangano, A. Rescifina and S. C. Carroccio, *Mater. Chem. Front.*, 2023, **7**, 2693-2705.
97. R. La Spina, D. C. Antonio, R. Bombera, T. Lettieri, A. S. Lequarre, P. Colpo and A. Valsesia, *Biosensors*, 2021, **11**, 142.
98. T. H. T. Trinh, L. Ye and S. Hajizadeh, *J. Sep. Sci.*, 2023, **46**, 2300017.
99. B. Wan, J. Li, F. Ma, N. Yu, W. Zhang, L. Jiang and H. Wei, *Langmuir*, 2019, **35**, 3284-3294.
100. R. G. Nascimento, M. C. P. Porfirio, A. N. Alves, P. A. Nascimento, L. S. Santos, C. M. Veloso, R. C. F. Bonomo and R. D. I. Fontan, *J. Polym. Environ.*, 2023, **31**, 2641-2652.
101. R. G. Nascimento, M. C. P. Porfirio, P. A. Nascimento, A. N. Alves, L. S. Santos, C. M. Veloso, R. C. F. Bonomo and R. D. I. Fontan, *J. Polym. Environ.*, 2022, **30**, 3230-3238.
102. K. S. Maciel, P. C. G. Mol, L. A. A. Verissimo, V. P. R. Minim and L. A. Minim, *J. Sep. Sci.*, 2023, **46**, 2200639.
103. M. Y. Kim and T. G. Lee, *Chemosphere*, 2019, **217**, 423-429.
104. T. Mecca, M. Ussia, D. Caretti, F. Cunsolo, S. Dattilo, S. Scurti, V. Privitera and S. C. Carroccio, *Chem. Eng. J.*, 2020, **399**, 125753.
105. J. Chen, C. Liao, X. X. Guo, S. C. Hou and W. D. He, *Eur. Polym. J.*, 2022, **171**, 111192.
106. N. Sahiner, S. Demirci, M. Sahiner, S. Yilmaz and H. Al-Lohedan, *J. Environ. Manag.*, 2015, **152**, 66-74.
107. G. Guven, S. Evli, M. Uygun and D. A. Uygun, *J. Liq. Chromatogr. Relat. Technol.*, 2019, **42**, 537-545.
108. D. Eigel, R. Schuster, M. J. Maennel, J. Thiele, M. J. Panasiuk, L. C. Andreae, C. Varricchio, A. Brancale, P. B. Welzel, W. B. Huttner, C. Werner, B. Newland and K. R. Long, *Biomaterials*, 2021, **271**, 120712.
109. J. Sievers, R. Zimmermann, J. Friedrichs, D. Pette, Y. D. P. Limasale, C. Werner and P. B. Welzel, *Biomaterials*, 2021, **278**, 121170.
110. P. Shrimali, M. Peter, A. Singh, N. Dalal, S. Dakave, S. V. Chiplunkar and P. Tayalia, *Biomater. Sci.*, 2018, **6**, 3241-3250.
111. L. Chambre, H. Maouati, Y. Oz, R. Sanyal and A. Sanyal, *Bioconjugate Chem.*, 2020, **31**, 2116-2124.
112. T. Mizoguchi, T. Edano and T. Koshi, *J. Lipid Res.*, 2004, **45**, 396-401.
113. W. Sun, J. H. Choi, Y. H. Choi, S. G. Im, K.-H. So and N. S. Hwang, *Biotechnol. Bioprocess Eng.*, 2022, **27**, 17-29.
114. M. Rezaeeyazdi, T. Colombani, L. J. Eggermont and S. A. Bencherif, *Mater. Today Bio*, 2022, **13**, 100207.
115. T. He, B. Li, T. Colombani, K. J. Navare, S. A. Bencherif and A. G. Bajpayee, *Osteoarthr. Cartil.*, 2020, **28**, 748-760.
116. H. Radhouani, S. Correia, C. Goncalves, R. L. Reis and J. M. Oliveira, *Polymers*, 2021, **13**, 1342.
117. A. Filippova, F. Bonini, L. Efremova, M. Locatelli, O. Preynat-Seauve, A. Beduer, K.-H. Krause and T. Braschler, *Biomaterials*, 2021, **270**, 120707.



118. L. Di Muzio, C. Sergi, V. C. Carriero, J. Tirillò, A. Adrover, E. Messina, R. Gaetani, S. Petralito, M. A. Casadei and P. Paolicelli, *React. Funct. Polym.*, 2023, **189**, 105607.
119. M. E. Han, S. H. Kim, H. D. Kim, H. G. Yim, S. A. Bencherif, T. I. Kim and N. S. Hwang, *Int. J. Biol. Macromol.*, 2016, **93**, 1410-1419.
120. C. Huynh, T. Y. Shih, A. Mammoo, A. Samant, S. Pathan, D. W. Nelson, C. Ferran, D. Mooney, F. LoGerfo and L. Pradhan-Nabzdyk, *PeerJ*, 2019, **7**, e7377.
121. R. H. Koh, J. Kim, S. H. L. Kim and N. S. Hwang, *Biomed. Mater.*, 2022, **17**, 024106.
122. M. J. Park, Y. H. An, Y. H. Choi, H. D. Kim and N. S. Hwang, *Macromol. Biosci.*, 2021, **21**, 2100234.
123. A. Singh, J. Mirgule, M. M. Pillai, N. Dalal and P. Tayalia, *Mater. Today Commun.*, 2022, **31**, 103494.
124. S. Hou, Y. Liu, F. Feng, J. Zhou, X. Feng and Y. Fan, *Adv. Healthcare Mater.*, 2020, **9**, 1901041.
125. S. H. Wu, M. Kuss, D. J. Qi, J. Hong, H. J. Wang, W. H. Zhang, S. J. Chen, S. L. Ni and B. Duan, *ACS Appl. Bio Mater.*, 2019, **2**, 4864-4871.
126. D. J. Qi, S. H. Wu, M. A. Kuss, W. Shi, S. Chung, P. T. Deegan, A. Kamenskiy, Y. N. He and B. Duan, *Acta Biomater.*, 2018, **74**, 131-142.
127. M. Zoughaib, K. Dayob, S. Avdokushina, M. I. Kamalov, D. V. Salakhieva, I. N. Savina, I. A. Lavrov and T. I. Abdullin, *Gels*, 2023, **9**.
128. A. Y. Durukan and I. A. Isoglu, *Mater. Technol.*, 2020, **35**, 853-862.
129. S. Pacelli, L. Di Muzio, P. Paolicelli, V. Fortunati, S. Petralito, J. Trilli and M. A. Casadei, *Int. J. Biol. Macromol.*, 2021, **166**, 1292-1300.
130. L. C. Bahlmann, A. E. G. Baker, C. Xue, S. Liu, M. Meier-Merziger, D. Karakas, L. K. Zhu, I. Co, S. Zhao, A. Chin, A. McGuigan, J. Kuruvilla, R. C. Laister and M. S. Shoichet, *Adv. Funct. Mater.*, 2021, **31**, 2008400.
131. M. E. Han, B. J. Kang, S. H. Kim, H. D. Kim and N. S. Hwang, *J. Ind. Eng. Chem.*, 2017, **45**, 421-429.
132. C. T. Liu, X. Liu, C. Q. Quan, X. Q. Li, C. Z. Chen, H. Kang, W. K. Hu, Q. Jiang and C. Zhang, *RSC Adv.*, 2015, **5**, 20227-20233.
133. D. Rana, T. Colombani, B. Saleh, H. S. Mohammed, N. Annabi and S. A. Bencherif, *Mater. Today Bio*, 2023, **19**, 100572.
134. S. Reichelt, J. Becher, J. Weisser, A. Prager, U. Decker, S. Möller, A. Berg and M. Schnabelrauch, *Mater. Sci. Eng. C*, 2014, **35**, 164-170.
135. M. Rezaeeyazdi, T. Colombani, A. Memic and S. A. Bencherif, *Materials*, 2018, **11**, 1374.
136. A. Singh and P. Tayalia, *J. Biomed. Mater. Res. A*, 2020, **108**, 365-376.
137. L. C. Bahlmann, C. Xue, A. A. Chin, A. Skirzynska, J. Lu, B. Theriault, D. Uehling, Y. Yerofeyeva, R. Peters, K. L. Liu, J. A. Chen, A. L. Martel, M. Yaffe, R. Al-award, R. S. Goswami, J. Ylanko, D. W. Andrews, J. Kuruvilla, R. C. Laister and M. S. Shoichet, *Biomaterials*, 2023, **297**, 122121.
138. M. Behl, Q. Zhao and A. Lendlein, *J. Mater. Res.*, 2020, **35**, 2396-2404.
139. I. Malakhova, Y. Privar, Y. Parotkina, M. Eliseikina, A. Golikov, A. Skatova and S. Bratskaya, *J. Environ. Chem. Eng.*, 2020, **8**, 104395.
140. Y. Privar, I. Malakhova, A. Pestov, A. Fedorets, Y. Azarova, S. Schwarz and S. Bratskaya, *Chem. Eng. J.*, 2018, **334**, 1392-1398.
141. Z. M. Sahin, D. Alimli, M. M. Tonta, M. E. Kose and F. Yilmaz, *Sens. Actuators B Chem.*, 2017, **242**, 362-368.
142. R. Mallik and D. S. Hage, *J. Sep. Sci.*, 2006, **29**, 1686-1704.
143. A. V. Pestov, Y. O. Privar, A. V. Mekhaev, A. N. Fedorets, M. A. Ezhikova, M. I. Kodess and S. Y. Bratskaya, *Eur. Polym. J.*, 2019, **115**, 356-363.
144. M. Gedikli, S. Ceylan, M. Erzenegin and M. Odabasi, *Acta Biochim. Pol.*, 2014, **61**, 731-737.
145. F. Yilmaz, N. Bereli, H. Yavuz and A. Denizli, *Biochem. Eng. J.*, 2009, **43**, 272-279.
146. Ş. Öncel, L. Uzun, B. Garipcan and A. Denizli, *Ind. Eng. Chem. Res.*, 2005, **44**, 7049-7056.
147. R. Zhai, B. Zhang, Y. Wan, C. Li, J. Wang and J. Liu, *Chem. Eng. J.*, 2013, **214**, 304-309.
148. N. Carballo-Pedrares, J. López-Seijas, D. Miranda-Balbuena, I. Lamas, J. Yáñez and A. Rey-Rico, *J. Control. Release*, 2023, **362**, 606-619.
149. C. Oelschlaeger, F. Bossler and N. Willenbacher, *Biomacromolecules*, 2016, **17**, 580-589.
150. M. D. Kerr, D. A. McBride, W. T. Johnson, A. K. Chumber, A. J. Najibi, B. R. Seo, A. G. Stafford, D. T. Scadden, D. J. Mooney and N. J. Shah, *Bioeng. Transl. Med.*, 2023, **8**, e10309.
151. M. D. Kerr, W. T. Johnson, D. A. McBride, A. K. Chumber and N. J. Shah, *Bioeng. Transl. Med.*, 2023, **8**, e10591.
152. A. M. Chaux-Gutierrez, E. J. Perez-Monterroza, D. M. Granda-Restrepo and M. A. Mauro, *J. Food Process. Preserv.*, 2020, **44**, e14843.
153. B. Tavsanlı and O. Okay, *Carbohydr. Polym.*, 2020, **229**, 115458.
154. N. Bölgen, M. R. Aguilar, M. D. Fernández, S. Gonzalo-Flores, S. Villar-Rodil, J. S. Román and E. Piskin, *Artif. Cells Nanomed. Biotechnol.*, 2015, **43**, 40-49.
155. N. Bölgen, P. Korkusuz, I. Vargel, E. Kiliç, E. Güzel, T. Çavusoglu, D. Uçkan and E. Piskin, *Artif. Cells Nanomed. Biotechnol.*, 2014, **42**, 70-77.
156. N. J. Shah, A. S. Mao, T. Y. Shih, M. D. Kerr, A. Sharda, T. M. Raimondo, J. C. Weaver, V. D. Vrbancak, M. Deruaz, A. M. Tager, D. J. Mooney and D. T. Scadden, *Nat. Biotechnol.*, 2019, **37**, 293-302.
157. N. Bölgen, F. Plieva, I. Y. Galaev, B. Mattiasson and E. Piskin, *J. Biomater. Sci. Polym. Ed.*, 2007, **18**, 1165-1179.
158. J. B. Leach, K. A. Bivens, C. W. Patrick and C. E. Schmidt, *Biotechnol. Bioeng.*, 2003, **82**, 578-589.
159. B. Tavsanlı, V. Can and O. Okay, *Soft Matter*, 2015, **11**, 8517-8524.
160. E. Hoch, T. Hirth, G. E. M. Tovar and K. Borchers, *J. Mater. Chem. B*, 2013, **1**, 5675-5685.
161. C. C. Zhou, P. Li, X. B. Qi, A. R. M. Sharif, Y. F. Poon, Y. Cao, M. W. Chang, S. S. J. Leong and M. B. Chan-Park, *Biomaterials*, 2011, **32**, 2704-2712.
162. S. I. Somo, K. Langert, C. Y. Yang, M. K. Vaicik, V. Ibarra, A. A. Appel, B. Akar, M. H. Cheng and E. M. Brey, *Acta Biomater.*, 2018, **65**, 53-65.
163. P. B. Welzel, M. Grimmer, C. Renneberg, L. Naujox, S. Zschoche, U. Freudenberg and C. Werner, *Biomacromolecules*, 2012, **13**, 2349-2358.
164. K. Salchert, T. Pompe, C. Sperling and C. Werner, *J. Chromatogr. A*, 2003, **1005**, 113-122.



## Abbreviations

<sup>1</sup> H NMR	Proton nuclear magnetic resonance	DexMA	Methacrylated dextran
AA	Acrylic acid	DF	Degree of functionalization
AAM	Acrylamide	Dil	1,1'-Dioctadecyl-3,3',3'-tetramethylindocarbocyanine perchlorate
AAPBA	<i>meta</i> -Acrylamidophenylboronic acid	DM	Degree of modification
AAS	Atomic absorption spectroscopy	DMAAm	<i>N,N</i> -Dimethylacrylamide
AATris	<i>N</i> -[Tris(hydroxymethyl)methyl]acrylamide	DMSP-HEMA	Dimethylsulfoniopropionate-hydroxyethyl methacrylate ester
Ac-Cys-OH	<i>N</i> -Acetyl-L-cysteine	DNS	3,5-Dinitrosalicylic acid
Acrylate-PEG-G <sub>4</sub> RGDSP	PEG acrylate based G <sub>4</sub> RGDSP peptide sequence	DOSY	Diffusion ordered spectroscopy
Acrylate-PEG-YRGDS/YRDGS	PEG acrylate based YRGDS/YRDGS peptide sequence	DS	Degree of substitution
Acryloyl-CD	Acrylated β-cyclodextrin	<i>E. coli</i>	<i>Escherichia coli</i>
Ada-Ahx-GGRGD/GGGHK	Adamantyl aminohexanoic acid	EA	Elemental analysis
AEMA-HCl	2-Aminoethyl methacrylate hydrochloride	ECH	Epichlorohydrin
AES	Mono(2-acryloyloxyethyl) succinate	ECM	Extracellular matrix
AGE	Allyl glycidyl ether	EDC	1-Ethyl-3-(3-dimethylaminopropyl) carbodiimide
Albumin-MA	Methacrylated albumin	EDTA	Ethylenediamine tetraacetic acid
Alg	Alginate	EDX	Energy-dispersive X-ray spectroscopy
Alg-MA	Methacrylated alginate	EGDGE	Ethylene glycol diglycidyl ether
AllAm	Allylamine	EGDMA	Ethylene glycol dimethacrylate
Amine-HA-MA	Amine terminated methacrylated hyaluronic acid	EH	Epoxy hexane
APTMAcI	Acrylamidopropyltrimethyl ammonium chloride	ELISA	Enzyme-linked immunosorbent assay
ARhoB	Acryloxyethyl thiocarbamoyl rhodamine B	EPL-A	Acrylated ε-poly-L-lysine
Asp-MA	<i>N</i> -Methacrylamido aspartic acid	ESI-MS	Electrospray ionization mass spectrometry
blgG	Bovine immunoglobulin G	FITC-ConA	Fluorescein isothiocyanate labelled Concanavalin A
Biotin-SH	Thiol-functionalized biotin	FTIR	Fourier-transform infrared spectroscopy
BODIPY	Boron-dipyrromethene	FuMaMA	Furan-protected maleimide-containing methacrylate
bPEI	Branched poly(ethyleneimine)	GA	Glutaraldehyde
BSA	Bovine serum albumin	GCMA	Methacrylated glycol chitosan
Calcein-AM	Calcein acetoxymethyl ester	GC-MS	Gas chromatography-mass spectrometry
CD	Cyclodextrin	GelMA	Methacrylated gelatin
C-MA	Methacrylated chitosan	GELox	Oxyamine-functionalized gelatin
CMFDA	5-Chloromethylfluorescein diacetate	Gel-UPY	2-ureido-4[1H]-6-methyl-pyrimidinone functionalized gelatin
<i>C</i> <sub>final</sub>	Final concentration in solution	GFP	Green fluorescent protein
CFU	Colony forming unit	GHK	Glycyl-L-histidyl-L-lysine peptide sequence
<i>C</i> <sub>initial</sub>	Initial concentration in solution	GlcNAc	<i>N</i> -Acetyl glucosamine
CLSM	Confocal laser scanning microscopy	GMA	Glycidyl methacrylate
CMC-MA	Methacrylated carboxymethylcellulose	HA	Hyaluronic acid
CNBr	Cyanogen bromide	HAa	Hyaluronan aldehyde
ConA	Concanavalin A	HA-MA	Methacrylated hyaluronic acid
CS-MA	Methacrylated chondroitin sulfate	HA-Nb	Norbornene-functionalized hyaluronic acid
CT	Computed tomography	HA-Tz	Triazine-functionalized hyaluronic acid
DAOS	<i>N</i> -Ethyl- <i>N</i> -(2-hydroxy-3-sulfopropyl)-3,5-dimethoxyaniline sodium salt	HEK	Human embryonic kidney
DAPI	4'6-Diamidino-2-phenylindole	HEMA	2-Hydroxyethyl methacrylate
		Hep-MA	Methacrylated heparin
		HPLC	

View Article Online  
DOI: 10.1039/D4MH00315B

## Journal Name

## ARTICLE

Journal Name	ARTICLE
HRP	High-performance liquid chromatography
hsTf	Horse radish peroxidase
ICP-AES	Human serum transferrin
ICP-MS	Inductive coupled plasma-atomic emission spectroscopy
ICP-OES	Inductive coupled plasma-mass spectrometry
IDA	Inductive coupled plasma-optical emission spectroscopy
IgG	Iminodiacetic acid
IMAC	Immunoglobulin G
KefMA	Immobilized metal-affinity chromatography
L-ASNase	Methacrylated kefiran
LDH	L-Asparaginase
LDL	Lactate dehydrogenase
LDL-C	Low-density lipoprotein
MAA	Low-density lipoprotein-cholesterol
MAAm	Methacrylic acid
MABP	Methacrylamide
MAETAC	Methyl acrylamide
MAG	Methacryloyl benzophenone trimethylammonium chloride
MAHis	2-(Methacryloyloxy)ethyl trimethylammonium chloride
MALDI-ToF	2-(Methacrylamido) glucopyranose
Mannose-SH	<i>N</i> -Methacrylamido-L-histidine
MA-Tyr-OMe	Matrix-assisted laser desorption/ionization-time of flight
MBAAm	Thiol-functionalized mannose
m <sub>cryogel</sub>	<i>N</i> -Methacryloyl-L-tyrosine methylester
MMA	<i>N,N'</i> -methylenebisacrylamide
mPEGA	Cryogel mass
NAA	Methyl methacrylate
NGF	Methoxy poly(ethylene glycol) acrylate
NHS	Nicotinamide
NiPAAm	Human neuronal growth factor
NIR680	<i>N</i> -Hydroxysuccinimide
NMR	<i>N</i> -Isopropyl acrylamide
OES	Near-Infrared dye 680
OPF	Nuclear magnetic resonance spectroscopy
ox-PHSRN-RGDSP	Optical emission spectroscopy
PAA	Oligo (poly(ethylene glycol) fumarate)
pABA	Oxyamine-functionalized PHSRN-RGDSP peptide sequence
pABSA	Poly(acrylic acid)
pAPyr	<i>para</i> -Amino benzoic acid
PCAPBA	<i>para</i> -Amino benzenesulfonamide
PEGDA	<i>para</i> -Amino pyridine
PEGDMA	3-(Prop3-ynyloxycarbonylamino)-phenylboronic acid
	Poly(ethylene glycol) diacrylate
	Poly(ethylene glycol) dimethacrylate
	PEGFuMaMA
	PEGMeMA
	PEI
	Phe
	PLL
	PPL
	retro-DA
	RGD
	Rhodamine-NHS
	RITC
	RT qPCR
	<i>S. epidermidis</i>
	SBMA
	SDF-1
	SDS-PAGE
	SEM
	SPA
	SPMA
	ssNMR
	Styrene-CD
	sulfoNHS
	TBO
	TMBEMPA-Br
	TNBS
	Tris
	TRITC
	Trp
	Tyr
	V
	VBMG
	VEGF
	VIm
	VP
	VPBA
	WDX
	XPS
	$\beta$ -CD
	Poly(ethylene glycol) based furan protected maleimide-containing methacrylate
	Poly(ethylene glycol) methyl methacrylate
	Polyethyleneimine
	L-Phenylalanine
	Poly(L-lysine)
	Porcine platelet lysate
	Retro-Diels Alder reaction
	L-Arginyl-glycyl-L-aspartic acid peptide sequence
	5/6-Carboxy tetramethyl rhodamine succinimidyl ester
	Rhodamine B isothiocyanate
	Real-time quantitative polymerase chain reaction
	Staphylococcus epidermidis
	Sulfobetaine methacrylate
	Stromal cell-derived factor 1
	Sodium dodecyl sulfate-polyacrylamide gel electrophoresis
	Scanning electron microscopy
	Sulfolpropyl acrylate
	Sulfolpropyl methacrylate
	Solid-state nuclear magnetic resonance spectroscopy
	Styrene-functionalized cyclodextrin
	<i>N</i> -Hydroxysulfosuccinimide sodium salt
	Toluidine blue O
	<i>N,N,N',N'</i> -Tetramethyl- <i>N,N'</i> -bis(2-ethylmethacrylate)-propyl-1,3-diammonium dibromide
	2,4,6-Trinitrobenzenesulfonic acid
	Tris(hydroxymethyl)aminomethane
	Tetramethylrhodamine isothiocyanate
	L-Tryptophan
	L-Tyrosine
	Volume
	(4-Vinyl-benzyl)- <i>N</i> -methyl-D-glucamine
	Vascular endothelial growth factor
	<i>N</i> -Vinylimidazole
	4-Vinylpyridine
	4-Vinylphenylboronic acid
	Wavelength-dispersive X-ray spectroscopy
	X-ray photoelectron spectroscopy
	$\beta$ -Cyclodextrin



## Data availability statement

View Article Online  
DOI: 10.1039/D4MH00315B

No primary research results, software or code have been included and no new data were generated or analysed as part of this review.

